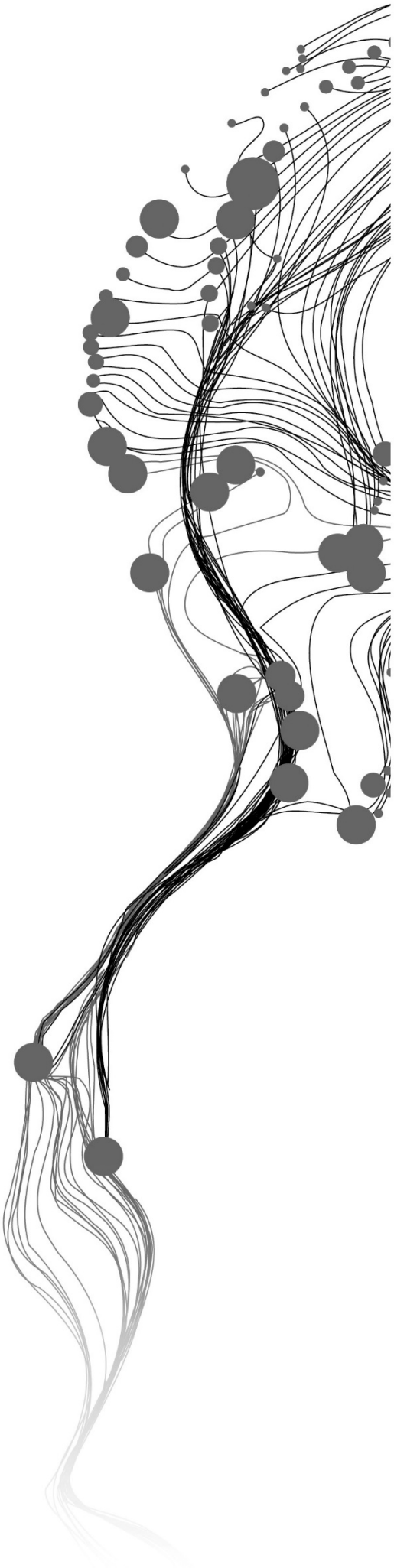

Is Heatwave A Risk in Enschede?

- A heat-health related assessment

TONG JIANG

August, 2024

Thesis submitted to the Faculty of Geo-Information Science and Earth Observation of the University of Twente in partial fulfilment of the requirements for the degree of Master of Science in Spatial Engineering

SUPERVISORS:

PROF.DR. J.I. BLANFORD

DR. S. AMER

THESIS ASSESSMENT BOARD:

PROF.DR.IR. C. PERSELLO

PROF.DR. M.J.C. VAN DEN HOMBERG MBA

ADVISOR:

C. PEREIRA MARGHIDAN MSC

DISCLAIMER

This document describes work undertaken as part of a programme of study at the Faculty of Geo-Information Science and Earth Observation of the University of Twente. All views and opinions expressed therein remain the sole responsibility of the author, and do not necessarily represent those of the Faculty.

ABSTRACT

Heat poses a significant threat to human health, with an increasing number of people worldwide being exposed to extreme temperatures due to the accelerating impacts of climate change. This trend is particularly concerning in urban areas, where the urban heat island effect exacerbates heat exposure. In the Netherlands, the frequency and intensity of heatwaves have markedly increased since 2000, presenting new challenges that the country faces a warming future. The unusual intensity of these extreme heat events can have severe consequences, particularly for those who are unprepared. Although there is a general consensus in Netherlands that heat is an imminent issue, a critical area that remains under-researched is the impact of heatwave events on local communities, highlighting the need for a deeper understanding of how these populations are affected.

This thesis focused on heat-related health risks, especially in relation to hazard, exposure, and their effects on liveability and human health through different vulnerabilities (sensitivity and adaptive capacity) at a localised level for the city of Enschede. The overall research objective was to assess the heat-related health risks in the urban area of Enschede and to understand why these areas were at high risk. The research was constructed at two levels: national level and neighbourhood level.

In the Netherlands, a heatwave is defined as having a maximum temperature of 25°C or higher in De Bilt for five consecutive days, with at least three tropical days within the period, which reach 30°C or higher. Thus, heatwave hazards were assessed at the national level, with hazards evaluated using data from the De Bilt weather station, compared against Enschede records to highlight potential local context deviations. Further spatial and temporal analyses showcased historical heatwave characteristics. In general, the southern and eastern parts of the Netherlands have experienced more frequent and intense heatwaves. Enschede, as one of the heat-prone areas, has faced more intense and prolonged heatwaves than De Bilt due to its higher summer temperatures. A total of 16 heatwaves were identified at Enschede using the KNMI heatwave definition, with 14 heatwave events occurring in De Bilt. The years 2018, 2019, and 2020 saw consecutive intense heatwave events, with an atypical heatwave in 2019 that recorded the highest air temperature of 40.2°C in Enschede

Focusing on the city level, this study identified heat risk across different neighbourhoods. Exposure factors included urban morphology, land use patterns, and population density, while vulnerability factors encompassed demographic characteristics, socio-economic status, health conditions, and the availability of cooling resources and green spaces. There are no neighbourhoods scored as “High” risk. Top 5 neighbourhoods with the higher risk scores are City, Getfert, De Bothoven, Hogeland-Noord, and Veldkamp-Getfert-West. They are all residing in 'Medium to High' risk levels. In all, around 95% of the population in urban neighbourhoods are found at a risk level greater than “Medium”.

To mitigate these risks, the city of Enschede could implement targeted interventions during this critical period. Strategies highlighted in the literature included enhancing urban greenery, planning cooling centres, and conducting public awareness campaigns on staying safe during extreme heat. These interventions could be functional for climate heat adaptation strategies, particularly for at-risk groups such as older adults and those with pre-existing health conditions.

Keywords: extreme heat, heatwaves, spatial and temporal analysis risk assessment, MCDA

ACKNOWLEDGEMENTS

I would like to express my deepest gratitude to everyone who has supported me throughout the process of completing this thesis.

First and foremost, I extend my sincerest thanks to my supervisors and advisor for their invaluable guidance, encouragement, and feedback throughout this journey. I am particularly thankful to Prof. Dr. Justine Blanford, who has been consistently supportive and encouraging each time I introduced a new idea. Her assistance in helping me organize my exploratory ideas into a structured and logical flow was indispensable. Her active involvement during the final stages of writing, along with her insightful feedback, was truly invaluable. I would also like to thank Dr. Sherif Amer, who consistently reminded me of the importance of structuring my writing and provided valuable suggestions on the overall framework I was describing. I am also deeply grateful to my advisor, Carolina Pereira Marghidan, with whom I have thoroughly enjoyed brainstorming sessions. Her insights into the potential of heat research and useful data resources have been truly inspiring. Each discussion with her led me to discover new and intriguing topics and literature to explore.

I would also like to acknowledge the Faculty of Geo-Information Science and Earth Observation (ITC) for providing the resources and environment that made this research possible.

Special thanks go to the participants of this study and the stakeholders Henk Broekhuizen from GGD Twenthe and Rik Meijer from Gemeente Enschede, whose cooperation and help were essential to this research.

I also want to thank my mentor, Janneke Ettema, for providing valuable guidance for my academic and career development throughout my two years of study.

To my colleagues and friends, thank you for your support, which made this journey more enjoyable. I would like to specifically thank my ITC friends Keke Duan, Katherine van Roon, Manuka Khan, and Tatenda Dzurume, who helped me review my extensive thesis paper. I am also grateful to all my friends who provided mental support during the stressful but fruitful and unforgettable last year.

Finally, I am deeply grateful to my mom and my grandma for their support and care during my final thesis writing phase.

DISCLAIMER

Some aspects of this work have been developed with the use of artificial intelligence (AI), such as ChatGPT 4o, GitHub Copilot and AI based literature searching platforms Consensus and SciSpace. The purpose of incorporating AI was to help literature finding, translate method to script, and debugging, and help fine-tuning writing through checking grammar and style.

It's important to note that while AI tools were employed, the content and ideas presented in this work remain the result of my personal understanding and efforts. I have taken care to ensure that any information submitted based on AI-generated content complies with intellectual property laws, is accurate, and aligns with ethical standards.

TABLE OF CONTENTS

LIST OF FIGURES

LIST OF TABLES

LIST OF ACRONYMS

CBS - Centraal Bureau voor de Statistiek / Statistics Netherlands

CHI - Cumulative Heatwave Intensity

EMWCF - European Monitoring and Evaluation Programme and World Climate Research Programme

GGD - Gemeentelijke Gezondheidsdienst / Municipal Public Health Service

HI - Heatwave Intensity

HVI - Heat Vulnerability Index

HWD - Heatwave Duration

IPCC - Intergovernmental Panel on Climate Change

KEA - Klimaateffectatlas / Climate Impact Atlas

KNMI - Koninklijk Nederlands Meteorologisch Instituut / Royal Netherlands Meteorological Institute

LST - Land Surface Temperature

MCDA - Multi-Criteria Decision Analysis

NAS - National Climate Adaptation Strategy

PET - Physiological Equivalent Temperature

PT - Perceived Temperature

RO - Research Objective

RQ - Research Questions

RIVM - Rijksinstituut voor Volksgezondheid en Milieu / National Institute for Public Health and the Environment

TD - Tropical Days

TG - Daily Average Temperature

TN - Minimum Temperature

TX - Maximum Temperature

UHI - Urban Heat Island

US EPA - United States Environmental Protection Agency

USGS - U.S. Geological Survey

UTCI - Universal Thermal Climate Index

VWS - Ministerie van Volksgezondheid, Welzijn en Sport / Ministry of Health, Welfare and Sport

WGBT - Wet-Bulb Globe Temperature

WHO - World Health Organization

1 INTRODUCTION

1.1 Background

1.1.1 Heatwaves: a severe climate-induced hazard worldwide

Heatwaves, intensified by climate change, are increasing in frequency globally (IPCC, 2023). Throughout recent years, a series of unprecedented heatwaves have caused record temperatures and severe disruptions worldwide (The Guardian, 2023, 2024; The New York Times, 2023; World Weather Attribution, 2022, 2023, 2024b, 2024a). 2023 was one of hottest years on record (ECMWF, 2023). Heatwaves are a deadly weather phenomenon (Mora et al., 2017). Heat-related deaths have been on the rise globally, with over 166,000 deaths recorded between 1998 and 2017, and approximately 125 million more individuals exposed to heatwaves between 2000 and 2016 (WHO, 2023). The devastating impact of heatwaves are evident in instances like heatwaves in Europe causing 70,000 excess deaths in 2003 and over 60,000 heat-related deaths in 2022 (Ballester et al., 2023; The Lancet, 2018).

1.1.2 Society is being impacted across different sectors

Heatwaves can have a negative impact on infrastructure (Klok & Kluck, 2018), workplace productivity (Tong et al., 2021) and the health and wellbeing of humans across different sectors e.g., urban areas, agriculture and construction (The Guardian, 2024), as shown in Figure 1–1. For example, heat can damage pavements, bridges, and rails and lead to blackouts with increasing demands for electricity (Klok & Kluck, 2018). Excess heat can also threaten labour productivity and outdoor work and reduce comfort in cities (Tong et al., 2021). With increasing heat, health concerns can escalate leading to heat-related illnesses, such as heat cramps, heat exhaustion, and heat stroke when the body cannot cool itself effectively, causing damage to the brain and other vital organs resulting in hospital admissions, higher demand for emergency services, and a rise in heat-related mortality rates (Amengual et al., 2014). The older adults, children, individuals with existing chronic diseases, and those with low socioeconomic backgrounds are the most vulnerable (Balmain et al., 2018; Kovats & Hajat, 2008). Furthermore, heatwaves can also intensify air pollution, leading to increased smog and ground-level ozone, which also have severe health implications (The Lancet, 2018). Lastly, with rising temperatures water availability can be reduced and water quality can be negatively affected with growth of algae pathogens (Klok & Kluck, 2018).

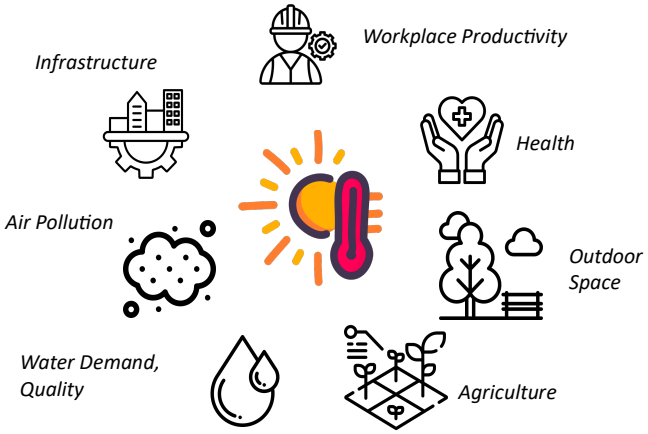

Figure 1–1 Heatwave impact, drawn by author

1.1.3 Heatwave in the Netherlands and the warming future

In the Netherlands, heatwaves have become an increasingly imminent issue attracting much more attention (Klok & Kluck, 2018). Heatwaves have occurred more frequently in the last few decades compared to previous centuries. For example, the heatwaves of 2003 and 2006 resulted in significant increases in mortality rates in the Netherlands, with estimated excess mortality up to 2200 deaths during each event (De Visser et al., 2022). These two deadly events led to heatwaves becoming a public health issue, which consequently pushed forward the development of the first heat plan in Netherlands initiated in 2007 (Hagens & van Bruggen, 2015). However, research on heat-related mortality is still underdeveloped, as heat is not listed as a cause of death in the Netherlands (CBS, 2019, 2020). Recent summers also highlight the problem of more extreme heat events, which is particularly crucial given the typically mild climate of the Netherlands. The highest temperature ever recorded in the Netherlands was 40.7°C on July 25, 2019 in Gilze-Rijen, North Brabant (KNMI, 2024). Further, research conducted among 140,000 respondents in Netherlands found that nearly half of the respondents, especially young adults, people with existing health conditions and low income, have difficulty to cool down in and around their homes (van Merwijk et al., 2023). Thus, unusual extreme heat can have significant effects when people are unprepared.

Moreover, the European continent is experiencing the fastest warming trend globally, which is twice the global average rate since the 1980s according to European Centre for Medium-Range Weather Forecasts (ECMWF) (ECMWF, 2022). Corresponding to that trend, in the latest KNMI climate scenarios, it was predicted that heatwaves will become more frequent, hotter and prolonged (KNMI, 2023c). In the high emissions scenarios according to KNMI (KNMI, 2023c), temperatures reaching 40°C could become an almost yearly occurrence by the end of the century. Meanwhile, even in low emission scenarios, the Netherlands is expected to face increasingly tropical weather conditions (maximum temperature surpassing 30°C) (KNMI, 2023c). These facts and trends highlight the necessity and importance of heatwave research in the Netherlands.

1.1.4 Current measures and the mitigations

Following the heatwave in 2006 in the Netherlands, the Ministry of Health, Welfare and Sport (VWS) drew up a National Heat Plan (NHP) in 2007, which was updated by the RIVM in 2015 (Hagens & van Bruggen, 2015), as indicated in Figure 1–2. The National Heat Plan is a risk- communication plan that describes how heat early warnings are issued by KNMI, and how the information will be conveyed via healthcare sector

organizations such as the National Institute for Public Health and the Environment (RIVM) to local public health services (GGDs) and other relevant stakeholders.

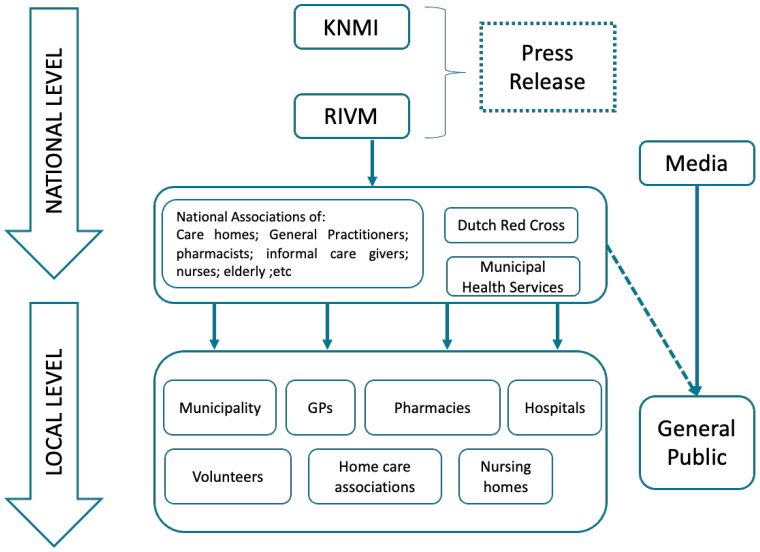

Figure 1–2 Stakeholders involved in Heat Action Plan in the Netherlands

However, the follow-up of the NHP by different stakeholders is without obligation. Not all organisations are aware of the NHP, for example, care organisations, including hospitals and elderly care services, were found to have limited awareness of the NHP (Van Loenhout et al., 2016). The NHP also lacks emphasis on other critical strategies that may be important during a heat event. For example, how to alleviate heat in the built environment or modification of working times and conditions during extreme heat days.

1.1.5 Towards an integrated approach

There is a growing call to develop local heat actions plans to not only efficiently implement the NHP but also investigate the critical strategies needed for involving cross-sectoral collaborations (European Environment Agency, 2022). This is not always easy, since it has been shown that heatwaves do not have a specific problem owner, therefore understanding different stakeholders' perceptions of heatwaves is crucial for developing effective local heat plans (Klok & Kluck, 2018). Although the awareness of heat impacts among stakeholders is on the rise, the lack of awareness or misunderstandings about the severity and frequency of heatwaves still exist and can lead to knowledge gaps regarding the characteristics and impacts of heatwaves (Klok & Kluck, 2018). The underlying factor is the possible insufficiency of localised research or data. In the mortality database from the Dutch health sector, so far, heat related death is not well documented (CBS, 2019, 2020). It is important to highlight that heat-related health data is often difficult to capture (Hajat & Kosatky, 2010). For this reason, examining the environments that contribute to health effects, which is often referred as vulnerabilities, is essential. By understanding these vulnerabilities, local governments and stakeholders can better target their interventions and develop more effective heat action plans.

Since 2015, local implementation of this National Heat Plan has been taken up in several regions in the Netherlands by GGDs and partners such as the Dutch Red Cross. Information products have been developed to reach vulnerable groups. To support municipalities in drawing up their own local heat plan, a guideline on local heat plan was published in 2019 from National Climate Adaptation Strategy (NAS, 2019)

and the Climate Effect Atlas (Klimaateffectatlas) was developed at the national level (Klimaateffectatlas, 2023). With respect to heatwave hazards, the atlas provides information on current and predicted climate change analysis, urban heat island effect, Physiologically Equivalent Temperature (PET) maps, distances to cooling centres, maps of loneliness and green base map and etc. More details regarding these are provided in section 2.3. Although these resources offer valuable information at a national level, these still lack calibration, integration, and application at the local level.

1.1.6 Stakeholder Involvement

Based on the framework (Figure 1–2), a focus of stakeholders could be identified. The potential stakeholders indicated by the "GGD guideline on local heat adaptation" include local authorities such as the municipality, public health organizations like the GGDs (local Public Health Service), general practitioners, pharmacists, social neighbourhood teams, home care organizations, geriatric networks, welfare foundations, religious organizations, childcare locations, sports clubs and etc.

In this thesis project, we managed to reach out to two main stakeholders GGD Twente and Gemeente Enschede (Municipality of Enschede). Several meetings were held to understand the local knowledge and existing mitigation interventions. They also helped to inform the research questions and provide feedback on the intermediate results. Due to the scope of the research and time constraints, no recorded interviews were conducted. Instead, stakeholder input was verified through published outputs that can be cited.

The main knowledge gained from the stakeholder information are as follows:

- A report on social perception of environmental health risks, which includes social perception of heat and identification of potential vulnerable groups (van Merwijk et al., 2023). These vulnerable groups involve young population between 18-34 years, people with limited mobility, people with poor perceived health, older adults with fragile health, people living in urbanised areas, people who feel that there is insufficient greenery in their environment.
- An existing heat stress analysis from Twents Waternet for Enschede using the standard process, estimating the Urban Heat Island effect, Physiologically Equivalent Temperature (PET) mapping and warm nights, these three heat stress indicators are combined to estimate the heat stress on each neighbourhood (Twents Waternet, 2023).
- Local heat action plan is being developed and will be published in year 2024.

1.2 Research significance (Wicked Problem)

This study aims to assess heat-related health risks at the local level in the Netherlands. A key area of limited understanding is the impact of heatwave events on local communities. Although there is a national climate effect atlas (Klimaateffectatlas) that illustrates heat impacts, there remains a gap in the integrated heat risk assessments that can support the cross-disciplinary coordination of local heat action plans in the Netherlands.

These challenges align with what is typically conceptualized as 'wicked problems' in environmental issues. The term 'wicked problem' is used here as defined by Balint et al. (2011): a problem characterised by an absence of definite knowledge and a lack of consensus on values among stakeholders, complicating the identification of optimal solutions. Effective public decision-making is contingent upon two dimensions: agreement on values and certainty of knowledge. These dimensions can lead to four distinct scenarios, ranging from simple decisions with clear knowledge and consensus, to wicked problems where both

knowledge and agreement are ambiguous (Balint et al., 2011). Therefore, although there is a general consensus that heat is an imminent issue, the challenge of addressing local heatwave hazards in the Netherlands can be classified as a wicked problem. This is marked by a lack of ownership of the problem and also lack of local knowledge.

1.3 Research objective (RO) and Research questions (RQ)

This thesis will focus on heat-related health risks, especially in relation to hazard, exposure and how this affects liveability and human health through different vulnerabilities (sensitivity and capacity) here at a localised level.

The overall research objective is to assess the heat-related health risk in the urban area of Enschede and why these areas are at high risk. To achieve this overall objective, two sub-objectives and subsequent research questions are defined as following:

RO1: To assess how heatwaves vary spatially and temporally in the Netherlands.

RQ 1.1 What are the temporal and spatial patterns of heatwaves across Netherlands?

RQ 1.2 How do heatwave events and characteristics vary between Enschede and De Bilt?

RO2: To identify who is at risk to heatwave in Enschede and where are the risk areas in Enschede.

RQ 2.1: What are the characteristics of intra-urban heat exposure distributions during a heatwave event in Enschede?

RQ 2.2: What demographic, socio-economic and capacity factors define the populations most vulnerable to heatwaves in Enschede?

RQ 2.3: Which areas in Enschede are at the highest risk during heatwaves, considering both exposure and vulnerability?

2 LITERATURE REVIEW

2.1 Heatwave definition and measurement

2.1.1 Heatwave definition

The IPCC (2023) defines a heatwave as a period of abnormally hot weather, often relative to a temperature threshold, lasting from two days to months. This abnormal hot weather is considered extreme, occurring as rarely as or rarer than the 90th percentile of observed probability. However, there are no universal heatwave definitions, as the characteristics of a heatwave can vary from place to place, resulting in a variety of definitions in different regions and countries (McGregor et al., 2015). In the Netherlands, a heatwave is defined as having a maximum temperature of 25°C or higher in De Bilt for five consecutive days, with at least three tropical days within the period, which reach 30°C or higher. For the heat warning system, the heatwave warning will be issued when the KNMI reports a high probability of at least four consecutive days with maximum temperatures exceeding 27°C (Hagens & van Bruggen, 2015).

2.1.2 Heatwave measurement

The ways of measuring the heatwave can be categorised into four different schematic types: extreme indices, event indices, multivariate indices, and risk indices (Barriopedro et al., 2023). The four categories are not separated from each other but are interconnected or evolving indices, which range from hazard focused indices to vulnerability and exposure related indices (Figure 2–1). The hazard-focused indices, such as extreme indices and event indices, typically evaluate heatwaves using temperature measurements based on absolute values or percentiles, examining characteristics like intensity, frequency, and duration. The multivariate indices are impact-based indices, incorporating temperature, wind, humidity, or physiology. There are also risk indices composed of hazard, exposure, and vulnerability, which are also an impact-based index but also involve the socio-economic factors. The differences in heatwave indices stem from various disciplines, each reflecting specific insights and criteria relevant to their respective fields (Boni et al., 2023). For example, climatologists and meteorologists define heatwaves as prolonged periods of excessively high temperatures to understand and predict weather patterns. Epidemiologists, however, focus on the health impacts, linking heatwaves to increased mortality rates. Policymakers view heatwaves as critical public health concerns, using specific thresholds and durations to determine the severity and necessary response measures (Boni et al., 2023). As there is a growing call for interdisciplinary research to cope with heatwave events better effectively, a more integrated heatwave measurement focusing on the risk indices is also on rise to bring all the necessary stakeholders together.

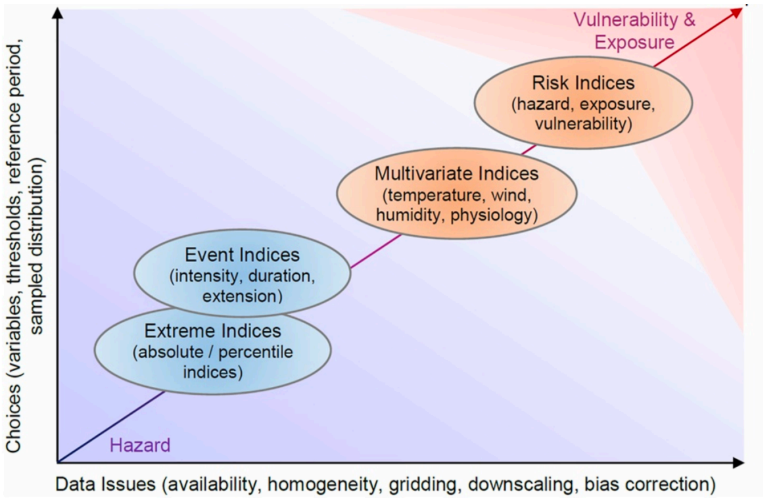

Figure 2–1 Different types of heat indices (Barriopedro et al., 2023)

Heatwave indices using extreme indices, event indices and multivariate indices are based on air temperature thresholds and other meteorological or physiological indicators (Table 2–1). Air temperature data such as daily maximum (TX), daily minimum (TN) and daily average (TG) are used as thresholds. Under the extreme index category, there are indices defined by absolute temperature thresholds, such as the monthly maximum temperature (TXx), the annual count of tropical nights (TR), and the annual count of summer days (SU). There's also the percentile-based extreme index, like TX90p, which counts the days with temperatures above the 90th percentile, and the Warm Spell Duration Index (WSDI), which tracks consecutive warm days.

Event indices focus on specific heatwave events, with the HW Magnitude Index daily (HWMId) measuring cumulative exceedances of daily maximum temperature, and the Excess Heat Factor (EHF) considering cumulative exceedances of mean temperature, with an acclimatization factor.

Multivariate indices consider additional variables such as humidity. These include the Heat Index/Apparent Temperature (HI/AT) and the Universal Thermal Climate Index (UTCI), which reflect the perceived heat based on human physiological response. Other indices like Airmass, Humidex, Perceived Temperature (PT), Physiological Equivalent Temperature (PET), and Wet-bulb Globe Temperature (WGBT) combine temperature with other environmental factors to gauge heat stress.

Table 2–1 Heatwave indices by category, adapted from (Barriopedro et al., 2023; McGregor et al., 2015)
**The temperature used in the table is by default air temperature; TX: daily maximum; TN: daily minimum; TG: daily average*

Category	HW index	Defined By	References
Extreme index (absolute, TX, TN, TG)	TXx	Monthly maximum temperature (TX).	(Alexander et al., 2006)
	TR	Annual count of tropical nights: days with minimum temperature (TN) > 20°C.	
	SU	Annual count of summer days: days with maximum temperature (TX) > 25°C.	
Extreme index (percentile, TX)	TX90p	Days with TX above the 90th percentile.	(Peterson et al., 2001)
	Warm spell duration index (WSDI)	Count of days in warm spells: at least six consecutive days with TX above the 90th percentile.	(Alexander et al., 2006)

Event index (TX)	HW Magnitude Index daily (HWMId)	Cumulative normalized exceedances of TX.	(Russo et al., 2015)
Event index (TM)	Excess Heat Factor (EHF)	Cumulative threshold exceedances of mean temperature (TM), weighted for acclimatization.	(Perkins & Alexander, 2013)
Multivariate index	Heat Index /Apparent Temperature (HI/AT)	Apparent temperature considering both temperature and humidity, indicating perceived heat.	(Steadman et al., 1984)
	Universal Thermal Climate Index (UTCI)	Equivalent temperature based on human physiological response to the thermal environment.	(Bröde et al., 2012)
	Airmass	Classification of weather types by a holistic set of atmospheric conditions affecting human responses.	(Sheridan & Kalkstein, 2004)
	Humidex	Combining temperature and humidity to express perceived heat.	(Smoyer-Tomic et al., 2003)
	Perceived temperature (PT)	Equates actual environment's thermal stress to a standard environment.	(Staiger et al., 1997)
	Physiological equivalent temperature (PET)	Based on a human heat budget model.	(Höppe, 1999)
	Wet-bulb globe temperature (WGBT)	Measure heat stress in direct sunlight, incorporating factors like temperature, humidity, wind speed, sun angle, and radiation.	(Budd, 2008)

2.2 Heat risk in the urban area

2.2.1 Intra-urban temperature variability

Urban areas are particularly vulnerable to heatwaves, where heat island effects are intensified during such periods (Jiang et al., 2019; Vanderplanken et al., 2021). This effect can be identified as urban areas being warmer than rural areas, thus experiencing more intense heat. It also highlights the intra-urban variability of temperature caused by the heat island effect. The term Urban Heat Island (UHI) has been broadly applied when quantifying the heat island effects, indicating not only that urban areas are under higher temperatures than rural areas, but also encompassing the varying temperatures within urban areas due to different urban design features and landscape arrangements(Stewart & Oke, 2012).

UHI effect occurs due to the disparity in the absorption and radiation of heat between urban constructions and natural landscapes(Oke, 1982). Urban construction materials such as metal, concrete, and brick are highly efficient at absorbing, storing and releasing heat (Mohajerani et al., 2017). In urban environments, the morphology, which includes the shape and layout of buildings and streets, can contribute to the trapping of heat, collectively, intensifying the heating effect (Yang et al., 2023). Conversely, natural landscapes originally featuring vegetation offer a cooling effect through evapotranspiration—evaporation from soil and

transpiration from plants—which can mitigate heat accumulation (Oke, 1982). Further, it leads to variations in thermal environment across different city morphology (e.g. Figure 2–2). To capture this intra-urban thermal variability, land surface temperature (LST) from satellite observations is usually used (Reiners et al., 2023).

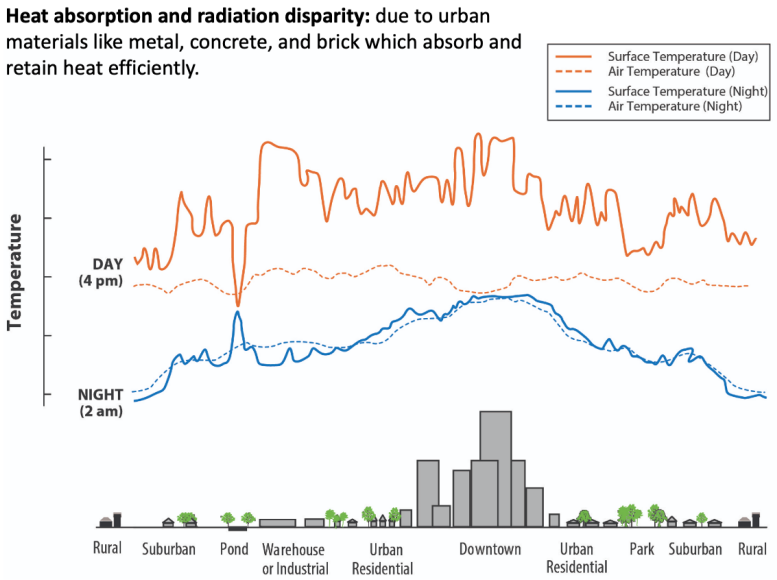

Figure 2–2 Causes of UHI effect (sources: US EPA, retrieved in 2024)

2.2.2 Heatwave risk evaluated by Land surface temperature (LST)

Urban heatwave hazards have been evaluated differently across different scales. The heat characteristics (calculating intensity, frequency, and duration) using air temperature data are usually applied at the macro level, continental, national or regional level with weather observations. Challenges arise when applying the methods to finer scale heatwave risk assessment. Often official meteorological measurements with long-term tracking are positioned on the outskirts of urban areas with limited stations, generally irregularly distributed across an urban landscape (e.g. weather stations). Thus, they cannot adequately capture intra-urban variability (Tomlinson et al. 2011). For city level, or even finer neighbourhood level, heatwave hazards can be intensified by UHI effect, thus finer resolution of data are needed.

Thus, heatwave measurements using meteorological or biometeorological indices tend to be applied at the national or regional scale while remotely sensed data such as satellite data are able to provide comprehensive spatial coverage, filling in the finer details, especially those needed for mapping urban characteristics. For this reason, Land Surface Temperature (LST) datasets, for instance, have found broader application in heat risk assessments. As LSTs can present local surface variations that directly affect the overlying air, studies have used LST as hazard indicators. For example, Buscail et al. (2012) used a Landsat ETM + image at a 60 m resolution during a heatwave in 2001 in Rennes to estimate LST and derive a hazard index. Tomlinson et al. (2011) used MODIS (Moderate Resolution Imaging Spectroradiometer) in 2006 to measure the magnitude of the surface UHI at a 1 km resolution on cloud free days on a specific heatwave day. More studies have used scaled LST obtained from a heatwave event to act as a hazard indicator proxy, areas with higher LST stands for higher risk (Chen et al., 2018a, 2018b; Dousset et al., 2011; Jenerette et al., 2016). Even though LST has been widely applied in the heatwave studies, challenges remain in the quality and processing complexity of long-duration thermal images (Reiners et al., 2023) . Additionally, the low temporal

accuracy of high-resolution clear sky LST datasets, often affected by cloud coverage, which could lead to limited LST data availability (Agathangelidis et al., 2022; Jenerette et al., 2016; Reiners et al., 2023).

2.2.3 Heatwave risk assessment - from macro to local scale

Heatwaves are hazardous due to their severe impact on both human and natural systems, with health-related risks often being represented by an increase in mortality. The relationship between heat and mortality has been a long-term concern and well documented in the epidemiology literature (Basu, 2009; Curriero et al., 2002; Mora et al., 2017; Vicedo-Cabrera et al., 2021). Geographical variation of this relationship was observed from a multi-country research study of people residing in moderately cold and moderately hot regions (Guo et al., 2017). Guo et al. (2017) found that people residing in moderate regions are more affected by heatwaves compared to those in extremely cold or hot regions. While at a more local scale, Clarke (1972) found that higher death rate in cities existed due to UHI effect.

Recent years have seen an increasing trend for local scale heatwave risk assessment, given the varying physical and socioeconomic characteristics of urban areas and cities. Heat vulnerability index (HVI) ,or in another way, the heat risk index has been widely explored across different spatial levels from countrywide to local level (Ahmed et al., 2023; Bradford et al., 2015; Estoque et al., 2020; Ho et al., 2018; Johnson et al., 2012; Kim et al., 2017; Voelkel et al., 2018; Wolf & McGregor, 2013). A well-used method is Spatial Multi-criteria Decision analysis (MCDA) (Dean, 2020; Malczewski & Rinner, 2015; Raines et al., 2010), to map risk analysis and use weights to combine different indicators together. Other research delved into how spatial configuration or urban morphology influences exposure to heat. For instance, Maiullari et al. (2021) employed a typo-morphology approach to quantitatively evaluate the urban microclimate in Rotterdam, uncovering that spatial conditions significantly impact both indoor and outdoor temperatures. This discovery aligns with Zinzi and Santamouris's (2019) research that the urban form and its configurations can either mitigate or exacerbate overheating. Similar studies also emphasised the relationship between heat and mortality is significantly affected not only by the heterogeneity of physical environments but also by different socio-demographic characteristics (Baccini et al., 2008; Bettaieb et al., 2020; Brooke Anderson & Bell, 2011; Curriero et al., 2002; De Visser et al., 2022; Klein Rosenthal et al., 2014; McGeehin & Mirabelli, 2001; Oudin Åström et al., 2011; Yang et al., 2019). Thus, in the cities, the health risk to populations from heat is driven by various sub-systems which include the characteristics of the built environment, land use, infrastructures, and the social-economic characteristics (Ellena et al., 2020).

2.2.4 Heat Risk Framework

Heat risk is commonly assessed through a framework (IPCC, 2023) that integrates three key components: hazard, exposure, and vulnerability where:

$$\text{Heat Risk} = \text{Hazard} \times \text{Exposure} \times \text{Vulnerability}$$

Figure 2–3 shows the common indicators often used in the heat risk framework.

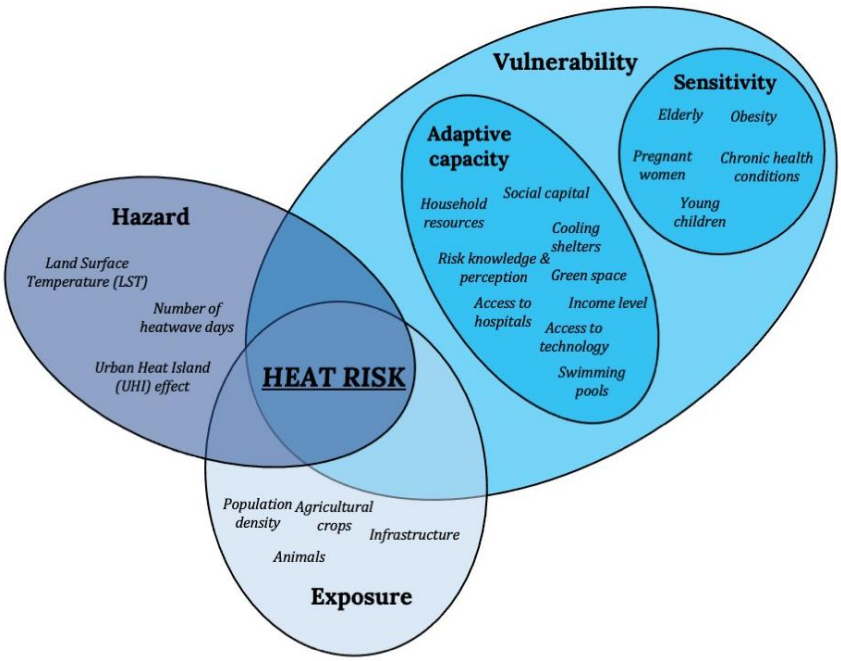

Figure 2–3 Indicators used in the heat risk index, source:(Marghidan, 2022)

Hazard refers to identifying the potential characteristics of extreme heat events, such as occurrence, intensity, duration etc . They are often defined and measured through specific temperature thresholds as discussed in 2.1. For example, the 2022 Lancet Countdown Europe report examines these characteristics by tracking the number of heatwave exposure days (van Daalen et al., 2022).

Exposure is defined as "the presence of people, livelihoods, species or ecosystems, environmental functions, services, resources infrastructure, or economic, social, or cultural assets in places and settings that could be adversely affected" (IPCC, 2023). The assessment of exposure involves identifying and quantifying these elements within the affected areas. Common indicators include population density, land surface temperature (LST). For instance, in the Philippines, a city-level study assessed heat-health risks across 139 cities, using LST to measure exposure and population density to assess the concentration of people at risk (Estoque et al., 2020).

Vulnerability refers to "the propensity or predisposition of an element exposed to extreme events to be adversely affected (IPCC, 2023). **Sensitivity** involves characteristics that increase the likelihood of adverse effects, such as age, health status, and socio-economic conditions. For instance, the older adults, individuals with chronic diseases, and low-income populations are often more sensitive to heat (van Daalen et al., 2022). **Adaptive capacity**, on the other hand, includes factors that enable populations to cope with and adapt to heat events, such as access to medical resources, availability of green spaces, and economic capacity. In Hangzhou, China, a socio-economic vulnerability assessment utilized indicators like GDP per capita and proximity to medical facilities to reflect both sensitivity and adaptive capacity (Sun et al., 2022).

The Table 2–2 below summarises how different regions assess heat-health risks using a combination of climatic, demographic, economic, and health-related data by integrating the conceptual framework of hazard, exposure, and vulnerability.

Table 2–2 Summary of different indicators used for determining risk
(Risk = Exposure x vulnerability (sensitivity and capacity). Examples from three case studies in China, Philippines and Europe)

Category	Data Type/Indicator	Description	Case Studies
Exposure	Land Surface Temperature (LST)	Temperature data	Philippine, Hangzhou
	Population Density	Number of people per area unit	Philippine (Estoque et al., 2020)
	Heatwave Exposure Days	Number of days with extreme heat	Lancet Countdown (Europe) (van Daalen et al., 2022)
Vulnerability Sensitivity	Chronic Diseases Prevalence	Incidence of cardiovascular, respiratory diseases, etc.	
	Urban Population Density	Number of people in urban areas	
	Age Structure	Proportion of population in specific age groups	Philippine, Hangzhou
	Socioeconomic Status	Poverty incidence, economic indicators	Philippine
	Age-Specific Population Density	Density of population in age groups	Hangzhou (Sun et al., 2022)
	Economic Points of Interest (POIs)	Density of economic activity POIs	
	Infrastructure Points of Interest (POIs)	Density of infrastructure-related POIs	
Vulnerability - Capacity	Availability of Urban Green Space	Vegetation coverage, using vegetation index	Philippine, Lancet Countdown (Europe)
	GDP Per Capita	Economic capacity indicator	Hangzhou, Philippine
	Waterbody and Vegetation Coverage Proportion	Environmental resources	
	Access to Medical Resources	Proximity to medical facilities	
	Air Conditioning Use and CO2 Emissions	AC use and related environmental impact	Lancet Countdown (Europe)
	Labour Supply in Temperature-Sensitive Sectors	Labour data in sectors like agriculture	Lancet Countdown (Europe)
	Heat Impacts on Economic Activity	GDP growth in relation to temperature anomalies	

2.2.5 Interventions in the urban context

Mitigating risk from heat requires strategic planning and the implementation of effective interventions. From a literature review on urban heat mitigation, among the most cited strategies is the enhancement of urban vegetation (Keith et al., 2020). This includes not only the addition of green spaces, such as urban forestry, green roofs, and parks but also an increase of surface reflectivity using materials with higher albedo. Studies (Dhalluin & Bozonnet, 2015; Guindon & Nirupama, 2015) have highlighted the role of vegetation in providing shade and evaporative cooling, which are essential for reducing surface and air temperatures.

In addition to greening, improving building and infrastructure standards is a critical component of heatwave mitigation (Table 2–3). The adaptation of building codes and enhancing urban designs to incorporate heat-resilient materials, the use of reflective and lighter-coloured materials in construction (Guindon & Nirupama, 2015; Stone et al., 2013; Zaidi & Pelling, 2015) and architecture can play a significant role in reducing heat (Hamilton et al., 2015). Change of urban morphology is also a category of interventions that often considered by city planners through land use configurations or urban form for reducing UHI effect (Steeneveld et al., 2011; Yang et al., 2023).

Implementation of heat action plans, which have shown promising results in reducing heat-related mortality and morbidity. These plans typically include establishing early warning systems, informative campaigns, and

mobilizing healthcare professionals, volunteers, and social workers to manage and survey vulnerable populations such as older adults and those with chronic conditions (Keith et al., 2020).

Table 2–3 Summary of potential interventions from Keith et al. (2020)

Category	Description
Vegetation	Increasing vegetation as a heat resilience design strategy, including urban forestry, green roofs, and parks.
	Urban canopy for increased shade and evaporative cooling, with context-specific effectiveness.
Buildings and Infrastructure	Improved building and urban infrastructure standards for heat mitigation.
	Energy efficient buildings and the recommendation for low energy cooling systems.
	Use of reflective and lighter-coloured materials in construction for UHI effect reduction.
Land Use and Urban Form	Land use configurations and urban form for reducing UHI effect.
Implementation of heat action plan	Establishing early warning systems, informative campaigns, and mobilizing healthcare professionals, volunteers, and social workers to manage and survey vulnerable populations.

2.3 Heat-related health impact in Dutch urban area

2.3.1 Health impacts of heat stress

Extreme heat weather significantly overwhelms the body's ability to regulate heat, leading to various health issues collectively known as heat stress. Heat stress has significant public health implications, ranging from mild to potentially fatal conditions. Common mild symptoms include lack of concentration, headaches, and fatigue (RIVM, 2024). Severe health issues, such as heat cramps, heat exhaustion, and heat stroke, can arise, particularly in the older adults and those with physical or mental impairments, who are at higher risk of mortality (RIVM, 2024). Heat stroke is a medical emergency requiring immediate intervention. Additionally, heat stress can negatively impact mental health, increasing rates of suicide, stress, and aggression (RIVM, 2024).

2.3.2 Thermal comfort

Thermal comfort (Kleerekoper, 2016) refers to the condition of mind that expresses satisfaction with the surrounding environment. It is influenced by various factors, including air temperature, humidity, wind speed, and radiation. Ensuring thermal comfort, both indoors and outdoors, is crucial for mitigating heat stress and protecting public health.

2.3.2.1 PET mapping for outdoor thermal comfort

Physiological Equivalent Temperature (PET) (Höppe, 1999) is an index used to assess outdoor thermal comfort by combining meteorological data to reflect the thermal perception of the human body. PET maps visually represent areas of thermal comfort or discomfort, aiding in urban planning and public health strategies to mitigate heat stress (Koopmans et al., 2020). PET calculations consider several factors, including air temperature, humidity, wind speed, radiation, and individual human characteristics and activities. For instance, the calculation might involve a 35-year-old male, 1.75m tall, weighing 75kg, with a clothing insulation value of 0.9, walking at a speed of 4 km/h (Koopmans et al., 2020). The PET method integrates multiple environmental factors. Air temperature directly influences the body's heat balance, while

humidity affects the body's ability to cool down through sweating. Wind speed enhances convective heat loss, and solar radiation impacts the heat load on the body. The sky view factor, representing the amount of visible sky from the ground, influences long-wave radiation loss. Additionally, the Bowen ratio, which indicates the ratio of sensible to latent heat fluxes, varies with surface characteristics like water bodies and vegetation, affecting local climate conditions. It could help to guide the implementation of interventions such as increasing green spaces, providing shaded areas, and improving urban design to enhance outdoor thermal comfort.

2.3.2.2 Warm nights and indoor comfort

Warm nights, where temperatures remain high, significantly affect indoor thermal comfort. High nighttime temperatures can disrupt sleep and increase the risk of heat-related health issues, as people typically stay indoors during the night. Addressing indoor comfort involves improving building insulation, ventilation, and cooling strategies to ensure a safe and comfortable indoor environment during heatwaves. Effective measures include installing better insulation materials, using energy-efficient cooling systems, and ensuring proper ventilation to reduce indoor temperatures and enhance thermal comfort during warm nights (RIVM, 2024).

2.3.3 Vulnerable groups

Heatwaves disproportionately affect certain vulnerable groups, making it crucial to identify and address their specific needs. RIVM (2024) identified the following Table 2–4:

Table 2–4 Potential vulnerable groups affected by heat

Group	Effects	Reasons
Older populations (>75 years)	Vulnerable to heat-related health effects.	Older adults with frail health are particularly susceptible during heatwaves due to their reduced ability to cool down and sense thirst.
Children and Infants	They also rely on adults for hydration and cooling.	Young children and infants have underdeveloped thermoregulatory systems and rely on adults for proper care during heatwaves.
Socially Isolated Individuals	Social isolation significantly increases vulnerability to heat.	Older adults living alone or in poorly ventilated homes are less likely to seek help or be noticed when experiencing heat stress.
People with limited mobility	Difficulty accessing cooler areas during heatwaves.	People with limited mobility face challenges in finding cool spots during heatwaves.
People with severe obesity	Increased risk of heat-related health issues.	Excess body weight can hinder the body's ability to regulate temperature effectively, leading to an increased risk of overheating and related health complications.
Outdoor Workers and Athletes:	Those who work or exercise outdoors face higher risks due to prolonged exposure to heat. This group includes construction workers, farmers, and athletes	They are often engaged in strenuous activities that increase body temperature and fluid loss through sweating.

Pregnant Women	Heat exposure can lead to adverse pregnancy outcomes, including dehydration and preterm labour.	They are susceptible to heat stress due to increased body temperature and metabolic rate during pregnancy.
People with Chronic Conditions	Individuals with chronic conditions such as cardiovascular, respiratory, and renal diseases are highly susceptible to heat stress.	These conditions can be aggravated by high temperatures, leading to severe health complications. For example, heart conditions may be exacerbated due to increased strain on the cardiovascular system, while respiratory issues can be worsened by hot and humid conditions.
Homeless People	They may not recognize and respond to heat stress effectively.	Homeless individuals may lack of access to cool environments and clean drinking water.

3 STUDY AREA AND METHODOLOGY

3.1 Study area

This research is centred on assessing the risk of heatwaves at a local scale within the Dutch City of Enschede. Pilot studies on heat mapping and the implementation of heat action plans have been explored in cities such as Amsterdam (Van Der Hoeven & Wandl, 2015), The Hague (Bergh et al., 2022), and Rotterdam (Van Der Hoeven & Wandl, 2018). Enschede was selected as the case study area for this research due to, as far as we are aware, the local heatwave risk assessment still being in a developmental stage of research there.

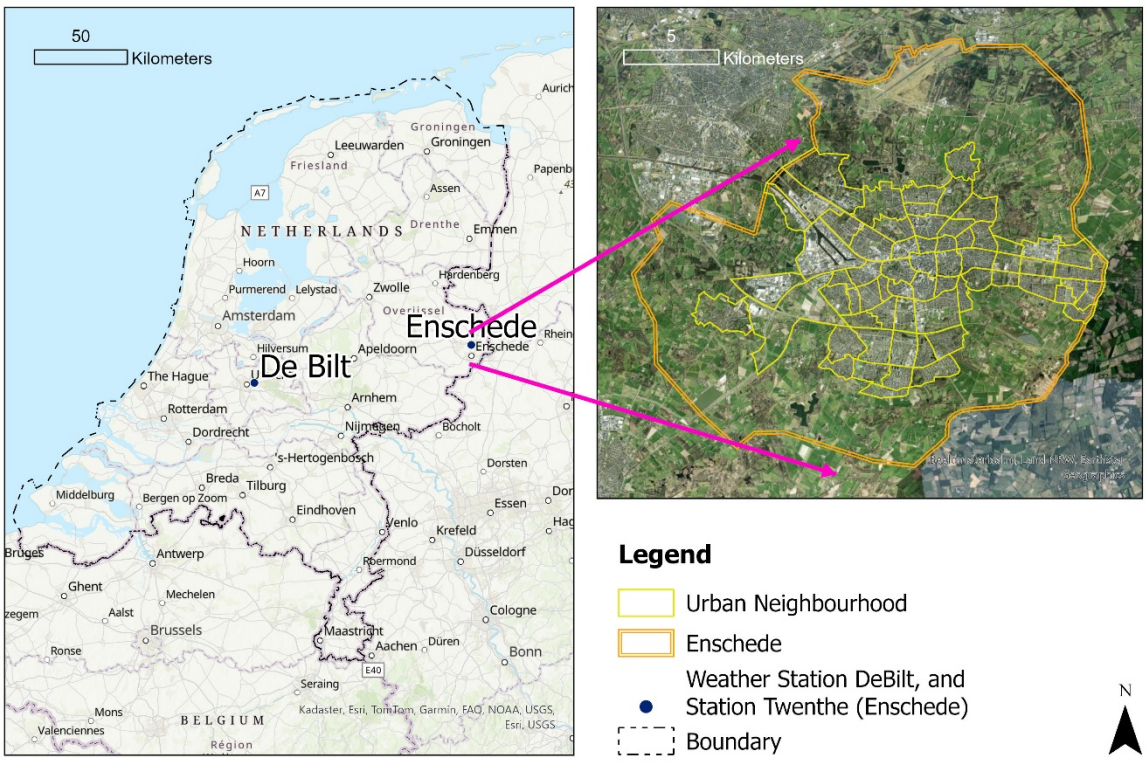

Figure 3–1 Study area

3.2 Heat risk framework

Heat risk will be evaluated through three components: hazard, exposure, and vulnerability, as described in section 2.2.4.

Hazard will be evaluated through the temperature-based heatwave definition, considering the consistency of data availability between temperature and other relevant meteorological or physiological. The heatwave hazard will be assessed though a time series analysis, identifying the frequency, duration, intensity of heatwave events. This analysis will identify the nature of heatwave events experienced in Enschede from 2000 to 2022 and compare the result with heatwave events identified based on De Bilt temperature observation.

Exposure is defined as "the presence of people, livelihoods, species or ecosystems, environmental functions, services, resources infrastructure, or economic, social, or cultural assets in places and settings that could be adversely affected"(IPCC, 2023). Hence, it refers to the elements in the area impacted by the hazard. As stated in section 1.3, this thesis focuses on heat-related health and livability issues, specifically considering intra-urban heat stress and population densities.

Vulnerability is "the propensity or predisposition of an element exposed to extreme events to be adversely affected" (IPCC, 2023), involving sensitivity to the hazard and the elements or systems lacking capacity to cope with the adverse effects of climate change. It involves both sensitivity and adaptive capacity. Sensitivity involves the vulnerable group (the older adults, people with low socio-economic status, the group with health issues). Adaptive capacity includes greenspace availability and cooling space accessibility.

3.3 Overview of Methodology

This research framed the risk assessment for Enschede at two different scales, regional scale and neighbourhood scale. Hazard was assessed through spatial and temporal analyses of heatwave characteristics. Exposure was assessed through investigating intra urban heat stress and population density. Vulnerability was evaluated based on sensitivity and adaptive capacity. The risk composite is combing exposure and vulnerability indicators through Spatial Multi-criteria Decision analysis (MCDA).

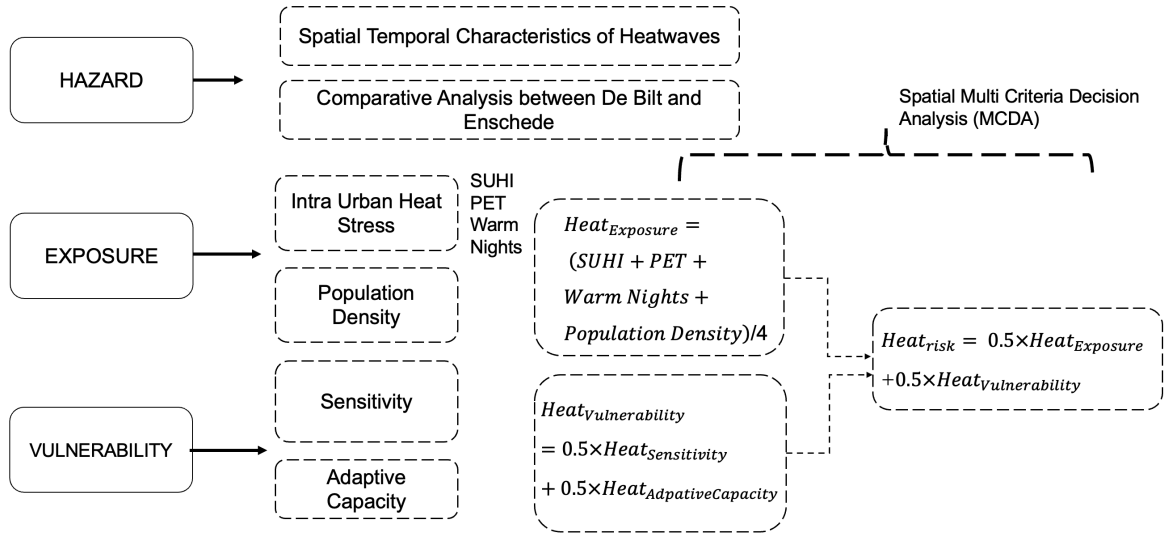

Figure 3–2 Overall risk assessment framework

4 RO1: HOW DO CHARACTERISTICS OF HEATWAVES VARY SPATIALLY AND TEMPORALLY IN THE NETHERLANDS?

Several heatwave characteristics (Table 2–1) and definitions exist (McGregor et al., 2015). In the Netherlands heatwaves are defined by data recorded at the De Bilt station, which is located in the middle of the country, just outside of Utrecht. In the Netherlands, a heatwave is defined as *a period of at least five consecutive days with a maximum air temperature of 25°C or higher, with at least three of those days having a tropical temperature of 30°C or above* (Hagens & van Bruggen, 2015). Thus, the objective of the first research question was to examine heat risks in the Netherlands and examine how heat risks vary across the country and, since Enschede is located approximately 115 km Northeast of De Bilt, determine if there are differences in temperatures between station De Bilt and station Twenthe (Enschede). To do so heatwaves between the De Bilt station and the local weather stations for the Netherlands were examined. A spatial and temporal analysis of heatwave events nationwide was first explored, followed by a comparative analysis between De Bilt and Twenthe station.

4.1 Methods and data

An overview of the methods used are provided in Figure 4–1:

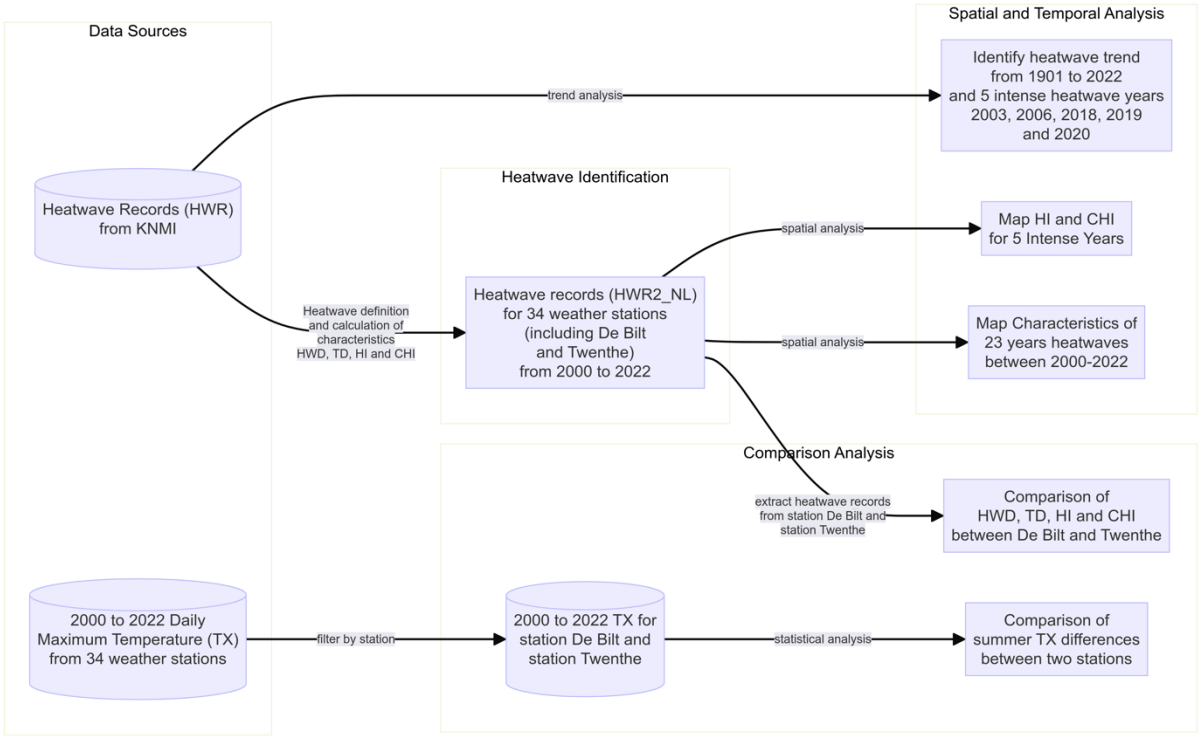

Figure 4–1 Flowchart of methods for RO1

4.1.1 Data Summary

For this study a variety of datasets were used and are summarised in Table 4–1.

Table 4–1 Summary of data used to evaluate heatwaves in the Netherlands.

Name	Data	Source
Daily Maximum Temperature (TX)	Daily maximum temperature TX observations from weather stations from 2000 to 2022	(KNMI, 2023a)
Heatwave records (HWR)	KNMI heatwave records identify from 1901 to 2022	(KNMI, 2023b)

Daily Maximum Temperature (TX) was used to identify heatwave occurrences in the Netherlands. TX records were obtained for 34 stations in the Netherlands. These 34 stations were selected from 51 stations because they are current operational automatic weather stations with TX records. Due to weather station relocations, decommissioning or change of observation method (KNMI, 2023a), not all weather stations had continuous and homogenous data (see Appendix 9.1 for further details). Among the 34 inland automatic weather stations, station 215 Voorschoten has data since July 15th, 2014; Station 257 Wijk aan Zee since April 30th, 2001 and Station 323 Wilhelminadorp has data since December 15th, 2017. All the other stations had complete daily temperature records from 2000 to 2022. For the purpose of this study, data were obtained from 2000 to 2022 for the summer months of June 1st to September 30th. A total number of N=2806 daily temperature records were obtained for each station, except the previous mentioned three stations. The three stations datasets were kept in the data collection and heatwave records identification process. They were handled separately in the subsequent analyses.

KNMI's 34 inland automatic weather stations are illustrated in Figure 4–2.

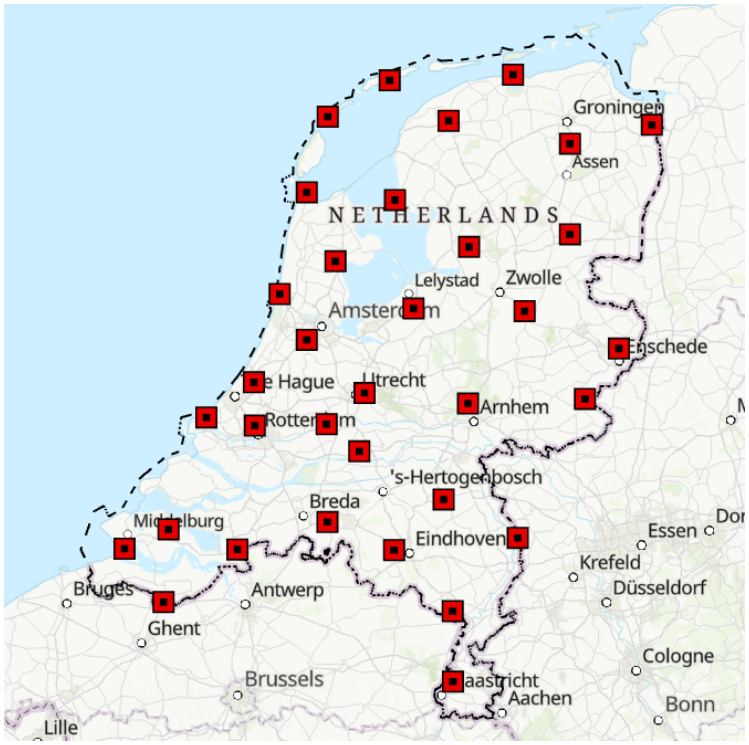

Figure 4–2 Location of the 34 weather stations selected

Heatwave records (HWR): The KNMI has recorded heatwave events for the Netherlands based on daily TX observations at the De Bilt station from 1901 to 2022 (For this study a variety of datasets were used and are summarised in Table 4–1.

A total of 30 events were recorded for the Netherlands. For each heatwave, a number of heatwave characteristics are available that include the start and end date, duration in days (HWD), the number of tropical days (with daily maximum temperatures (TX) of 30.0°C or higher) (TD), the highest recorded TX temperature (HI), the date of this highest temperature, and a cumulative heatwave intensity (CHI) number (KNMI, 2023b). The CHI was derived by summing all TX above 25°C during the heatwave. Each of these characteristics are defined below (Eq 4b-4e).

Heatwave event $HWEvent\_NL$ is defined as:

$$HWEvent\_NL = \sum_{i=0}^{N-1}\left(\left(\sum_{j=i}^{i+4} T_j \geq 25℃ \geq 5\ days\right) \cap \left(\sum_{k=i}^{i+4} T_k \geq 30℃ \geq 3\ days\right)\right) \qquad Eq\ 4\text{–}a$$

Where a heatwave event ($HWEvent\_NL$) was identified when:

for 5 consecutive days from day $i=1...N$, temperature $T_j \geq 25℃$ $\left(\sum_{j=i}^{N-1} T_j \geq 25℃ \geq 5\ days\right)$, and

for at least 3 days from day $i=1...N$, temperature $T_k \geq 30℃$. $\left(\sum_{k=i}^{N-1} T_k \geq 30℃ \geq 3\ days\right)$

The *HWEvent_NL* counts the heatwave days from a start date day i. The outputs for each heatwave event were then used to calculate the following corresponding heatwave characteristics:

Heatwave Duration (HWD): The length of heatwave days per year. It was used to assess the frequency and severity of heatwaves over time.

$$HWD = \sum_{i=1}^{N}(TX_i \geq 25℃) \qquad Eq\ 4\text{–}b$$

Tropical Days (TD): Defined as numbers of days with maximum daily temperature TX ≥ 30 °C. It was used to assess severity of tropical days over time.

$$TD = \sum_{i=1}^{N}(TX_i \geq 30℃) \qquad Eq\ 4\text{–}c$$

Heatwave Intensity (HI): Highest TX temperature of the heatwave events.

$$HI = max\ (TX_i) \qquad Eq\ 4\text{–}d$$

Cumulative Heatwave Intensity (CHI): the CHI provided a combined index of heatwave intensity and duration, capturing not just the occurrence of a heatwave but also its cumulative severity over a series of days. To be consistent with the KNMI definition, it was calculated by adding all temperature values above 25°C per day for each heatwave event. A low CHI indicates low-intensity heatwaves, whereas a high CHI reflects high-intensity heatwaves.

$$CHI = \sum_{i=1}^{n}(TX_i - 25) \qquad Eq\ 4\text{–}e$$

4.1.2 Heatwave trends in the Netherlands 1901-2022 using current HWR at De Bilt

The heatwave events (HWR) were visualised from 1901-2022 to identify years with intensive heatwaves. The visualisation of HWRs involved two heatwave characteristics by year: Heatwave Intensity (HI) and the Cumulative Heatwave Intensity (CHI). For years with multiple heatwave events, the visualisation summarised the heatwave records by year, showing the highest HI and summed up CHI were calculated by year.

Based on the findings from this temporal analysis, five intensive heatwave years between 2000 and 2022 were selected for further analysis. The years with CHI exceeding 67.4 (the CHI value of 2003) were selected. This threshold was chosen because 2003 was recorded as a year with atypical heatwave event, which caused thousand deaths (De Visser et al., 2022).

4.1.3 Spatial Patterns of Heatwaves for 34 weather stations in Netherlands

4.1.3.1 Heatwave events from 34 weather stations between 2000 and 2022

A Python script was developed to identify heatwave periods, and to compute the heatwave characteristics HWD, TD, HI and CHI using the TX datasets referred in 4.1.1. The script involves the following steps:

To successfully identify heatwave records for each station (N=34),

- The TX dataset was firstly classified by each station and then sorted by date.
- Next, each heatwave event was identified using Eq 4-a. The start date, end date of each heatwave event period was recorded.
- For each heatwave event, the heatwave characteristics were calculated using Eq 4-b, 4-c, 4-d, 4-e

These heatwave events dataset, referred to as **HWR2_NL** then served as inputs for the following analyses.

4.1.3.2 Spatial patterns of heatwaves in Netherlands between 2000 and 2022

The spatial distribution of heatwaves between 2000 and 2022 across the Netherlands were mapped using HWR2_NL. Of the three stations with data available at different time span to the other stations, after further investigation, station 215 and station 323 were removed. Station 257, with data starting from April 30th, 2001, was kept in the analysis as there was no heatwave identified in 2000. Thus, a total of 367 heatwave events were identified.

The total number of heatwave events were summarised by station. For the following characteristics, the mean duration (Heatwave Duration (HWD)) and total number of Tropical Days (TD) were calculated. For the Highest Temperature (HI) and Cumulative Heatwave Intensity (CHI) the mean and maximum values were calculated. These summaries were then used to create surfaces to show the mean duration of heatwaves, locations with the highest number of tropical days, hottest and most intense temperatures. The Inverse Distance Weighting (IDW) method was used. A power parameter of 2.0 was used with a search radius of 12 neighbouring points. The surfaces were created with an output cell size of 1km. All analyses were conducted in ArcGIS Pro.

4.1.3.3 Spatial patterns of heatwaves during intense heatwave years 2003, 2006, 2018, 2019, and 2020

HWR2_NL was used in this spatial analysis, and records from five intense heatwave years were extracted from HWR2_NL. The five years identified through the temporal analysis in section 4.1.2, were further analysed to examine spatial variations of intense heatwaves. These included years 2003, 2006, 2018, 2019, and 2020. For each of the stations, the yearly summed CHI and highest HI were mapped. The three stations (215, 323 and 257) were included in this analysis as heatwave events were recorded during these five intense heatwave years. CHIs were mapped as points identified at each station, while the HIs from the 34 stations were interpolated as continuous surfaces. The Inverse Distance Weighting (IDW) method was used in ArcGIS Pro, using power parameter 2.0, with search radius of 12 neighbouring points and output cell size 1km.

4.1.4 Comparison of heatwaves between De Bilt and Twenthe (Enschede) during 2000 and 2022

Since official heatwave events are typically based on temperatures recorded in De Bilt and given that Enschede is approximately 115 km northeast of De Bilt, a comparison was conducted to determine if differences between De Bilt and Enschede existed. For this analysis, the temperatures recorded at Station Twenthe will represent those of Enschede.

The heatwave events for Enschede, based on the Station Twenthe record (total number of records N=16), were extracted from the HWR2_NL results obtained in 4.1.3.1. Similarly, the heatwave events for the De Bilt Station (total number of records N=14) were extracted.

For each station a descriptive analysis was conducted that captures the Heatwave Duration (HWD), Tropical Days (TD), Heatwave Intensity (HI), and Cumulative Heatwave Intensity (CHI) was calculated for years 2000 to 2022 and compared visually.

4.1.5 Variation of summer temperature (TX) between De Bilt and Twenthe (Enschede)

When temperatures are close to these critical thresholds that define a heatwave, 25°C for a standard heatwave day and 30°C for a tropical day, even small changes can affect whether a day is classified as part of a heatwave or not, influencing the overall heatwave event count and characterisation at each station. To

further investigate this issue, variation of temperatures between De Bilt and Twenthe were conducted. Normality checks indicated that the data did not follow a normal distribution Table 4–2, therefore a non-parametric Wilcoxon signed-rank test was used to test if the temperatures between the two stations differed.

Two analyses were conducted using daily TX:

- The first analysis used all of the data for the summer, named the Full Summer Dataset. The Full Summer Dataset covers the entire summer season including June 1st until September 30th from 2000 to 2022 (total number of summer days = 2806).
- The second analysis used TX temperatures greater or equal to 25°C, the threshold temperature used to define a heatwave in the Netherlands. Data were obtained from 2000 to 2022 and referred to as the TX over 25°C (total number of TX>25°C, days =715). The High-Temperature Dataset focuses on days where the TX exceeded 25°C from the Full Summer Dataset at either De Bilt or Twenthe stations.

Several visualisation methods were employed to illustrate the TX differences between the two stations. Scatter plots were used to compare the TX between De Bilt and Twenthe, with points above the diagonal line indicating higher TX at the y-axis station compared to the x-axis station. Boxplots by station depicted the overall distribution of TX differences for each data series.

Table 4–2 Statistical test of TX differences (Twenthe – De Bilt) from 2000 to 2022

	Full Summer Dataset (June 1st until September 30th)	TX over 25°C
Shapiro-Wilk normality test p value	4.75E-22	2.04E-10
Total number of records	Total N = 2806	Total N = 715

4.2 Results

4.2.1 Temporal pattern of heatwave events in the Netherlands 1901-2022 using current HWR at De Bilt

In the Netherlands, a total of 30 heatwave events were recorded between 1901 and 2022, see Figure 4–3. There have been 14 heatwaves recorded since 2000. Table 4–3 shows the descriptive analysis of heatwave records. The average highest temperature(HI) during heatwaves was 33.2°C, with a maximum recorded temperature of 37.5°C in 2019. Heatwaves lasted an average of 9.17 days (HWD), with tropical days (TD) averaging 4.43 days per event. The Cumulative Heatwave Intensity (CHI), indicating yearly summed up heatwave severity, averaged 43.49, with a peak value of 96.3.

Table 4–3 Descriptive statistics of heatwave records

	HI(°C)	**HWD (Days)**	**TD (Days)**	**CHI (°C)**
mean	**33.20**	**9.17**	**4.43**	**43.49**
std	1.52	3.63	1.92	19.37
min	31.1	5	3	24
25%	32.2	7	3	29.7

50%	32.8	8	4	36.6
75%	34.05	10	5	48.28
max	**37.5**	18	10	**96.3**

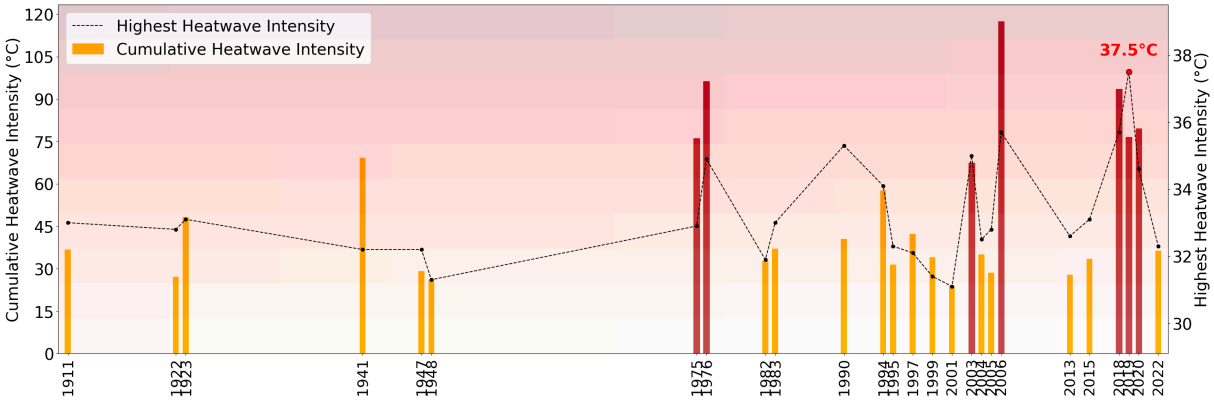

Figure 4–3 Heatwave events in the Netherlands summed by year from 1901 to 2022. from 1901 to 2022. Red bars highlight the notable hot years with a yearly CHI over 67.4 (CHI of year 2003)

Figure 4–3 captures heatwave patterns in the Netherlands across a century, showing both the HI and CHI. The dotted line shows the highest HI for each event, with the peak at 37.5°C in 2019. The bars represent the CHI for all the individual heatwave events for that year. The red bars highlighted the hotter years with yearly CHI over 67.4. Since 1975, the frequency of heatwave events has increased. The yearly total CHI ranged from 24 to 117.5 with an average of 50.18. The CHI captured the duration and intensity of a heatwave event. Notable years included 1975, 1976, 2003, 2006, and the consecutive years of 2018, 2019 and 2020 (red bars, Figure 4–3).

4.2.2 Spatial Patterns of Heatwaves for 34 weather stations in Netherlands

4.2.2.1 Spatial patterns of heatwaves during intense heatwave years 2003, 2006, 2018, 2019, and 2020

The spatial distribution of heatwaves characteristics across the Netherlands are shown in Figure 4–4 for the years 2003, 2006, 2018, 2019, and 2020. The HI, shows the highest TX found at each station in each year, ranging from 30°C (light yellow) to 40°C (dark red). The CHI of all the heatwave records at each station represented by dots on each map ranged from 22-40 (smaller dots) to 191-225 (larger dots).

Table 4–4 shows that not all 34 stations consistently recorded heatwave events each year, with the highest number of events recorded in 2019. In 2003, 23 stations recorded 24 heatwave events. In 2006, 26 stations reported 36 heatwave events. Similarly, in 2018, 26 stations observed 29 heatwave events. In 2020, 31 stations recorded a total of 35 heatwave events.

Table 4–4 Summary of heatwave records for year 2003, 2006, 2018, 2019 and 2020

	2003	**2006**	**2018**	**2019**	**2020**
Number of stations having heatwave events	23	26	26	34	31
Total number of heatwave events	24	36	29	62	35

Generally, higher HI are consistently observed in the southern and eastern parts of the country. These regions, marked in darker red, experienced more extreme heat compared to northern and coastal areas, with temperature 2°C to 4°C higher than De Bilt. Conversely, the northern and coastal regions are cooler, with temperatures often 2°C to 6°C lower than those in De Bilt, represented by lighter colours on the maps.

The years 2018 (Figure 4–4c) and 2019 (Figure 4–4d) stand out with particularly severe and widespread heatwave conditions. In 2019, southern regions experienced some of the highest temperatures recorded, with HI values reaching up to 39°C to 40°C. On 25th July 2019, De Bilt recorded its highest temperature of 37.5°C, while Gilze-Rijen reached a national record for the hottest day to date with a temperature of 40.7°C. In Enschede, within our study area, a temperature of 40.2°C was recorded. Similarly, 2018 saw high temperatures and intense CHI, reflecting widespread and longer heatwave conditions which affected broad area across the country.

Overall, Enschede, located inland, is depicted by these darker zones in the figures, signifying that it experiences higher HI than De Bilt during these identified periods of extreme heat. The variation in CHI is not clearly visible except in year 2018.

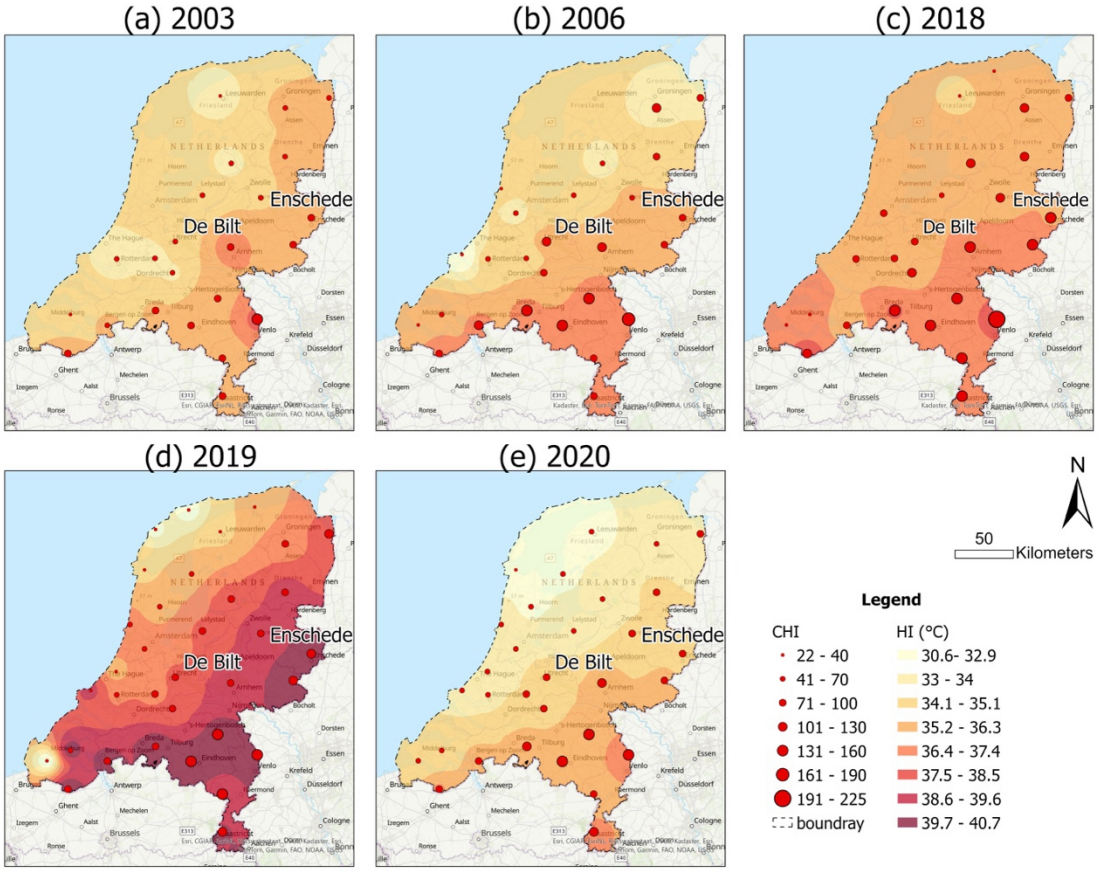

Figure 4–4 Spatial distribution of CHI and HI in 2003, 2006, 2018, 2019 and 2020

4.2.2.2 Spatial patterns of heatwaves in Netherlands between 2000 and 2022

There were 367 heatwave events identified in the 32 weather stations from 2000 to 2022. The HWR duration ranged from 6.01 to 11.73 days (Figure 4–5a), the number of tropical days varied between 3.01 and 6.13

days (Figure 4–5b), the average HI ranged from 32.21°C to 35.1°C (Figure 4–5c), and the mean CHI spans from 26.31°C to 59.73°C (Figure 4–5d). Similar to Figure 4–4, the east and southern part of the Netherlands generally experience more frequent and intense heatwaves. Enschede is located in a hot zone with, on average, the longest number of tropical days, relatively longer average heatwave durations and comparatively higher HI and CHI while De Bilt resides in a comparatively milder heatwave zone.

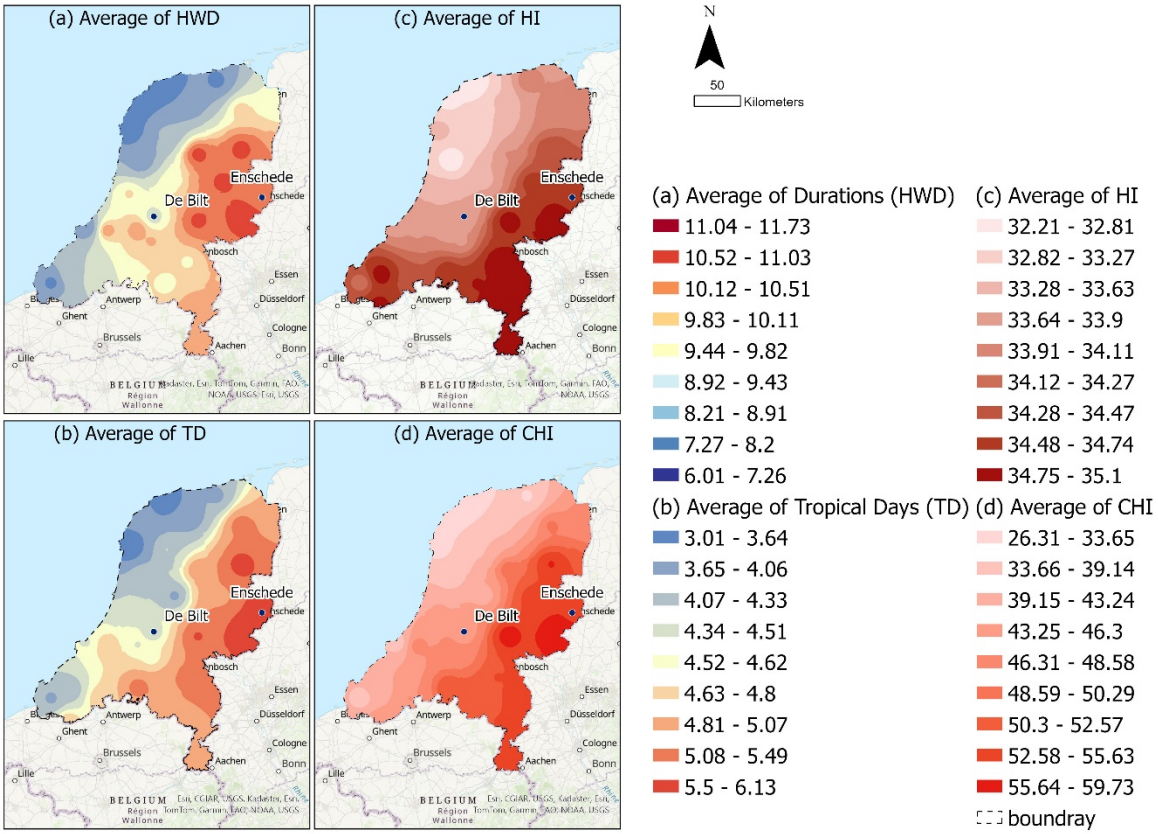

Figure 4–5 Spatial distribution of heatwave characteristics between 2000 and 2022

4.2.3 Comparison of heatwaves between De Bilt and Twenthe (Enschede) during 2000 and 2022

In total, during 2000 to 2022, 16 heatwave events were identified for Station Twenthe (Enschede), compared with 14 heatwave events for De Bilt (Table 4–5). Table 4–5 shows the summary of heatwaves and characteristics between Twenthe and De Bilt. Station. Twenthe recorded higher average values for the CHI (55.2) and maximum temperature (30.7°C) compared to De Bilt, which had a CHI of 44.3 and a maximum temperature of 29.3°C. Additionally, the mean duration of heatwaves and the average number of tropical days were also greater in Twenthe, at 10.5 days and 5.8 days respectively, compared to De Bilt's 9.1 days and 4.4 days.

Table 4–5 Summary heatwaves between station De Bilt and Twenthe

2000-2022	Twenthe	De bilt
Total no. Events	16	14
Time of year	June-August	June-August
Mean CHI	55.2	44.3

Mean duration	10.5	9.1
Mean number TD	5.8	4.4
Mean TX	30.7	29.3

Figure 4–6 shows the variations in heatwave duration between De Bilt and Twenthe. Discrepancies are highlighted by the grey bars. For example, station Twenthe recorded a heatwave in 2015 which was not recorded for the De Bilt. Additional events included 2008, 2010, 2014, and 2021 which were exclusive to Twenthe. Table 4–6 summarises the differences between the heatwave events recorded at both stations. Specifically, there were 4 events where heatwaves in Twenthe matched the duration of those in De Bilt, 1 event in Twenthe was shorter in duration than the corresponding event in De Bilt, and 5 events in Twenthe lasted longer than those in De Bilt. Additionally, 4 heatwaves were recorded in De Bilt that did not occur in Twenthe, while 6 heatwaves were recorded in Twenthe that did not occur in De Bilt.

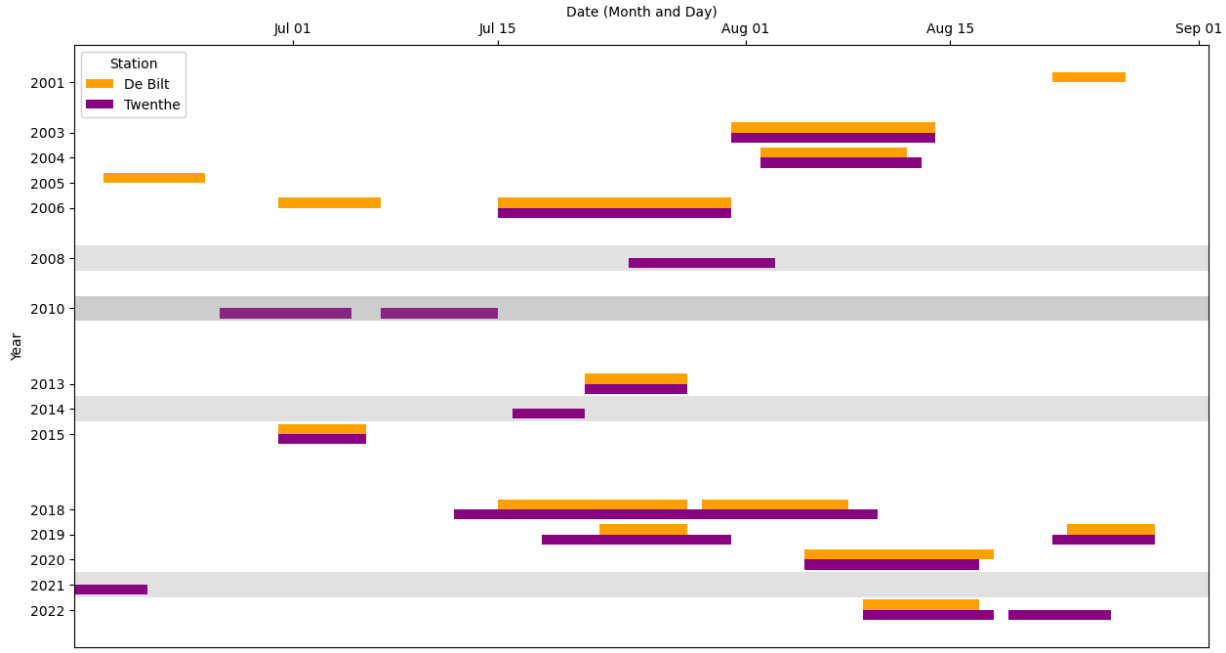

Figure 4–6 Heatwave events between 2000 and 2022 for De Bilt and Twenthe between June and September. Grey bars show years where heatwave events are only identified in Twenthe.

Table 4–6 Summary of discrepencies at both stations

	Same as De Bilt	Shorter than De Bilt	Longer than De Bilt	Heatwave at De Bilt but not at Enschede	Heatwave at Enschede but not at De Bilt
Number of heatwave events at Twenthe	4	1	5	4	6

Figure 4–7 (a) and (b) further illustrates that Twenthe records more frequent and extended heatwave events as well as tropical days than De Bilt. Figure 4–7 (c) and (d) also shows that Twenthe records consistently higher HI and CHI values than De Bilt. Figure 4–7 (c) shows maximum temperatures vary by 3°C in 2015 and 2.7°C 2019. In Figure 4–7 (d), the gaps in CHI for the years 2003, 2006, 2018, 2019 indicate not only longer durations but also more severe heat conditions at Twenthe. These trends showcase that Twenthe may be experiencing more intense heatwave events than those recorded in De Bilt.

Figure 4–7 (a)HWD, (b) TD, (c) HI and (d) CHI for De Bilt and Twenthe, the purple is the trend line for Twenthe while yellow line is for De Bilt

4.2.4 Variation of summer temperature (TX) between De Bilt and Twenthe (Enschede)

Scatter plots of TX temperatures for De Bilt and Twenthe are shown in Figure 4–8. Figure 4–8a showed that temperatures recorded on most days were closely aligned or above the diagonal line, indicating that on most summer days, the temperatures at the station on the Twenthe were close to those recorded at De Bilt. When TX was greater than 25°C (Figure 4–8b), some TX variability between the two stations was observed, suggesting that there was more variability between the two stations on hotter days.

In Figure 4–9 and Table 4–7, the range of TX differences between Station Twenthe and De Bilt are summarised. They ranged from -6.8 to 7.3°C and -4 to 7.3°C in the two series, the full summer datasets (June 1st to September 30th) and TX over 25°C, respectively. The mean and median of TX differences also varied. The average TX difference was 0.43°C for the full summer datasets and 1.09°C for TX over 25°C. The median TX difference for the summer datasets was 0.4°C during the full summer datasets, while it was 0.9°C for TX over 25°C.

Table 4–7 also summarises the results of the statistical test of the significance of the variation in TX between the two stations. The non-parametric Wilcoxon signed-rank test was implemented, revealing very small p-values (less than 0.05) for both datasets. Considering that the mean differences in temperatures for all datasets were positive, it suggests that Enschede experienced significantly higher temperatures than De Bilt during the analysed periods. The varied TX differences from two data series, the full summer datasets (June

1st to September 30th) and TX over 25°C , indicate that when TX was over 25°C, there were significantly greater differences between the two stations, with Enschede being notably hotter than De Bilt.

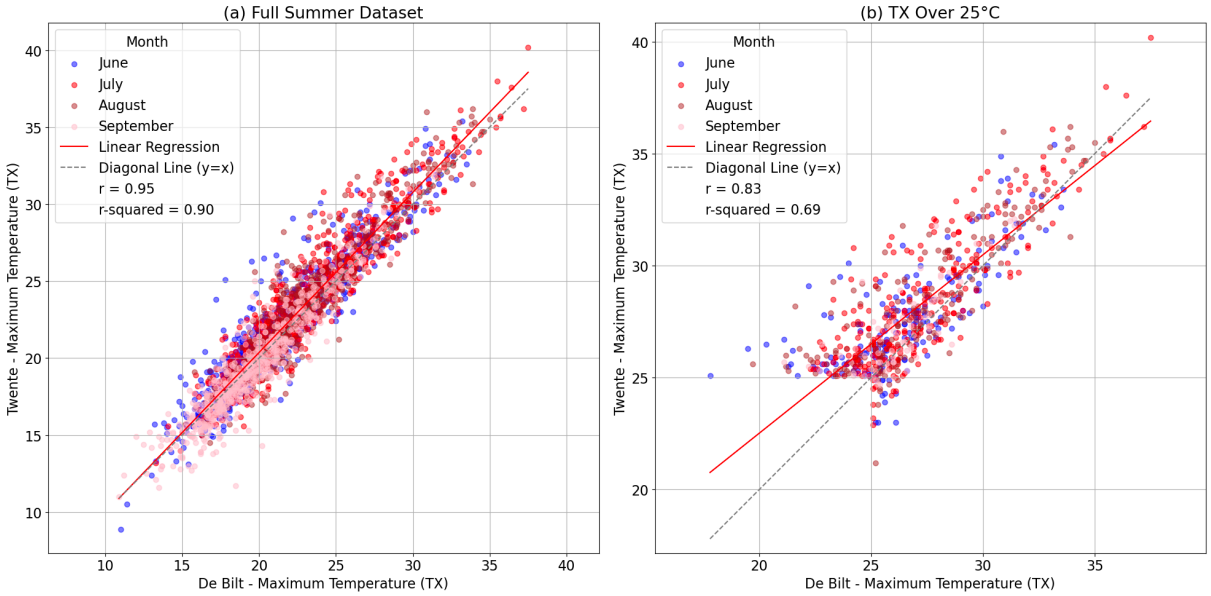

Figure 4–8 Scatter plots of TX at two stations using two TX series

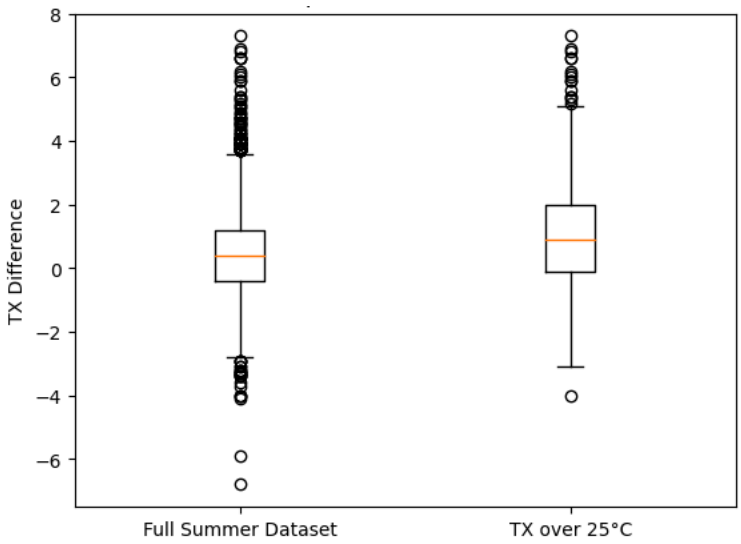

Figure 4–9 Distribution of TX differences for the two data series

Table 4–7 Statistical test and summary of TX differences (Twenthe – De Bilt)

	Full Summer Dataset	**TX over 25°C**
Total number of records	Total N = 2806	Total N = 715
Wilcoxon signed rank_test_stat	1239161	40888
p_value	2.52E-51	9.98E-53
min_TX differences	-6.8	-4

max_TX differences	7.3	7.3
mean_TX differences	0.43	1.09
median_TX differences	0.4	0.9

4.3 Conclusion

In general, the southern and eastern regions of the Netherlands have generally experienced more frequent and severe heatwaves. Enschede, being particularly prone to heat, has encountered more intense and prolonged heatwaves compared to De Bilt, due to its higher summer temperatures. A total of 16 heatwaves were identified in Enschede based on the KNMI heatwave definition, with 14 of these occurring in De Bilt. The years 2018, 2019, and 2020 experienced consecutive intense heatwave events, including an atypical heatwave in 2019, during which Enschede recorded the highest Heatwave Intensity of 40.2°C.

5 RO2: WHO IS AT RISK TO HEATWAVES IN ENSCHEDE? WHERE ARE THE RISK AREAS IN ENSCHEDE?

This research employed a risk framework consisting of hazard, exposure, and vulnerability components as discussed in section 2.2.4. Heat-health risk is understood as the potential for adverse health outcomes due to extreme heat events, which are becoming increasingly frequent and intense due to climate change. The risk framework aimed to investigate how various factors influence the risk of heat-related health impacts in urban settings. Due to the nature of heatwave definitions, it was not feasible to directly assess heatwaves at the intra-urban level. Therefore, this research framed the risk assessment for Enschede at two different scales, national scale and neighbourhood scale.

The extreme heat hazards were analysed in RQ1 (Chapter 4). The occurrence and characteristics of extreme heat events were identified and used for this analysis. A total of 5 heatwave events were recorded during three consecutive years (2018-2020); two events were recorded in 2018 (15-27 July and 29 July – 7 August), two events were recorded in 2019 (22 -27 July and 23-28 August) with one event recorded during 2020 (5-17 August) (Table 5–1). During 2019 the most intense heatwave was recorded with maximum temperatures reaching 40.2°C on July 25th (Table 5–1). Thus, for the purpose of this analysis July 25th was selected to perform city level analysis.

Table 5–1 Heatwave summary in station Twente during 2018 to 2020

Year	Heatwave Start	Heatwave End	HWD (days)	TD (days)	HI (°C)	Date of TX	CHI (°C)	No. Warm nights (TN>= 20°C)
2018	12-7-2018	9-8-2018	29	15	36.2	7-8-2018	145.7	2
2019	18-7-2019	30-7-2019	13	7	40.2	25-7-2019	77.7	2
2019	22-8-2019	28-8-2019	7	5	33.8	27-8-2019	37.5	0
2020	5-8-2020	16-8-2020	12	10	34.7	8-8-2020	83.3	2

**TX, maximum air temperature; TN, minimum air temperature*
**HWD: heatwave duration days; TD: tropical days; HI: heatwave intensity; CHI: cumulative heatwave intensity*

Since heat risk integrates three components: hazard, exposure, and vulnerability (*Heat Risk = Hazard × Exposure × Vulnerability*) Chapter 4 focused on hazard and this chapter focused on exposure and vulnerability at the neighbourhood level. Exposure was defined by the presence of populations and assets within areas affected by extreme heat, with particular attention given to intra-urban heat variation. Spatial variability in heat exposure across different neighbourhoods was primarily due to the Urban Heat Island (UHI) effects, with some areas experiencing more intense heat stress as a result of urban morphology and land use patterns.

Vulnerability was assessed by examining both sensitivity and adaptive capacity within Enschede's population. Sensitivity indicators included demographic and socio-economic factors such as age, health status, and income levels, which affected how different groups within the population responded to heat. Adaptive capacity, on the other hand, considered the availability of resources and infrastructure that enabled people's ability of coping with heat stress, including access to green spaces, water bodies, and cooling facilities. The study utilised data from sources like the Klimaat Effect Atlas (KEA), CBS, and RIVM to map these vulnerabilities at a neighbourhood level.

The final risk was combined by integrating exposure, and vulnerability indicators spatial multi-criteria decision analysis (MCDA), a method in heat risk assessment that combines multiple factors into a single index (Ho et al., 2015) . This chapter addressed the research questions: "Who is at risk to heatwaves in Enschede?" and "Where are the high-risk areas within the city?" This chapter aimed to provide a detailed understanding of heat-health risks among neighbourhoods in Enschede.

5.1 Methods and Data

An overview of the data and methods used for this analysis are generalised in Figure 5–1.

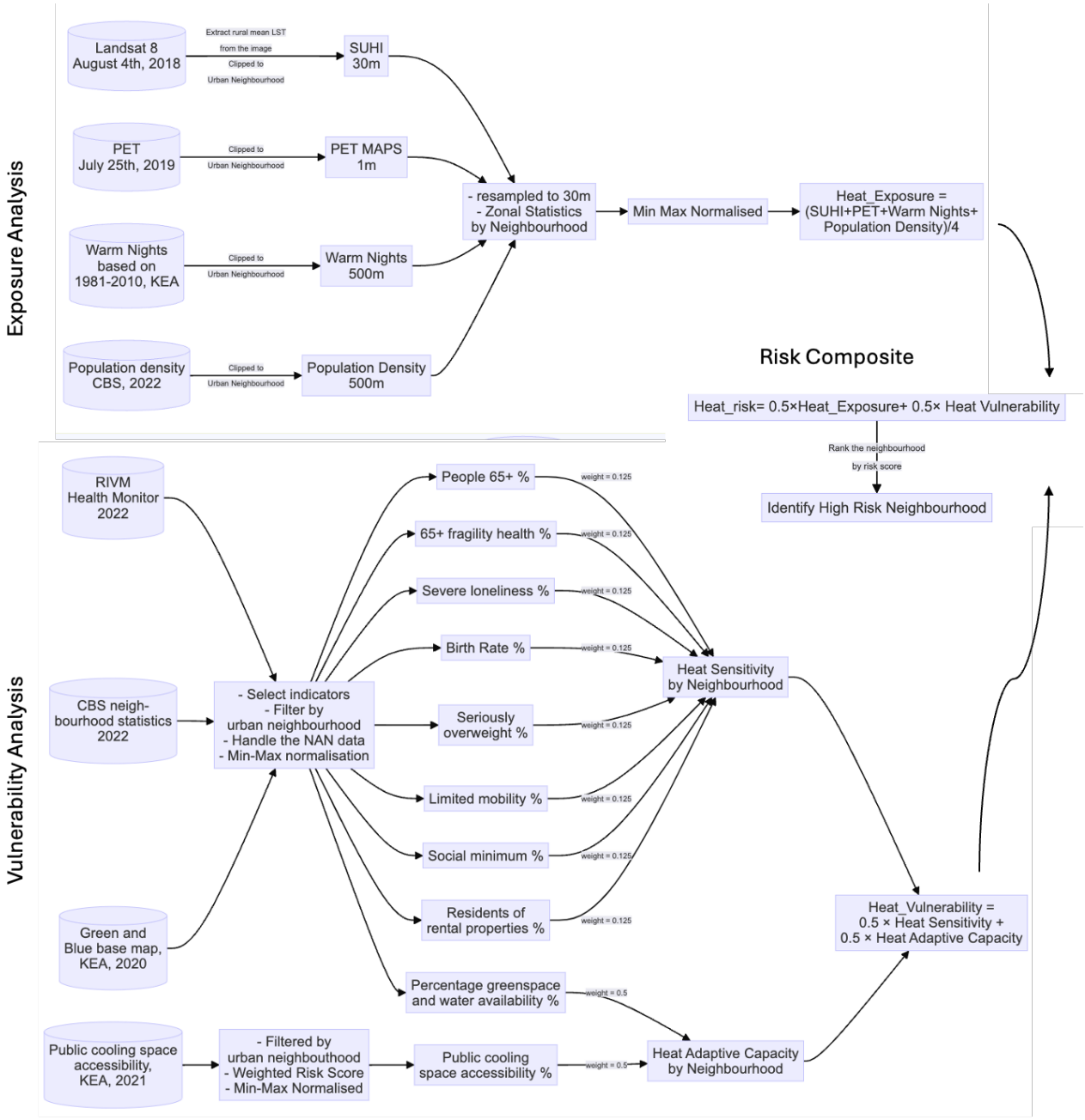

Figure 5–1 Flowchart of methods for RO2

5.1.1 Data Summary

The data used for this analysis is summarised in Table 5–2.

Table 5–2 Summary of the data used in this analysis.

Name	Indicator/ Data	Spatial and temporal resolution	Sources
SUHI	SUHI, calculated from Landsat 8 Land Surface Temperature (LST) , accessed from Google Earth Engine	August 4th, 2018 Raster, 30m	USGS, 2024
PET	Physiological equivalent temperature, modelled through a digital twin tool for heat stress assessment	July 25th, 2019 Raster, 1m	Cárdenas-León et al., 2024
Warm Nights	Warm Nights layer obtained from Klimaateffectatlas (KEA)	Modelled based on 1981 to 2010 climate Raster, 100m	Wageningen Environmental Research, 2016
Population Density	Population Density	2022 Raster, 100m	CBS, 2022
Health Monitors	The following indicators were obtained from Health Monitors: 65 and older_frailty health; severe loneliness aged 75+; people who are seriously overweight and people with limited mobility	2022 Recorded by neighbourhood (buurt)	GGD/CBS/RIVM, 2024
CBS neighbourhood statistics	The following socio-economic characteristic indicators were obtained from CBS neighbourhood statistics: Births per 1000 inhabitants; People aged 65 and older; Percentage of social minimum households; Percentage rental properties	2022 Vector, neighbourhood level (buurt)	CBS, 2024
Greenspace and water	Greenspace and water availability obtained from KEA	2020 Vector, neighbourhood level (buurt)	Cobra Groeninzicht, 2021
Cooling space	Public cooling space accessibility obtained from KEA	2021 Vector, neighbourhood level (buurt)	TAUW & Amsterdam University of Applied Science, 2021
Built areas	Built-up area	2017 Vector, neighbourhood level (buurt)	CBS, 2017

Surface Urban Heat Islands (SUHI) represents the variability of heat across different areas within a city. In this study, SUHI was calculated by subtracting the mean rural LST of 33.87°C (Table 5–3) from the urban reference LST layer (Table 5–3). This method, commonly used in previous studies (Peng et al., 2012), considered the size of the built-up area and surrounding land use. The urban area was defined based on the urban neighbourhood boundary, and the rural area for Enschede was created using a 1000-meter buffer around the urban area.

Table 5–3 Statistics of LST from Landsat 8 LST image in Enschede on Aug 4th, 2018

	Max (°C)	Mean (°C)	Median (°C)	Min (°C)

Urban	53.04	37.04	37.44	24.20
Rural	47.67	33.87	33.69	24.11

SUHI output from GEE had a spatial resolution of 30m. It was reprojected to EPSG 28992 and extracted by the urban neighbourhood. There were no NaN values in this layer.

The Physiological Equivalent Temperature (PET) was used to assess human thermal comfort by considering weather inputs, wind speed, relative humidity, greenspace, and urban morphology. For the purpose of this study, the 1km spatial resolution PET map created by Cárdenas-León et al. (2024) was used., The PET was calculated using the following equation:

$$PET_{sun} = -13.26 + 1.25 \times Ta + 0.011 \times Q_s - 3.37 \times ln(u_{1.2}) + 0.078 \times T_w + 0.0055 \times Q_{sln(u_{1.2})} + 5.56 \times sin(\varphi) - 0.0103 \times Q_{sln(u_{1.2})} \times sin(\varphi) + 0.0546 \times B_b + 1.94 \times S_{vf} \quad Eq\ 5\text{–}a$$

where:
T_a = air temperature at 2m
Q_s = solar irradiation
u_1.2 = wind speed at 1.2m height
T_w = wet-bulb temperature
φ = solar elevation angle
B_b = Bowen Ratio
S_vf = Sky-view factor

Warm nights, defined as nights when minimum temperature over 20°C. This data layer representing the occurrences of warn nights per year, was obtained from the KEA. (Wageningen Environmental Research, 2016).The spatial resolution is 100 metres. Warm Nights Layer was extracted based on urban neighbourhoods. The data obtained from KEA did not directly indicate the duration of warm nights; instead, pixel values ranging from 0 to 1 were classified into categories such as 1 day, 1 week, and 1 month. For this research, the original pixel values were utilised, with NaN values being treated as 0.

Population Density: As humans are the main target when measuring the heat exposure levels, integrating population data within intra urban heat stress is essential. For example, industrial zones might exhibit high LST, but the population density in these areas are low, thus lessens the overall risk. In this study, population density data from CBS 2022 statistics was used to capture population density. This data has a spatial resolution of 100 metres. Population Density was originally a polygon file representing 100m square grids. It was rasterised and then clipped to the urban neighbourhoods. NaN values were also handled as 0.

Health Monitors are a series of datasets containing neighbourhood statistics of human health in the Netherlands (GGD/CBS/RIVM, 2024). Previous research Table 2–4 highlighted that those more vulnerable to heat are those aged 65+ fragility health, severe loneliness, serious overweight and limited mobility etc. For the purpose of this study neighbourhoods where populations with these characteristics were extracted. A layer capturing the percentage of inhabitants potentially at risk of experiencing these conditions were created. The datasets were utilised for heat sensitivity analysis.

CBS neighbourhood statistics provided statistics on socio-demographical factors related to heat sensitivity analysis, such as birth rates, people over 65 years, social minimum and residents of rental properties. This vector data was also used to identify urban neighbourhood boundaries. Firstly, in conjunction with the built-up area in Enschede, the urban neighbourhoods were selected as the analysis extent. Furthermore, the selected urban neighbourhood boundary was employed for further zonal statistics.

Klimaateffectatlas (KEA) gathers various datasets useful for climate impact and adaptation. Two layers were selected to capture heat stress coping capacity. These included greenspace and water availability per neighbourhood (Cobra Groeninzicht, 2021) and public cooling space accessibility (TAUW & Amsterdam University of Applied Science, 2021).

- The **greenspace and water** availability layer showed the percentage of green and water areas per neighbourhood. Green features included trees (tree crowns and the area underneath) and low green (grass and shrubs). Agriculture was not included in the analysis.
- The **public cooling space accessibility** dataset showed the distances from each building polygon to the surrounding cooling spaces. A public cooling space is defined as a public outdoor area of at least 200 m², with a perceived temperature of 35 degrees Celsius or lower, typically shaded, and adequately distanced from roads. The distance to cooling refers to the total distance between a building and the closest cool space, measured using network analysis based on the road network. The map included five distance categories to cooling places: 0 - 200 metres, 200 - 300 metres, 300 - 400 metres, 400 - 500 metres, and 500+ metres.

All spatial data were projected to the EPSG 28992 coordinate system before further analysis.

5.1.2 Heat exposure during a heatwave event in Enschede

Exposure, as defined by the IPCC (2023) encompasses people, livelihoods, ecosystems, and infrastructure that could be adversely affected by a hazard, in this case heat during a heatwave. Since, this thesis focuses on heat and heat-related health, intra-urban heat stress and population density were considered in Enschede.

Intra-urban heat stress refers to the heat stress experienced within urban areas, influenced by urban morphology and surface characteristics. Heat stress is assessed using Urban Heat Island (UHI) effect, Physiological Equivalent Temperature (PET), and the occurrence of Warm Nights). The intra-urban heat stress in this study built on the 2006 study by incorporating Land Surface Temperature (LST). For the purpose of this study, exposure was determined using the following formula:

$$Heat_{Exposure} = \frac{SUHI+PET+Warm\ Nights+Population\ Density}{4} \qquad Eq\ 5\text{–}b$$

$Heat_{Exposure}$: The exposure composite was calculated as the mean of normalised raster layers SUHI, PET, Warm Nights, and Population Density, using Equation g.

- SUHI captured the variation of heat distributed in the urban area using the satellite derived LST.
- PET represented the spatial distribution of human perceived temperature modelled under the recorded extreme heat event (TX=40.7°C, July 25th, 2019).
- Warm Nights captured the frequency of warm nights (with temperature over 20 °C) within one year.
- Population Density captured the number of people per 100 metres.

All input layers, PET, Warm Nights and Population Density were resampled to a spatial resolution of 30 m and aligned to the SUHI layer. PET, Warm Nights and Population Density were then calculated the average for each neighbourhood through zonal statistics. All the indicators per neighbourhood were then normalised using the Min-Max Normalisation (Eq 5-c) method to produce standardised raster layers.

$$X_{normalised} = \frac{X - Xmin}{Xmax - Xmin}$$ Eq 5–c

After normalization, the heat exposure score for each neighbourhood was determined using Equation 5-b through averaging the PET, Warm Nights and Population Density. The exposure composite ranged from 0 (indicating low heat exposure) to 1 (indicating high heat exposure).

5.1.3 Heat vulnerability indicated by demographic, socio-economic and capacity factors

This vulnerability analysis builds upon existing research from the Klimaateffectatlas. The study on social vulnerability to heat (RIVM, 2023) explored how certain population groups are more affected by extreme heat due to factors such as age, health, income, and social networks. This is based on senior citizens in poor health and families living around or below the social minimum. Based on that, in this study, vulnerable populations were identified by identifying the populations most at risk from heat stress based on their sensitivity to heat and adaptive capacity. This was calculated using the following equation:

$$Heat_{Vulnerability} = 0.5 \times Heat_{Sensitivity} + 0.5 \times Heat_{AdpativeCapacity}$$ Eq 5–d

- $Heat_{Sensitivity}$ refers to the sensitivity of different populations to heat stress based on the Health Monitors.
- $Heat_{AdpativeCapacity}$ refers to the capacity to adapt during a heatwave based on greenspace and water and cooling space accessibility and CBS socio-economic characteristics.

Indicators for sensitivity and adaptive capacity were assigned equal weights within each category to calculate the overall $Heat_{Vulnerability}$ score. The final $Heat_{Vulnerability}$ scores by neighbourhood ranged from 0 to 1.

5.1.3.1 Heat sensitivity

The 4 indicators selected from the Health Monitor and the 4 CBS socio-economic characteristic included:

Table 5–4 The heat sensitivity indicators

Indicators	Unit	Description
People Aged 65 and Older	(%)	The proportion of the population aged 65 and older
65 and older_Frailty Health	(%)	This measures the percentage of older adults in poor health
Severe Loneliness aged 75+	Count per km²	The prevalence of severe loneliness among those aged 75 and above
Infants Births per 1000 Inhabitants:	Count per 1000 Inhabitants	The number of infants in the population
People Who Are Seriously Overweight	(%)	Percentage of adults who are severely overweight
People with Limited Mobility	(%)	Percentage of the population (18 and older) with limited mobility
Percentage of Social Minimum Households	(%)	The proportion of households living at or below the social minimum income level.
Percentage Rental Properties	(%)	The percentage of rental properties

The proportion of the population for each of the 8 indicators was determined for each neighbourhood and standardised using Eq 5-c. $Heat_{Sensitivity}$ was calculated as the mean of the eight indicators.

5.1.3.2 Heat Adaptive Capacity

Heat Adaptive Capacity refers to the ability of individuals or communities to adjust to and manage the impacts of extreme heat. This capacity includes access to resources such as water, air conditioning, and cool spaces, which are essential for mitigating the effects of heat stress (Keith et al., 2020). Additionally, urban planning interventions, such as the creation of green spaces and the use of reflective materials in buildings, can enhance the adaptive capacity of communities by providing cooling effects and reducing urban heat island effects (Dhalluin & Bozonnet, 2015; Guindon & Nirupama, 2015). Thus, the following categories were chosen to assess heat adaptive capacity:

Greenspace and Water Availability: The greenspace and water availability layer from KEA shows the percentage of green and water areas per neighbourhood. There were three indicators from this datasets used in the study:

- Percentage of public green space per neighbourhood(%)
- Percentage of non-public green space per neighbourhood (%)
- Percentage of water per neighbourhood (%)

Since a higher percentage of greenspace and water indicates greater adaptive capacity, it was necessary to ensure consistency with the scoring criteria of other indicators. To maintain this consistency, where a higher score corresponds to greater vulnerability, these indicators were negatively normalised using the following Equation 5-e:

$$X_{normalised} = \frac{Xmax - X}{Xmax - Xmin} \qquad \text{Eq 5–e}$$

Accessibility to Public Cooling Spaces: The accessibility to public cooling spaces is a dataset that categorises the distance from building polygons to nearby cooling spaces. To determine the risk scores for a neighbourhood, weighted risk scores were calculated using specific steps and equations. It is crucial for health, especially for vulnerable populations, that every home has access to a cool space within a 300-metre walking distance. Based on this, each distance category was given a linear risk score:

- 0 - 200 metres: 1
- 200 - 300 metres: 2
- 300 - 400 metres: 3
- 400 - 500 metres: 4
- 500+ metres: 5
- Cool space: 0

The weighted risk score for a neighbourhood was calculated using Eq 5-f:

$$Weighted_{Risk_{Score_i}} = \sum_j \left(\frac{Count_{ij}}{Total_{Count_i}} \times Risk_{Score_j} \right) \qquad \text{Eq 5–f}$$

$Count_{ij}$ the number of buildings in neighbourhood i that are within distance category j.
$Total\_Count_i$: the total number of buildings in neighbourhood i.
$Risk\_Score_j$: the risk score assigned to distance category j.

The indicator of accessibility to public cooling spaces was then normalised use Eq 5-e.

After the previous processing, the four normalised indicators Percentage of Public Green Space(%) , Percentage of non-public Green Space (%) , Percentage of Water(%) and Accessibility to Public Cooling Space were normalised and recorded for each neighbourhood.

Finally, the $Heat_{AdpativeCapacity}$ was calculated as the mean of the four indicators.

5.1.4 Which areas (neighbourhoods) in Enschede are at the highest risk during heatwaves, considering both exposure and vulnerability?

To assess the neighbourhoods, each neighbourhood was normalised as described earlier and ranked to capture areas of highest (5) and lowest risk (1) using equal range. More details on the range of each indicator corresponding to its normalisation score could be found in Appendix 9.3, Table 9–2 to Table 9–4.

$$Heat_{\text{risk}} = 0.5 \times Heat_{Exposure} + 0.5 \times \text{Heat}_{\text{Vulnerability}} \quad \text{Eq 5–g}$$

The overall risk levels was generated by calculating risk aggregating the Heat Exposure and Heat Vulnerability score per neighbourhood using Eq 5-g. The aggregated result was further categorised into five levels using: Low 1, Low to Medium 2, Medium 3, Medium to High 4, and High 5. A risk map was then created to show the spatial distribution of heat risk in Enschede. To further quantify this risk, the number of neighbourhoods that fall into each of these five risk zones were summarised.

5.2 Results

5.2.1 Exposure Composite

Figure 5–2 captures the heat exposure risk for each neighbourhood. High heat exposure neighbourhoods were concentrated in five neighbourhoods located predominantly in the city center. These neighbourhoods included City, Hogeland-Noord, and Getfert. Neighbourhoods with mid to high-level exposure included De Bothoven, Pathmos, De Laares, Lasonder, Zeggelt. Neighbourhoods such as Roombeek-Roomveldje, Wesselerbrink Zuid-Oost, and Stadsveld-Zuid showed middle exposure levels but with variations due to high population density.

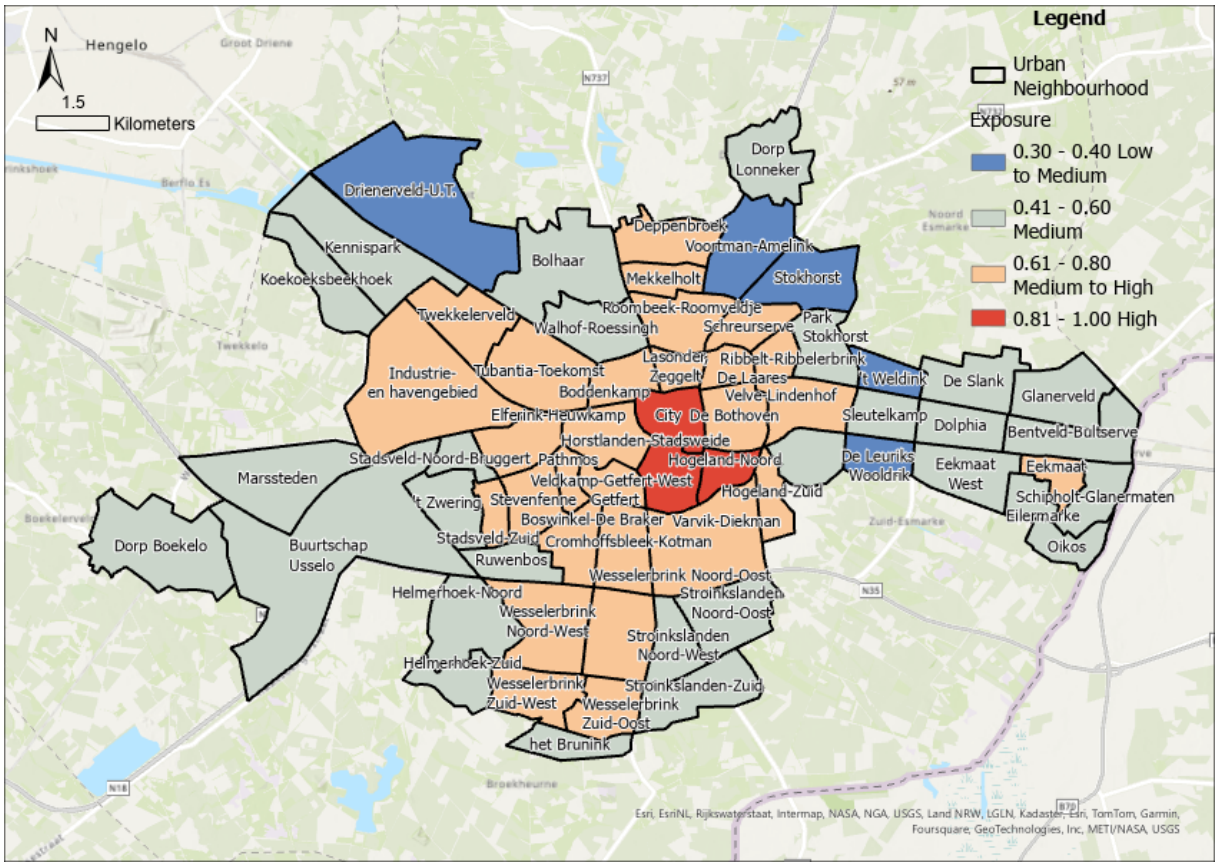

Figure 5–2 Exposure score per neighbourhood

Table 5–5 shows the summary of the neighbourhoods with Highest Rank and Lowest Rank Exposure, and the scores of corresponding individual indicators.

Table 5–5 Summary of the neighbourhoods with Highest Rank and Lowest Rank Exposure

Highest ranked	Neighbourhood Name	Exposure Score	SUHI		PET		Warm Nights		Population Density	
			Original | Normalised		Original | Normalised		Original | Normalised		Original | Normalised	
1	City	0. 89	5. 92	0. 77	41. 57	0. 84	0. 70	1. 00	91. 42	0. 94
2	Getfert	0. 83	7. 27	0. 88	41. 53	0. 77	0. 62	0. 88	79. 32	0. 81
3	Hogeland-Noord	0. 83	6. 64	0. 83	41. 46	0. 64	0. 60	0. 86	96. 25	1. 00
4	De Bothoven	0. 79	5. 31	0. 72	41. 43	0. 57	0. 62	0. 88	96. 46	1. 00
5	Veldkamp-Getfert-West	0. 74	5. 69	0. 75	41. 51	0. 72	0. 59	0. 85	64. 86	0. 65

Lowest ranked										
5	't Weldink	0. 36	−0. 51	0. 26	41. 41	0. 55	0. 43	0. 62	10. 56	0. 04
4	Voortman-Amelink	0. 36	−0. 09	0. 29	41. 26	0. 25	0. 44	0. 63	31. 29	0. 27
3	De Leuriks	0. 36	1. 78	0. 44	41. 23	0. 20	0. 47	0. 67	17. 60	0. 12
2	Drienerveld-U.T.	0. 32	−3. 82	0. 00	41. 13	0. 00	0. 50	0. 71	58. 09	0. 57
1	Stokhorst	0. 30	−0. 91	0. 23	41. 24	0. 21	0. 44	0. 63	18. 19	0. 12

5.2.1.1 Surface UHI (°C)

The SUHI map (Figure 5–3) shows Urban Heat Island effects in Enschede on August 4th, 2018, during the daytime. The SUHI values ranged from approximately -9.67°C to 19.17°C where positive values highlighted regions that hotter than rural areas, and negative values showed regions cooler than rural areas. Notable high UHI neighbourhoods included Industrie-en havengebied, Marssteden, Getfert, De Slank, and Varvik-Diekman. Negative SUHI values indicated cooler areas included Drienerveld-UT, Stokhorst.

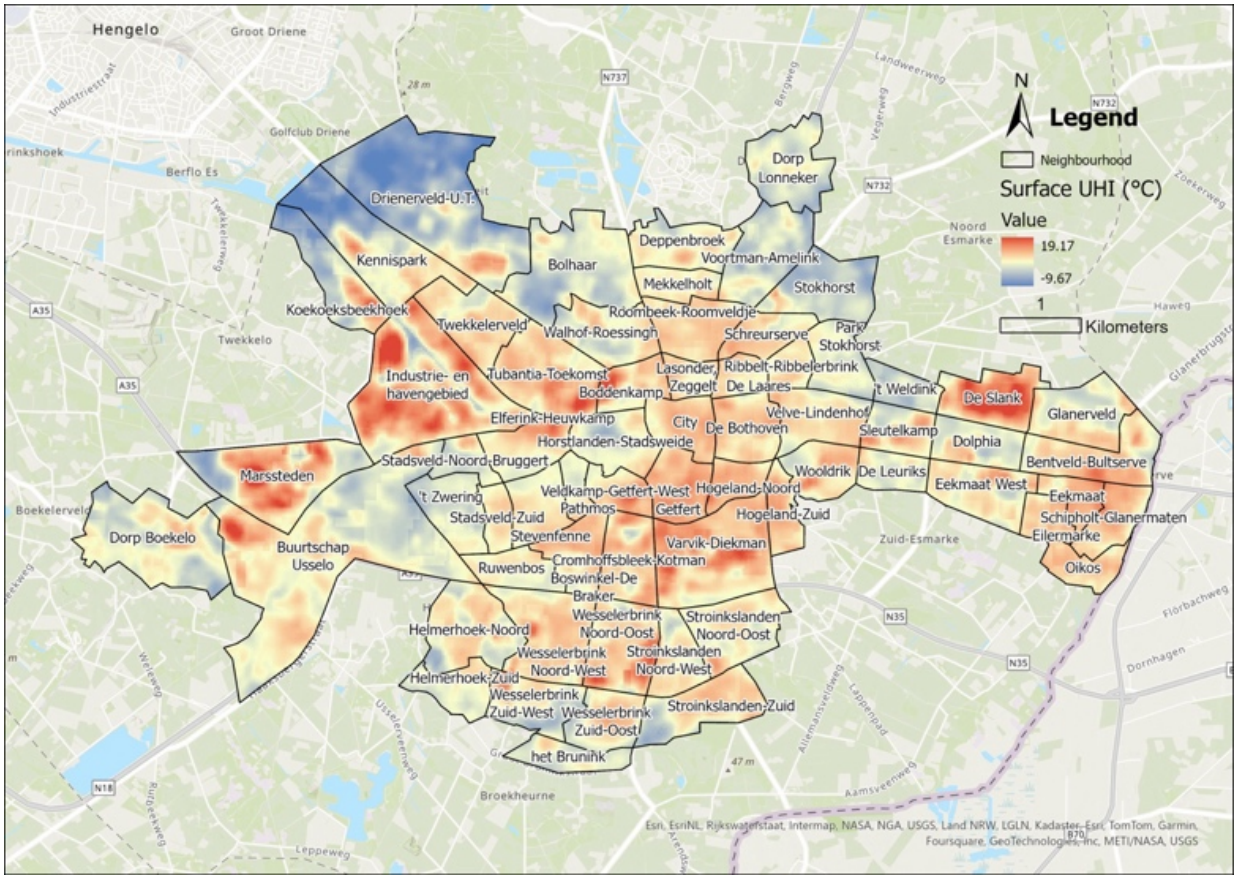

Figure 5–3 SUHI

5.2.1.2 PET (°C)

The PET map (Figure 5–4) shows the thermal comfort levels across Enschede in July 25th, 2019. The meteorological TX record reached an extreme of 40.2 °C. The calculated PET values ranged from 39.93°C to 42.13°C, across the city. The darker the colours showed the higher thermal stress.

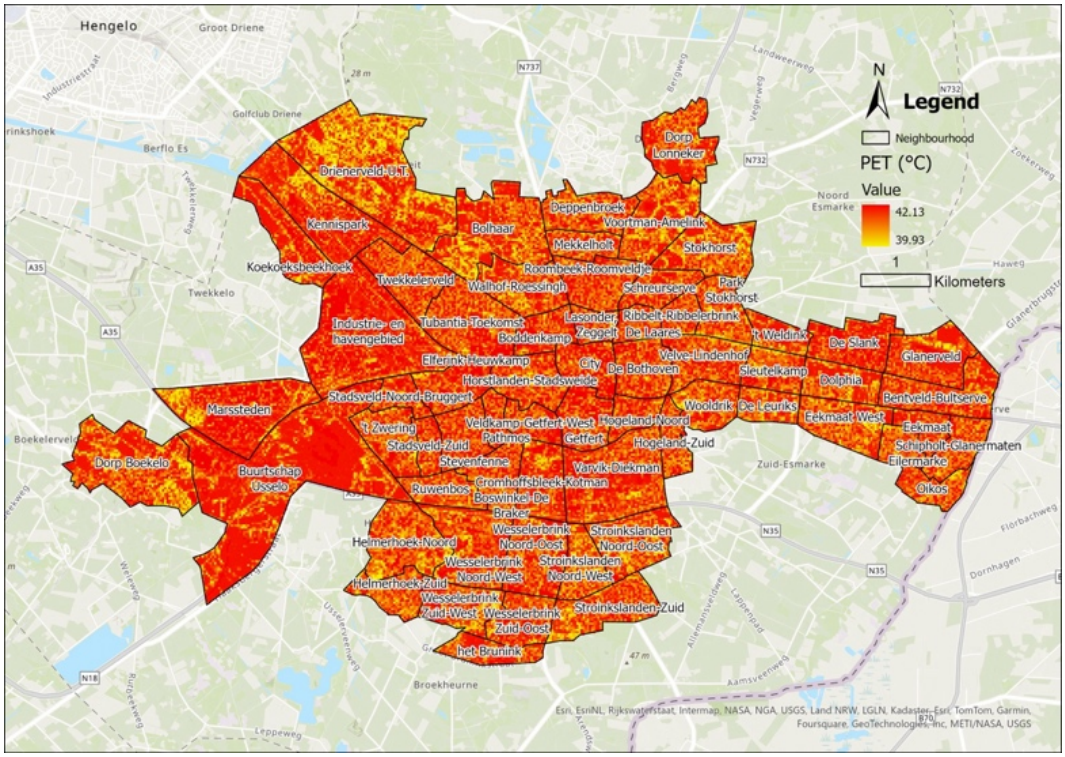

Figure 5–4 PET

5.2.1.3 Number of Warm Nights

Figure 5–5 illustrats the frequency of warm nights across Enschede, ranging from1 night to 1 week. Darker orange areas experienced more warm nights. Lighter orange areas had fewer warm nights due to natural cooling effects.

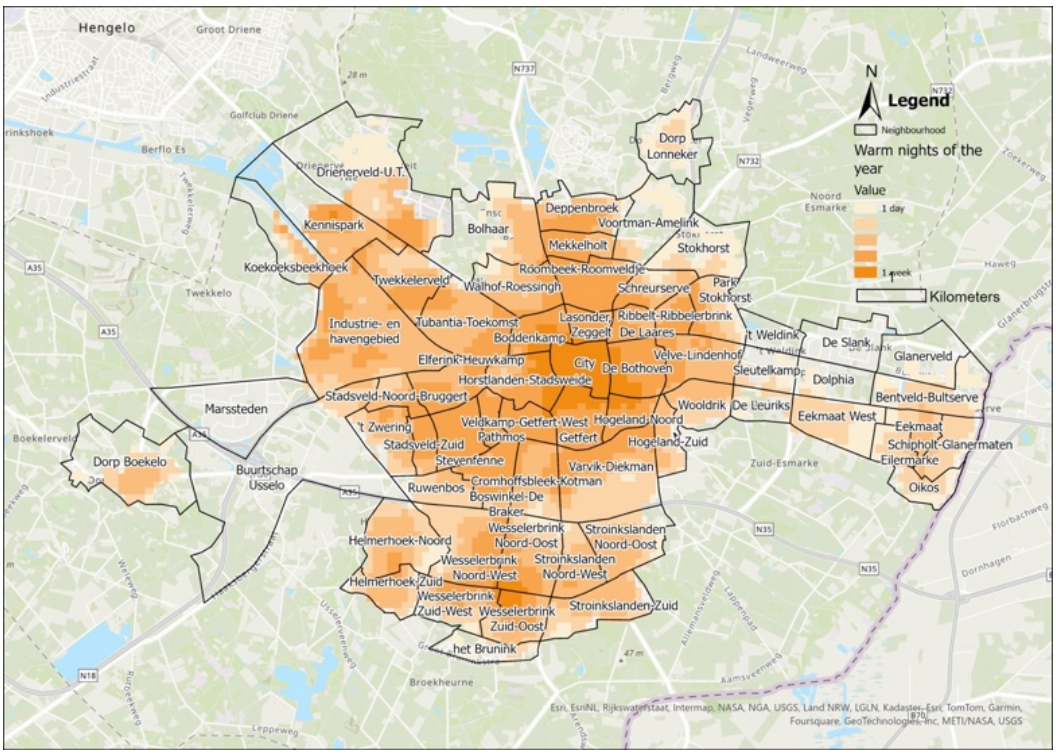

Figure 5–5 Warm Nights

5.2.1.4 *Population Density*

The population density map (Figure 5–6) represents the number of people per unit area with values ranging from 5 to 385. Higher population density areas, shown in darker blue, included central neighbourhoods like City and Getfert indicating a higher concentration of residents. Lower density areas, depicted in lighter blue, were found in neighbourhoods such asIndustrie-en havengebied.

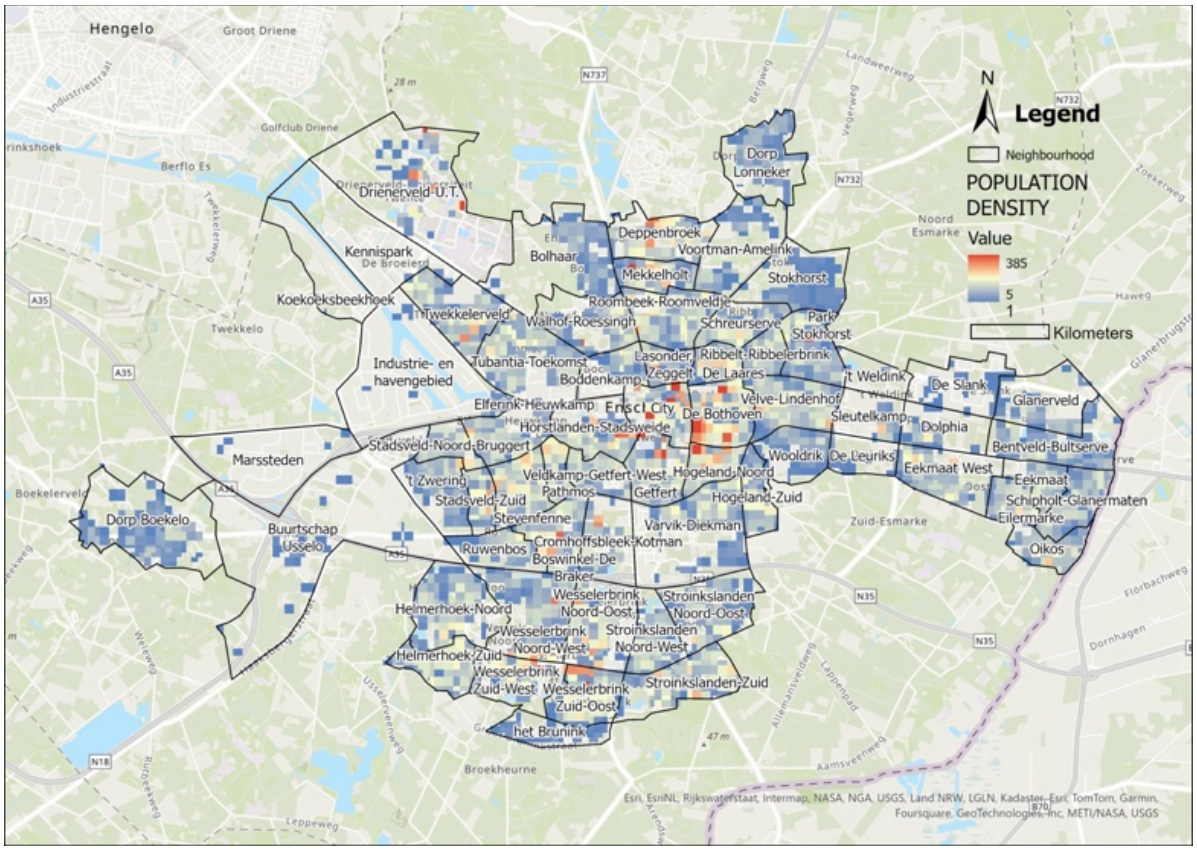

Figure 5–6 Population Density

5.2.2 Vulnerability Analysis

Figure 5–7 showes the vulnerability level for each neighbourhood. In Table 5–6, the top 5 neighbourhoods with the highest vulnerability scores are De Bothoven (0.72), Pathmos (0.72), Getfert (0.71), Wesselerbrink Zuid-Oost (0.71), and Eekmaat (0.70). These neighbourhoods are characterised by varying levels of sensitivity and adaptive capacity, making them more prone to heat-related challenges. In contrast, the 5 neighbourhoods with the lowest vulnerability scores, are Koekoeksbeekhoek (0.16), 't Weldink (0.17), Kennispark (0.20), De Leuriks (0.25), and Drienerveld-U.T. (0.26). These areas have lower sensitivity and higher adaptive capacity, making them less vulnerable to heat stress.

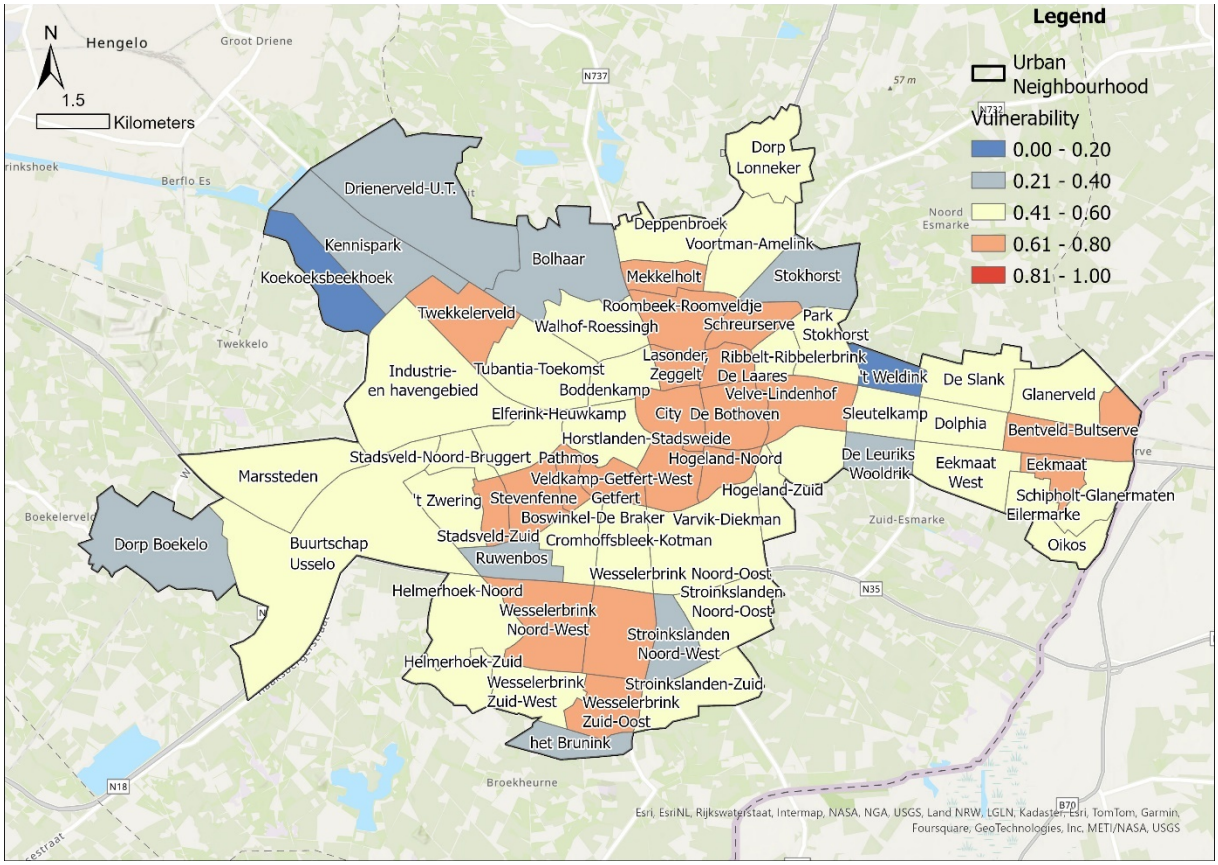

Figure 5–7 Map capturing Vulnerability to heat in Enschede

Table 5–6 Summary of the neighbourhoods with Highest Rank and Lowest Rank Vulnerability

Highest ranked	Neighbourhood Name	Vulnerability	Sensitivity	Capacity
1	De Bothoven	0.72	0.67	0.78
2	Pathmos	0.72	0.63	0.80
3	Getfert	0.71	0.51	0.91
4	Wesselerbrink Zuid-Oost	0.71	0.78	0.63
5	Eekmaat	0.70	0.56	0.84
Lowest ranked				
5	Drienerveld-U.T.	0.26	0.28	0.24
4	De Leuriks	0.25	0.27	0.22
3	Kennispark	0.20	0.00	0.40
2	't Weldink	0.17	0.18	0.15
1	Koekoeksbeekhoek	0.16	0.06	0.26

5.2.2.1 *Sensitivity Analysis*

Figure 5–8 shows the sensitivity level for each neighbourhood. The top 5 neighbourhoods with the highest sensitivity scores, indicating greater vulnerability to heat risk, are Wesselerbrink Zuid-Oost (0.78), Wesselerbrink Noord-Oost (0.75), De Bothoven (0.67), Wesselerbrink Noord-West (0.65), and Mekkelholt (0.65). These neighbourhoods show higher percentages of older adults residents, frailty in those over 65, and severe loneliness among those aged 75+, as well as higher rates of severe overweight, limited mobility, social minimum households, and rental properties. In contrast, the least ranked 5 neighbourhoods, with the lowest sensitivity scores are Kennispark (0.00), Koekoeksbeekhoek (0.06), 't Weldink (0.18), het Brunink (0.21), and De Leuriks (0.27).

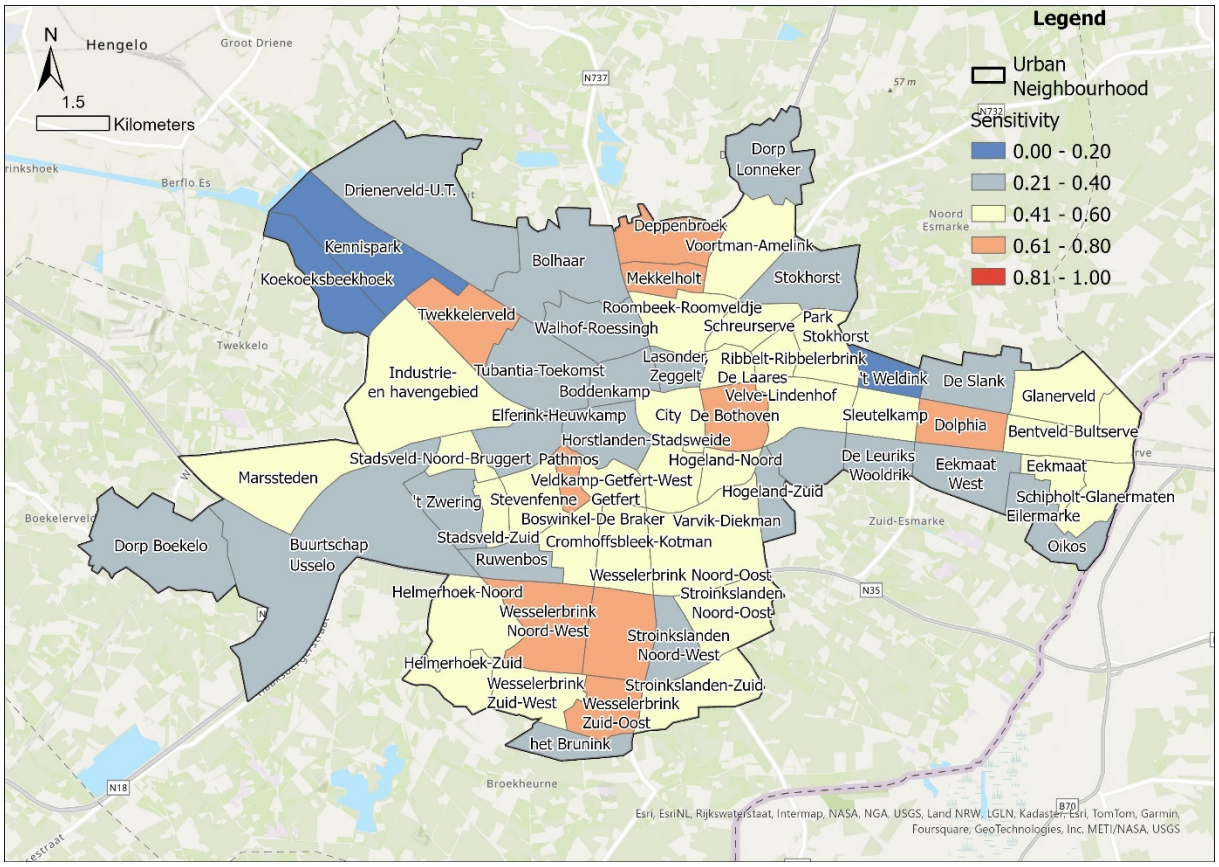

Figure 5–8 Map of Enschede capturing sensitivity to heat

Table 5–7 Summary of the neighbourhoods with Highest Rank and Lowest Rank Sensitivity

Highest ranked	Neighbourhood	Sensitivity	**Percentage 65 years and older (%)**		**65 and older Frailty Health (%)**		**Severe Lonely aged 75+ per km2**		**Births per 1000 inhabitants**	
			Original/	Normalised	Original/	Normalised	Original/	Normalised	Original/	Normalised
1	Wesselerbrink Zuid-Oost	0.78	28	0.82	44.8	0.97	180	0.92	7	0.21
2	Wesselerbrink Noord-Oost	0.75	24	0.71	46.1	1.00	58	0.30	6	0.18
3	De Bothoven	0.67	27	0.79	35.4	0.77	196	1.00	5	0.15
4	Wesselerbrink Noord-West	0.65	23	0.68	40.6	0.88	75	0.38	10	0.30
5	Mekkelholt	0.65	20	0.59	41.4	0.90	152	0.78	6	0.18

Lowest ranked										
5	De Leuriks	0.27	18	0.53	22.2	0.48	0	0.00	11	0.33
4	het Brunink	0.21	10	0.29	18.5	0.40	0	0.00	7	0.21
3	't Weldink	0.18	0	0.00	18.6	0.40	0	0.00	0	0.00
2	Koekoeksbeekhoek	0.06	0	0.00	0	0.00	0	0.00	0	0.00
1	Kennispark	0.00	0	0.00	0	0.00	0	0.00	0	0.00
Highest ranked	Neighbourhood	Sensitivity	**18 and older Severe Overweight (%)**		**18 and older Limited mobility(%)**		**Percentage of social minimum households(%)**		**Percentage rental properties (%)**	
			Original/ Normalised		Original/ Normalised		Original/ Normalised		Original/ Normalised	
1	Wesselerbrink Zuid-Oost	0.78	23.2	0.88	30.2	0.93	18.8	0.80	69	0.75
2	Wesselerbrink Noord-Oost	0.75	23.9	0.90	32.5	1.00	23.6	1.00	82	0.89
3	De Bothoven	0.67	18.4	0.69	21.3	0.66	12.6	0.53	73	0.79
4	Wesselerbrink Noord-West	0.65	20.6	0.78	25.9	0.80	14.9	0.63	72	0.78
5	Mekkelholt	0.65	18.8	0.71	22.1	0.68	14	0.59	74	0.80
Lowest ranked										
5	De Leuriks	0.27	11.4	0.43	9.4	0.29	0	0.00	11	0.12
4	het Brunink	0.21	11.3	0.43	7.7	0.24	2.7	0.11	1	0.01
3	't Weldink	0.18	16.8	0.63	11.8	0.36	0	0.00	0	0.00
2	Koekoeksbeekhoek	0.06	9	0.34	5.5	0.17	0	0.00	0	0.00
1	Kennispark	0.00	0	0.00	0	0.00	0	0.00	0	0.00

Distribution of vulnerable populations represented by sensitivity indicators as follows:

5.2.2.2 Percentage 65 years and older (%) (Figure 5–9a)

The proportion of the population aged 65 and older spans from 0% to 34%, with higher concentrations in neighbourhoods like Stokhorst, Stroinkslanden Noord-Oost, Wesselerbrink Zuid-Oost, De Bothoven, and Dorp Boekelo. These areas have larger older adults populations, who are generally more vulnerable to heat stress.

5.2.2.3 65 and older Frailty Health (Figure 5–9b)

The percentage of frail individuals aged 65 and older varies significantly across neighbourhoods, ranging from 0% to 46.1%. High frailty percentages are primarily concentrated in neighbourhoods such as City, Helmerhoek Zuid, Getfert, Wesselerbrink Noord-Oost, and De Bothoven. Older adults with frail health are particularly susceptible during heatwaves due to their reduced ability to cool down and sense thirst, necessitating targeted healthcare and social support services in these areas.

5.2.2.4 Births per 1000 Inhabitants (Figure 5–9c)

Birth rates in the neighbourhoods ranged from 0 to 33 per 1000 inhabitants, with higher rates in Boswinkel - Stadsveld, Stroinkslanden Noord-West, Wesselerbrink Zuid-Oost, Wesselerbrink Noord-Oost, and Wesselerbrink Noord-West. These areas likely have younger children who need help to keep cool during heat.

5.2.2.5 Severe Loneliness aged 75+ per km² (Figure 5–9d)

The density of severely lonely individuals aged 75 and older ranged from 0 to 196 per km², with significant concentrations in neighbourhoods like De Bothoven, Pathmos, Hogeland-Zuid, Boswinkel - Stadsveld, and Helmerhoek Noord. Severely lonely individuals are at higher risk of dehydration and overheating during heatwaves due to limited social interactions and support.

5.2.2.6 18 and older Severe Overweight (%) (Figure 5–9e)

Severe overweight percentages among individuals aged 18 and older range from 6.6% to 31.4%. Neighbourhoods such as Pathmos, Helmerhoek Zuid, Wesselerbrink Noord-Oost, De Bothoven, and Twekkelerveld.

5.2.2.7 18 and older Limited Mobility (%) (Figure 5–9f)

The percentage of individuals aged 18 and older with limited mobility varies from 7% to 32.5%, with higher percentages in neighbourhoods like Helmerhoek Zuid, Pathmos, Twekkelerveld, Wesselerbrink Noord-Oost, and Getfert. People with limited mobility face challenges in finding cool spots during heatwaves.

5.2.2.8 Percentage of Social Minimum Households (%) (Figure 5–9g)

This indicator ranges from 0% to 23.6%, highlighting neighbourhoods where economic vulnerability is more pronounced. Areas such as City, Pathmos, Wesselerbrink Noord-Oost, Helmerhoek Zuid, and Twekkelerveld have higher percentages of households at the social minimum income level. Households at or below the social minimum have limited budgets for heat mitigation measures.

5.2.2.9 Percentage Rental Properties (%) (Figure 5–9h)

The proportion of rental properties ranges from 0% to 92%, with the highest percentages in neighbourhoods like City, Drienerveld-U.T., Pathmos, Wesselerbrink Noord-Oost, and Twekkelerveld. Residents of rental homes have fewer options for large-scale home adaptations such as installing cooling systems or screens.

Figure 5–9 Sensitivity indicators.
(Top 5 high scored neighbourhoods are labelled for each indicator)

5.2.2.10 *Adaptative Capacity Analysis*

In Figure 5–10, the score of adaptive capacity is mapped. Higher Score means less capacity to adapt to heat. Table 5–8 shows the top 5 neighbourhoods with the highest scores are Getfert (0.91), Roombeek-Roomveldje (0.89), Veldkamp-Getfert-West (0.87), Eekmaat (0.84), and Stevenfenne (0.82). These areas have less green space and are farther from cooling spaces, making them more less capable of adapting to heat stress. In contrast, the bottom 5 neighbourhoods, with the lowest scores showing good capacity are 't Weldink (0.15), De Leuriks (0.22), Drienerveld-U.T. (0.24), Koekoeksbeekhoek (0.26), and het Brunink (0.33).

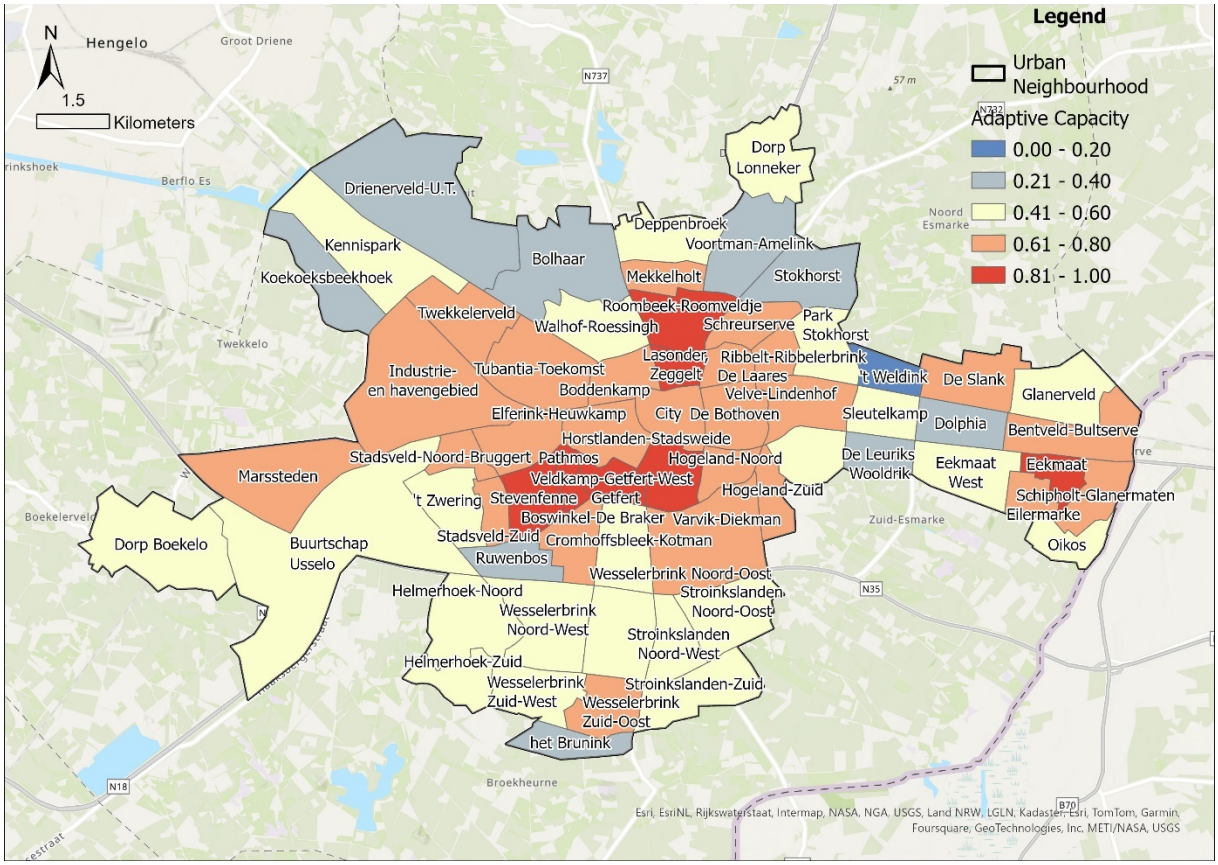

Figure 5–10 Map of Enschede capturing capacity
**Higher Score means less capacity to adapt to heat*

Table 5–8 Summary of the neighbourhoods with Highest Rank and Lowest Rank Adaptative Capacity

Highest ranked	Neighbourhood	Adaptive Capacity	Percentage of Green Space in Public		Percentage of Green Space non-Public		Percentage of Water		Distance to cooling space	
			Original/ Normalised		Original/ Normalised		Original/ Normalised		Original/ Normalised	
1	Getfert	0.91	11	0.99	21	0.81	0	1.00	2.09	0.85
2	Roombeek-Roomveldje	0.89	16	0.92	29	0.69	0.97	0.95	2.35	1.00
3	Veldkamp-Getfert-West	0.87	10	1.00	21	0.81	0	1.00	1.75	0.66
4	Eekmaat	0.84	23	0.82	25	0.75	0.54	0.97	2.00	0.80
5	Stevenfenne	0.82	24	0.80	25	0.75	0.05	1.00	1.87	0.73
Lowest										

Ranked										
5	het Brunink	0.33	67	0.20	60	0.24	5.78	0.71	0.93	0.19
4	Koekoeksbeekhoek	0.26	54	0.38	30	0.68	19.69	0.00	0.59	0.00
3	Drienerveld-U.T.	0.24	73	0.11	64	0.18	7.17	0.64	0.66	0.04
2	De Leuriks	0.22	77	0.06	76	0.00	5.22	0.73	0.76	0.10
1	't Weldink	0.15	81	0.00	73	0.04	9.86	0.50	0.73	0.08

5.2.2.11 Greenspace and Water Availability

Public green spaces (Figure 5–11a), varied from 10% to 80% across different neighbourhoods. Neighbourhoods with higher percentages of public green spaces, such as 't Weldink, De Leuriks, Stokhorst, Drienerveld-U.T., and Bolhaar., help mitigate the urban heat island effect and provide residents with places to cool down during heatwaves.

In addition to public green spaces, private gardens and institutional grounds also play a role in reducing heat. These non-public green areas (Figure 5–11b), ranged from 10% to 70%, are notably prevalent in neighbourhoods like 't Weldink, De Leuriks, Stokhorst, Drienerveld-U.T., and Dolphia.

Areas with significant water coverage, included 't Weldink, Koekoeksbeekhoek, Kennispark s (Figure 5–11c).The proportion of water in these neighbourhoods ranges from 0% to 17.5%.

5.2.2.12 Accessibility to Public Cooling Spaces

The Accessibility to Public Cooling Spaces is calculated a risk score (Figure 5–11d). Higher score per neighbourhood means it takes more distance to the cooling space. This risk score was calculated based on the distance residents in each neighbourhood must travel to reach a cooling space. In this map, areas with yellow shade represented neighbourhoods with higher risk scores, indicating that residents must travel further to access public cooling spaces. For example, neighbourhoods Getfert, Roombeek-Roomveldje, Eekmaat, Lasonder - Zeggelt and Bentveld-Bultserve. Darker areas showed neighbourhoods with lower risk scores, meaning that residents have better access to these spaces.

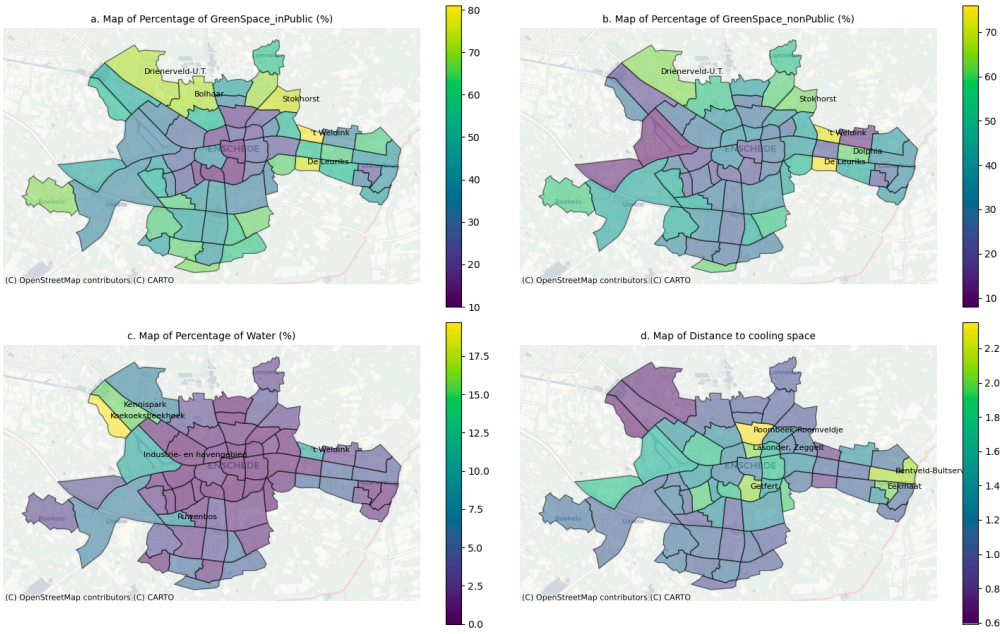

Figure 5–11 Adaptative Capacity indicators

5.2.3 Heat Risk in Enschede

Figure 5–12 shows the overall risk level of each neighbourhood. Table 5–9 shows the top 5 neighbourhoods with the highest risk scores, showing greater vulnerability to heat risk, are **City**, **Getfert**, **De Bothoven**, **Hogeland-Noord**, and **Veldkamp-Getfert-West**. These areas are more likely to be affected by heat due to a combination of high exposure and sensitivity, with potentially lower adaptive capacity. Conversely, the bottom 5 neighbourhoods with the lowest risk scores, indicating better resilience to heat, are **'t Weldink**, **Drienerveld-U.T.**, **De Leuriks**, **Koekoeksbeekhoek**, and **Stokhorst**.

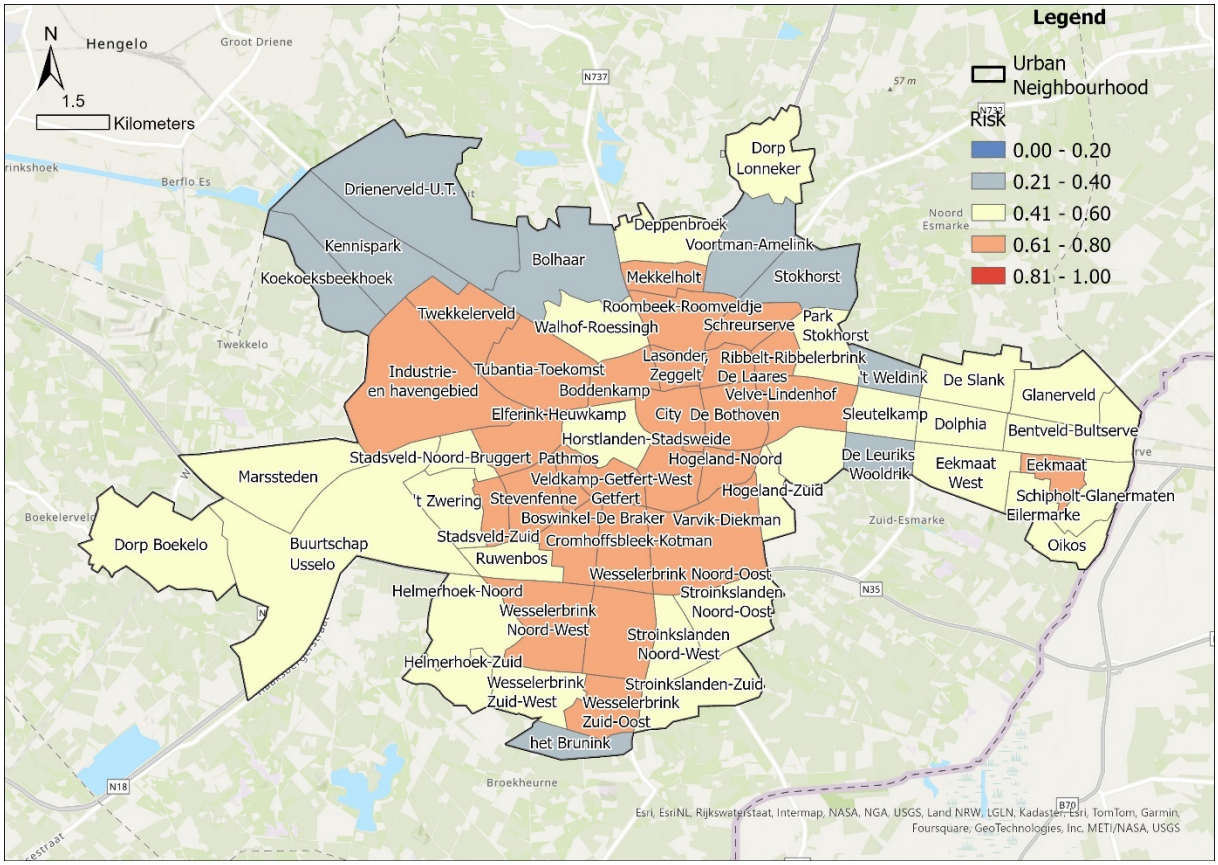

Figure 5–12 Map of Heat Risk per neighbourhood

Table 5–9 Summary of the neighbourhoods with Highest Rank and Lowest Rank Risk

Highest ranked	Neighbourhood Name	Risk	Exposure	Vulnerability	Sensitivity	Capacity
1	City	0.77	0.89	0.66	0.52	0.79
2	Getfert	0.77	0.83	0.71	0.51	0.91
3	De Bothoven	0.76	0.79	0.72	0.67	0.78
4	Hogeland-Noord	0.74	0.83	0.65	0.55	0.75
5	Veldkamp-Getfert-West	0.72	0.74	0.69	0.52	0.87
Lowest ranked						
5	Stokhorst	0.31	0.30	0.32	0.29	0.34
4	Koekoeksbeekhoek	0.30	0.44	0.16	0.06	0.26
3	De Leuriks	0.30	0.36	0.25	0.27	0.22
2	Drienerveld-U.T.	0.29	0.32	0.26	0.28	0.24

1	't Weldink	0.26	0.36	0.17	0.18	0.15

A summary table (Table 5–10) illustrates the percentage of neighbourhoods within each level for Exposure, Vulnerability, and the Final Risk Score.

- Exposure Level Distribution: The "High" exposure category included 4.69% of neighbourhoods (3 total). The majority fell into "Medium" (43.75%) and "Medium to High" (43.75%) categories, indicating a moderate to high exposure for most neighbourhoods.
- Vulnerability Level Distribution: Only 3.13% of neighbourhoods were classified as 'Low' vulnerability. Most neighbourhoods were in the "Medium" category (51.56%), followed by "Medium to High" (31.25%).
- Risk Level Distribution: 42.19% of neighbourhoods were in the "Medium to High" risk category, with 43.75% in the "Medium" category. "Low to Medium" accounted for 14.06%. There were no neighbourhoods "Low" and "High" risk.

Table 5–10 Summary of the neighbourhoods and population at different level

	Exposure Level				Vulnerability Level				Risk Level			
	neighbourhood count		total population		neighbourhood count		total population		neighbourhood count		total population	
High	3	4.69%	10850	6.98%		0.00%		0.00%		0.00%		0.00%
Medium to High	28	43.75%	86580	55.69%	20	31.25%	67175	43.21%	27	42.19%	84515	54.36%
Medium	28	43.75%	52770	33.94%	33	51.56%	75610	48.63%	28	43.75%	63450	40.81%
Low to Medium	5	7.81%	5275	3.39%	9	14.06%	12655	8.14%	9	14.06%	7510	4.83%
Low		0.00%		0.00%	2	3.13%	35	0.02%		0.00%		0.00%

5.3 Conclusion

Overall no neighbourhoods were scored as "High" risk. However, a significant share of urban neighbourhoods are at both 'Medium to High' and 'Medium' risk levels. Around 95% of the population in urban neighbourhoods are found at a risk level greater than "Medium".

6 DISCUSSION

6.1 Evaluation of results

6.1.1 RO 1 How do characteristics of heatwaves, daily TX data, vary spatially and temporally in the Netherlands?

6.1.1.1 Temporal pattern of heatwave events

Historical data from the De Bilt station (1901-2022) showed an increase in heatwave frequency, especially since 2000, with 14 of the 30 (in total) recorded events occurring in this period. The average highest temperature during these heatwaves was 33.2°C, and the average duration was 9.17 days. The years 1975, 1976, 2003, 2006, 2018, 2019, and 2020 were particularly notable for their high cumulative heatwave intensity (CHI) values, indicating more severe and prolonged heatwave conditions.

6.1.1.2 Spatial distribution of heatwaves characteristics

Spatial analysis during the intense heatwave years (2003, 2006, 2018, 2019, 2020) revealed that southern and eastern regions experienced more severe heatwaves. On 25th July 2019, De Bilt recorded its highest temperature of 37.5°C, while Gilze-Rijen reached a national record for the hottest day to date with a temperature of 40.7°C. In Enschede, within our study area, a temperature of 40.2°C was recorded. The year 2018 was also notable for high CHI values nationwide. A 23-year summary (2000-2022) from 32 weather stations further confirmed that southern and eastern regions consistently recorded higher maximum temperatures (HI) compared to northern and coastal areas. This indicates that the southern and eastern regions of the Netherlands experience more severe and prolonged heatwaves. This pattern is attributed to their inland location, which lacks the moderating influence of the sea, leading to higher summer temperatures. Additionally, Enschede also resided in the zones with more intense heatwave characteristics than De Bilt.

6.1.1.3 Comparison between station De Bilt and Twenthe (Enschede)

Comparing heatwave events between De Bilt and Twenthe (Enschede) from 2000 to 2022 revealed some differences. Enschede experienced 16 heatwave events, while De Bilt had 14. Heatwaves in Enschede were more frequent and prolonged, with higher HI and CHI values from heatwave events.

The observed differences in counts of heatwave records between two stations are attributed to differences in TX temperatures. First, it roots from the local climate variation considering Enschede inland located. Furthermore, these are also related to the temperature thresholds set for defining heatwaves. When temperatures are close to these critical thresholds that define a heatwave, 25°C for a standard heatwave day and 30°C for a tropical day, even small changes can affect whether a day is classified as part of a heatwave or not, influencing the overall heatwave event count and characterisation at each station.

The analysis of summer temperatures between De Bilt and Twenthe showed significant differences confirmed by Wilcoxon signed-rank tests. From June 1 to September 30, focusing on days with temperatures of 25°C or higher, Enschede consistently recorded higher temperatures than De Bilt during 2000 to 2022. The mean temperature difference was 0.43°C for the entire summer dataset and 1.09°C for temperature over 25°C days. It further supports higher TX in Enschede, particularly during heatwaves.

6.1.2 RO 2 Who is at risk to heatwave in Enschede? Where are the risk areas in Enschede?

6.1.2.1 The characteristics of intra-urban heat exposure distributions during an atypical heatwave event in Enschede

Heat exposure in this study employed the IPCC definition, where it was defined by the presence of populations and assets within areas affected by extreme heat, with a focus on intra-urban heat variation. Spatial differences in heat exposure across neighbourhoods were primarily driven by the Urban Heat Island (UHI) effect, with some areas experiencing increased heat stress due to urban morphology and land use patterns. Thus, three indicators were chosen to assess the intra-urban heat exposure: Surface Urban Heat Islands (SUHI), Physiological Equivalent Temperature (PET), and Warm Nights, alongside population density.

Significant variations were identified in heat exposure across different neighbourhoods in Enschede. The overall high exposure neighbourhoods are **City, Hogeland-Noord, and Getfert**. Areas such as **Industrie- en havengebied, Marssteden, Getfert, De Slank, and Varvik-Diekman** were found to have higher SUHI values on 2018 Aug 4th. PET values during a 2019 heatwave event ranged from 39.93°C to 42.13°C, with a high thermal stress across the city. Additionally, the occurrence of warm nights (minimum temperatures above 20°C) further illustrated heat stress in certain neighbourhoods, **City and Boddenkamp, De Bothoven and Getfert**, as neighbourhoods with higher frequencies of warm nights are particularly vulnerable as the lack of nighttime cooling exacerbates heat stress. High population density areas, such as the central neighbourhoods of **City and Getfert**, contribute to increased heat exposure due to the concentration of people in these heat-prone areas.

6.1.2.2 What demographic, socio-economic, and capacity factors define the populations most vulnerable to heatwaves in Enschede?

Vulnerability was assessed using the IPCC definition, focusing on both sensitivity and adaptive capacity within Enschede's population. Sensitivity indicators included people aged 65 and older, frailty health in those 65 and older, severe loneliness among those aged 75 and above, infants (births per 1000 inhabitants), people who are seriously overweight, people with limited mobility, the percentage of social minimum households, and the percentage of rental properties. Adaptive capacity was evaluated based on the percentage of public and non-public green spaces, the percentage of water per neighbourhood, and accessibility to public cooling spaces.

6.1.2.3 Which areas in Enschede are at the highest risk during heatwaves, considering both exposure and vulnerability?

The summary of the classification level showed a small portion of neighbourhoods (4.69%) fell into the "High" exposure category. Most areas experiencing "Medium to High" to "Medium" exposure levels, with an 87.5% population in urban neighbourhoods. In terms of vulnerability, none of neighbourhoods were at high level, with most portion (51.6%) in the "Medium" category.

Overall, there are no neighbourhoods were scored as "High" risk. However, a significant share of urban neighbourhoods are at both 'Medium to High' and 'Medium' risk levels. Around 95% of the population in urban neighbourhoods are found at a risk level greater than "Medium".

Top 5 neighbourhoods with the highest risk scores, showing greater vulnerability to heat risk, are **City**, **Getfert**, **De Bothoven**, **Hogeland-Noord**, and **Veldkamp-Getfert-West**. These areas are more likely to be affected by heat due to a combination of high exposure and sensitivity, with potentially lower adaptive capacity.

6.1.3 Wickedness of the problem mitigated by the study

Heat health related risk was identified as a wicked problem, characterised by a lack of consensus among stakeholders, which complicates the development of effective interventions. As defined by Balint et al. (2011), a 'wicked problem' is marked by uncertainties in knowledge and differing values among stakeholders, making it difficult to reach agreement on the best course of action. Although various datasets are available that provide insights into heat impact or social vulnerability to heat, this information remains fragmented and lacks integrated detailed combination of information. Furthermore, as there is a growing call for local heat action plan, in Enschede a heat action plan has been discussed and drafted. Current neighbourhood-level (spatial) heat health risk assessments focus predominantly on the exposure component on heat stress, overlooking the spatial distribution of vulnerability.

This research first mitigated the wickedness by identifying the spatial and temporal characteristics of heatwaves in Netherlands. It helped to further necessitate a more localised heat stress view. It provided useful information for assessing the heatwave hazard. It could be useful for the local heat early warning systems to further set the threshold or identifying local heat early warning system thresholds. This research further addressed this gap by combining all available spatial data to create a comprehensive risk assessment that identifies at-risk neighbourhoods. The resulting map could serve as a vital tool for supporting heat adaptation interventions, enabling the identification of hotspot neighbourhoods and the prioritisation of projects based on localised needs.

The risk map and the analysis of individual indicators could assist in designing interventions (Keith et al., 2020). One potential intervention to climate heat action is to increase urban greening. This could involve prioritising or adding new green and blue infrastructure in risk areas identified as having high intra-urban heat stress and lower capacities. Additionally, public awareness campaigns could be implemented to provide practical advice on staying safe and hydrated during extreme heat events. These campaigns should specifically target at risk neighbourhoods with the most vulnerable groups, ensuring that residents have the necessary information and resources to protect themselves. Furthermore, areas with higher exposure could be utilised for establishing drinking water resources for the urban area or opening cooling centres by repurposing existing buildings for this purpose.

6.2 Limitations

6.2.1 Spatial and temporal availability heterogeneity from different sources

In the heat risk mapping for Enschede, the objective was to assess risk during a recorded extreme heatwave day. However, due to limited data availability, the indicators used were extracted from different time, leading to potential inconsistencies. The intra-urban heat stress analysis relied on data from three different dates. The 2018 Aug 4th Landsat 8 LST datasets was selected instead of 2019 July 25th LST from available datasets to approximate a typical heatwave scenario. The warm night data was directly sourced from the Climate Effect Atlas (KEA) due to time constraints and the complexity of re-modelling, which used climate data from 1981 to 2010, potentially leading to underestimated results.

The vulnerability indicators were intended to reflect conditions in 2019, but data from 2022 was used instead. This was done for two reasons: firstly, it provided more recent socio-demographic information; and secondly, the latest health monitor records were from 2022, and thus data from CBS are chosen for consistent social demographic factors to ensure alignment. The time of the two capacity indicators were also constrained by the availability and recency of research outputs updates.

6.2.2 Limited Spatial Data Availability of TX

The analyses in the Chapter 4 primarily relied on daily TX, the maximum air temperature recorded at weather stations. Across the Netherlands, 34 automatic weather stations continuously record daily TX. However, considering the heterogeneous distribution of temperature, the observations are relatively coarse. Additionally, with the Urban Heat Island (UHI) effect, weather stations typically located outside city centres may miss crucial urban heat information.

6.2.3 Limited Temporal Data Availability of higher Resolution of LST

Another limitation is the limited availability of high-resolution temporal data for LST, as the data used is constrained by specific times of day due to the satellite's orbit and the need for cloud-free conditions, resulting in only a snapshot view of surface temperatures. For example, Landsat 8 has a 14-day revisit time, and the image quality is significantly affected by clear sky conditions. Although higher temporal resolution datasets, such as LST datasets from the MODIS (Moderate Resolution Imaging Spectroradiometer), are available and can provide daily observations, they are limited to a coarser spatial resolution of 1 km, which may not accurately capture fine-scale temperature variations, particularly in urban areas.

6.3 Further Recommendations

6.3.1 Systematic stakeholder input or judgement in the weight designing

This research employed a straightforward approach to developing the heat risk composite by assigning equal weights at each hierarchical level. However, a more refined method, such as the Analytic Hierarchy Process (AHP), could have been used (Taherdoost & Madanchian, 2023). Time permitting and future work should further explore to design weights and choose indicators by incorporating systematic stakeholder input. Involving multiple stakeholders in the weight and indicator designing process allows for more understanding of the factors influencing heat risk.

6.3.2 Quantify the heat stress impact at local level

In this research, the level of intra-urban heat stress was normalised and classified using the equal. However, exploring more impact-based heat stress indicator thresholds could provide deeper insights. For instance, examining the relationship between LST and mortality or even morbidity datasets could offer valuable understanding. This impact-based analysis could help to identify specific thresholds where heat stress significantly affects health outcomes, enabling a more targeted approach in identifying and protecting vulnerable groups at the local level.

7 CONCLUSION

This thesis provided an integrated assessment of heatwave risks in the Netherlands, with a focus on Enschede, a city particularly prone to heatwaves. The risk was assessed through the hazard, exposure and vulnerability. This work highlighted the increasing frequency and severity of heatwaves in the Netherlands, particularly in eastern and southern regions like Enschede. Vulnerable populations were particularly at risk during the peak heatwave period from mid-July to mid-August.

This study also identified heat risk across different neighbourhoods. Exposure factors such as urban morphology, land use patterns, and population density. Vulnerability factors included demographic characteristics, socio-economic status, health conditions, and the availability of cooling resources and green spaces.

To mitigate these risks, the city of Enschede could implement targeted interventions during this critical period. Strategies highlighted in the literature included enhancing urban greenery, planning cooling centres, and conducting public awareness campaigns to educate residents on staying safe during extreme heat. These interventions could be functional for climate heat adaptation strategies, particularly for at-risk groups such as the older adults and those with pre-existing health conditions.

The study also faced limitations, including inconsistencies in spatial and temporal data, which may have introduced uncertainties in the risk assessment. The lack of high-resolution maximum air temperature data from weather stations and continuous high-resolution Land Surface Temperature (LST) data limited the ability to fully capture heatwave dynamics and heat impact on intra-urban environments.

Despite these challenges, this research offered insights for developing more localised and effective heatwave mitigation strategies. Future research should focus on integrating more comprehensive datasets, incorporating stakeholder input, and exploring impact-based thresholds to better understand and address heat-related health risks. These steps would help refine the understanding of heat risks and contribute to the development of more effective adaptation strategies for urban areas like Enschede.

8 LIST OF REFERENCES

Agathangelidis, I., Cartalis, C., Polydoros, A., Mavrakou, T., & Philippopoulos, K. (2022). Can Satellite-Based Thermal Anomalies Be Indicative of Heatwaves? An Investigation for MODIS Land Surface Temperatures in the Mediterranean Region. Remote Sensing 2022, Vol. 14, Page 3139, 14(13), 3139. https://doi.org/10.3390/RS14133139

Ahmed, I., van Esch, M., & van der Hoeven, F. (2023). Heatwave vulnerability across different spatial scales: Insights from the Dutch built environment. Urban Climate, 51, 101614. https://doi.org/10.1016/J.UCLIM.2023.101614

Alexander, L. V., Zhang, X., Peterson, T. C., Caesar, J., Gleason, B., Klein Tank, A. M. G., Haylock, M., Collins, D., Trewin, B., Rahimzadeh, F., Tagipour, A., Rupa Kumar, K., Revadekar, J., Griffiths, G., Vincent, L., Stephenson, D. B., Burn, J., Aguilar, E., Brunet, M., … Vazquez-Aguirre, J. L. (2006). Global observed changes in daily climate extremes of temperature and precipitation. Journal of Geophysical Research: Atmospheres, 111(D5), 5109. https://doi.org/10.1029/2005JD006290

Amengual, A., Homar, V., Romero, R., Brooks, H. E., Ramis, C., Gordaliza, M., & Alonso, S. (2014). Projections of heat waves with high impact on human health in Europe. Global and Planetary Change, 119, 71–84. https://doi.org/10.1016/J.GLOPLACHA.2014.05.006

Baccini, M., Biggeri, A., Accetta, G., Kosatsky, T., Katsouyanni, K., Analitis, A., Anderson, H. R., Bisanti, L., D'Ippoliti, D., Danova, J., Forsberg, B., Medina, S., Paldy, A., Rabczenko, D., Schindler, C., & Michelozzi, P. (2008). Heat effects on mortality in 15 European cities. Epidemiology, 19(5), 711–719. https://doi.org/10.1097/EDE.0B013E318176BFCD

Balint, P. J., Stewart, R. E., Desai, A., & Walters, L. C. (2011). Wicked Environmental Problems. Wicked Environmental Problems. https://doi.org/10.5822/978-1-61091-047-7

Ballester, J., Quijal-Zamorano, M., Méndez Turrubiates, R. F., Pegenaute, F., Herrmann, F. R., Robine, J. M., Basagaña, X., Tonne, C., Antó, J. M., & Achebak, H. (2023). Heat-related mortality in Europe during the summer of 2022. Nature Medicine 2023 29:7, 29(7), 1857–1866. https://doi.org/10.1038/s41591-023-02419-z

Balmain, B. N., Sabapathy, S., Louis, M., & Morris, N. R. (2018). Aging and Thermoregulatory Control: The Clinical Implications of Exercising under Heat Stress in Older Individuals. BioMed Research International, 2018. https://doi.org/10.1155/2018/8306154

Barriopedro, D., García-Herrera, R., Ordóñez, C., Miralles, D. G., & Salcedo-Sanz, S. (2023). Heat Waves: Physical Understanding and Scientific Challenges. Reviews of Geophysics, 61(2), e2022RG000780. https://doi.org/10.1029/2022RG000780

Basu, R. (2009). High ambient temperature and mortality: A review of epidemiologic studies from 2001 to 2008. Environmental Health: A Global Access Science Source, 8(1), 1–13. https://doi.org/10.1186/1476-069X-8-40

Bergh, S. I., Longman, A. R., & Van Tuijl, E. (2022). Heatwaves and vulnerable populations: Mapping their needs in The Hague. https://pure.eur.nl/ws/portalfiles/portal/79274217/Heatwaves_and_vulnerable_populations_report_final.pdf

Bettaieb, J., Toumi, A., Leffondre, K., Chlif, S., & Ben Salah, A. (2020). High temperature effect on daily all-cause mortality in Tunis 2005–2007. Revue d'Epidemiologie et de Sante Publique, 68(1), 37–43. https://doi.org/10.1016/J.RESPE.2019.09.007

Boni, Z., Bieńkowska, Z., Chwalczyk, F., Jancewicz, B., Marginean, I., & Serrano, P. Y. (2023). What is a heat(wave)? An interdisciplinary perspective. Climatic Change, 176(9), 1–23. https://doi.org/10.1007/S10584-023-03592-3

Bradford, K., Abrahams, L., Hegglin, M., & Klima, K. (2015). A Heat Vulnerability Index and Adaptation Solutions for Pittsburgh, Pennsylvania. Environmental Science and Technology, 49(19), 11303–11311. https://doi.org/10.1021/ACS.EST.5B03127

Bröde, P., Fiala, D., Błażejczyk, K., Holmér, I., Jendritzky, G., Kampmann, B., Tinz, B., & Havenith, G. (2012). Deriving the operational procedure for the Universal Thermal Climate Index (UTCI). International Journal of Biometeorology, 56(3), 481–494. https://doi.org/10.1007/S00484-011-0454-1

Brooke Anderson, G., & Bell, M. L. (2011). Heat waves in the United States: Mortality risk during heat waves and effect modification by heat wave characteristics in 43 U.S. communities. Environmental Health Perspectives, 119(2), 210–218. https://doi.org/10.1289/EHP.1002313

Budd, G. M. (2008). Wet-bulb globe temperature (WBGT)--its history and its limitations. Journal of Science and Medicine in Sport, 11(1), 20–32. https://doi.org/10.1016/J.JSAMS.2007.07.003

Buscail, C., Upegui, E., & Viel, J. F. (2012). Mapping heatwave health risk at the community level for public health action. International Journal of Health Geographics, 11. https://doi.org/10.1186/1476-072X-11-38

Cárdenas-León, I., Morales-Ortega, L. R., Koeva, M., Atun, F., & Pfeffer, K. (2024). Digital Twin-based Framework for Heat Stress Calculation. https://doi.org/10.2139/SSRN.4861693

CBS. (2017). Bestand Bodemgebruik 2017 ATOM. https://service.pdok.nl/cbs/bestandbodemgebruik/2017/atom/index.xml

CBS. (2019). More deaths during recent heat wave. https://www.cbs.nl/en-gb/news/2019/32/more-deaths-during-recent-heat-wave

CBS. (2020). More heat-related deaths, mainly in long-term care. https://www.cbs.nl/en-gb/news/2020/35/more-heat-related-deaths-mainly-in-long-term-care

CBS. (2022). CBS Square Statistics of Population 100m. https://www.pdok.nl/introductie/-/article/cbs-vierkantstatistieken-100m

CBS. (2024). CBS Wijken en Buurten 2022 versie 2. https://service.pdok.nl/cbs/wijkenbuurten/2022/atom/index.xml

Chen, Q., Ding, M., Yang, X., Hu, K., & Qi, J. (2018a). Spatially explicit assessment of heat health risk by using multi-sensor remote sensing images and socioeconomic data in Yangtze River Delta, China. International Journal of Health Geographics, 17(1), 1–15. https://doi.org/10.1186/S12942-018-0135-Y/FIGURES/8

Chen, Q., Ding, M., Yang, X., Hu, K., & Qi, J. (2018b). Spatially explicit assessment of heat health risk by using multi-sensor remote sensing images and socioeconomic data in Yangtze River Delta, China. International Journal of Health Geographics, 17(1), 1–15. https://doi.org/10.1186/S12942-018-0135-Y

Clarke, J. F. (1972). Some effects of the urban structure on heat mortality. Environmental Research, 5(1), 93–104. https://doi.org/10.1016/0013-9351(72)90023-0

Cobra Groeninzicht. (2021). Green and Grey Base Map. KEA. https://www.klimaateffectatlas.nl/en/green-and-grey-base-map

Curriero, F. C., Heiner, K. S., Samet, J. M., Zeger, S. L., Strug, L., & Patz, J. A. (2002). Temperature and Mortality in 11 Cities of the Eastern United States. American Journal of Epidemiology, 155(1), 80–87. https://doi.org/10.1093/AJE/155.1.80

De Visser, M., Kunst, A. E., & Fleischmann, M. (2022). Geographic and socioeconomic differences in heat-related mortality among the Dutch population: a time series analysis. BMJ Open, 12(11). https://doi.org/10.1136/BMJOPEN-2021-058185

Dean, M. (2020). Multi-criteria analysis. Advances in Transport Policy and Planning, 6, 165–224. https://doi.org/10.1016/BS.ATPP.2020.07.001

Dhalluin, A., & Bozonnet, E. (2015). Urban heat islands and sensitive building design – A study in some French cities' context. Sustainable Cities and Society, 19, 292–299. https://doi.org/10.1016/J.SCS.2015.06.009

Dousset, B., Gourmelon, F., Laaidi, K., Zeghnoun, A., Giraudet, E., Bretin, P., Mauri, E., & Vandentorren, S. (2011). Satellite monitoring of summer heat waves in the Paris metropolitan area. International Journal of Climatology, 31(2), 313–323. https://doi.org/10.1002/JOC.2222

ECMWF. (2022). European State of the Climate 2022 Summary. https://climate.copernicus.eu/esotc/2022/european-state-climate-2022-summary

ECMWF. (2023). 2023 on track to become the warmest year after record October. https://climate.copernicus.eu/2023-track-become-warmest-year-after-record-october

Ellena, M., Breil, M., & Soriani, S. (2020). The heat-health nexus in the urban context: A systematic literature review exploring the socio-economic vulnerabilities and built environment characteristics. Urban Climate, 34, 100676. https://doi.org/10.1016/J.UCLIM.2020.100676

Estoque, R. C., Ooba, M., Seposo, X. T., Togawa, T., Hijioka, Y., Takahashi, K., & Nakamura, S. (2020). Heat health risk assessment in Philippine cities using remotely sensed data and social-ecological indicators. Nature Communications 2020 11:1, 11(1), 1–12. https://doi.org/10.1038/s41467-020-15218-8

European Environment Agency. (2022). Climate change as a threat to health and well-being in Europe : focus on heat and infectious diseases. In Publications Office of the European Union. . https://doi.org/10.2800/67519

GGD/CBS/RIVM. (2024). Health Monitor Adults and Elderly 2020 (edited based on SMAP methodology, RIVM). CC-BY-SA 4.0 Licensed. https://buurtatlas.vzinfo.nl/#gebruikslicentie

Guindon, S. M., & Nirupama, N. (2015). Reducting risk from urban heat island effects in cities. Natural Hazards: Journal of the International Society for the Prevention and Mitigation of Natural Hazards, 77(2), 823–831. https://doi.org/10.1007/S11069-015-1627-8

Guo, Y., Gasparrini, A., Armstrong, B. G., Tawatsupa, B., Tobias, A., Lavigne, E., De Sousa Zanotti Stagliorio Coelho, M., Pan, X., Kim, H., Hashizume, M., Honda, Y., Leon Guo, Y. L., Wu, C. F., Zanobetti, A., Schwartz, J. D., Bell, M. L., Scortichini, M., Michelozzi, P., Punnasiri, K., … Tong, S. (2017). Heat Wave and Mortality: A Multicountry, Multicommunity Study. Environmental Health Perspectives, 125(8). https://doi.org/10.1289/EHP1026

Hagens, W. I., & van Bruggen, M. (2015). Nationaal Hitteplan versie 2015 RIVM Briefrapport 2014-0051. https://www.rivm.nl/bibliotheek/rapporten/2014-0051.pdf

Hajat, S., & Kosatky, T. (2010). Heat-related mortality: a review and exploration of heterogeneity. Journal of Epidemiology & Community Health, 64(9), 753–760. https://doi.org/10.1136/JECH.2009.087999

Hamilton, I. G., Davies, M., & Gauthier, S. (2015). London's urban heat island: a multi-scaled assessment framework. Https://Doi.Org/10.1680/Udap.10.00046, 166(3), 164–175. https://doi.org/10.1680/UDAP.10.00046

Ho, H. C., Knudby, A., Chi, G., Aminipouri, M., & Lai, D. Y. F. (2018). Spatiotemporal analysis of regional socio-economic vulnerability change associated with heat risks in Canada. Applied Geography, 95, 61–70. https://doi.org/10.1016/J.APGEOG.2018.04.015

Ho, H. C., Knudby, A., & Huang, W. (2015). A Spatial Framework to Map Heat Health Risks at Multiple Scales. International Journal of Environmental Research and Public Health 2015, Vol. 12, Pages 16110-16123, 12(12), 16110–16123. https://doi.org/10.3390/IJERPH121215046

Höppe, P. (1999). The physiological equivalent temperature - A universal index for the biometeorological assessment of the thermal environment. International Journal of Biometeorology, 43(2), 71–75. https://doi.org/10.1007/S004840050118

Intergovernmental Panel on Climate Change (IPCC). (2023). Climate Change 2022 – Impacts, Adaptation and Vulnerability. Climate Change 2022 – Impacts, Adaptation and Vulnerability. https://doi.org/10.1017/9781009325844

Jenerette, G. D., Harlan, S. L., Buyantuev, A., Stefanov, W. L., Declet-Barreto, J., Ruddell, B. L., Myint, S. W., Kaplan, S., & Li, X. (2016). Micro-scale urban surface temperatures are related to land-cover features and residential heat related health impacts in Phoenix, AZ USA. Landscape Ecology, 31(4), 745–760. https://doi.org/10.1007/S10980-015-0284-3

Jiang, S., Lee, X., Wang, J., & Wang, K. (2019). Amplified Urban Heat Islands during Heat Wave Periods. Journal of Geophysical Research: Atmospheres, 124(14), 7797–7812. https://doi.org/10.1029/2018JD030230

Johnson, D. P., Stanforth, A., Lulla, V., & Luber, G. (2012). Developing an applied extreme heat vulnerability index utilizing socioeconomic and environmental data. Applied Geography, 35(1–2), 23–31. https://doi.org/10.1016/J.APGEOG.2012.04.006

Keith, L., Meerow, S., & Wagner, T. (2020). Planning for Extreme Heat: A Review. Https://Doi.Org/10.1142/S2345737620500037, 06(03n04), 2050003. https://doi.org/10.1142/S2345737620500037

Kim, D. W., Deo, R. C., Lee, J. S., & Yeom, J. M. (2017). Mapping heatwave vulnerability in Korea. Natural Hazards, 89(1), 35–55. https://doi.org/10.1007/S11069-017-2951-Y

Kleerekoper, L. (2016). Urban Climate Design: Improving thermal comfort in Dutch neighbourhoods. A+BE | Architecture and the Built Environment, 6(11), 1–424. https://doi.org/10.7480/abe.2016.11.1359

Klein Rosenthal, J., Kinney, P. L., & Metzger, K. B. (2014). Intra-urban vulnerability to heat-related mortality in New York City, 1997–2006. Health & Place, 30, 45–60. https://doi.org/10.1016/J.HEALTHPLACE.2014.07.014

Klimaateffectatlas. (2023). Viewer - Klimaateffectatlas. https://www.klimaateffectatlas.nl/en/

Klok, E. J. (Lisette), & Kluck, J. (Jeroen). (2018). Reasons to adapt to urban heat (in the Netherlands). Urban Climate, 23, 342–351. https://doi.org/10.1016/J.UCLIM.2016.10.005

KNMI. (2023a). Daily data of the weather in the Netherlands. https://www.knmi.nl/nederland-nu/klimatologie/daggegevens

KNMI. (2023b). KNMI - Hittegolven. https://www.knmi.nl/nederland-nu/klimatologie/lijsten/hittegolven

KNMI. (2023c). Nieuwe KNMI-klimaatscenario's: 'Nederland moet zich voorbereiden op zwaardere weersextremen.' https://www.knmi.nl/over-het-knmi/nieuws/knmi23klimaatscenario-s

KNMI. (2024). Tropische dagen. https://www.knmi.nl/kennis-en-datacentrum/uitleg/tropische-dagen

Koopmans, S., Heusinkveld, B. G., & Steeneveld, G. J. (2020). A standardized Physical Equivalent Temperature urban heat map at 1-m spatial resolution to facilitate climate stress tests in the

Netherlands. Building and Environment, 181, 106984. https://doi.org/10.1016/J.BUILDENV.2020.106984

Kovats, R. S., & Hajat, S. (2008). Heat Stress and Public Health: A Critical Review. Https://Doi.Org/10.1146/Annurev.Publhealth.29.020907.090843, 29, 41–55. https://doi.org/10.1146/ANNUREV.PUBLHEALTH.29.020907.090843

Maiullari, D., Pijpers-Van Esch, M., & van Timmeren, A. (2021). A Quantitative Morphological Method for Mapping Local Climate Types. Urban Planning, 6(3), 240–257. https://doi.org/10.17645/UP.V6I3.4223

Malczewski, J., & Rinner, C. (2015). Multicriteria Decision Analysis in Geographic Information Science. https://doi.org/10.1007/978-3-540-74757-4

Marghidan, C. P. (2022). Extreme heat in MOZAMBIQUE: a rising risk for public health [Faculty of Geo-Information Science and Earth Observation of the University of Twente]. https://www.researchgate.net/profile/Carolina-Pereira-Marghidan/publication/375224042_MSc_Thesis_Extreme_heat_in_Mozambique_a_rising_risk_for_public_health/links/6543a651b6233776b7443922/MSc-Thesis-Extreme-heat-in-Mozambique-a-rising-risk-for-public-health.pdf

McGeehin, M. A., & Mirabelli, M. (2001). The potential impacts of climate variability and change on temperature-related morbidity and mortality in the United States. Environmental Health Perspectives, 109(suppl 2), 185–189. https://doi.org/10.1289/EHP.109-1240665

McGregor, G., editor Bessemoulin, lead P., Ebi, K., & Menne, B. (2015). Heatwaves and Health: Guidance on Warning-System Development. https://durham-repository.worktribe.com/output/1130319

Mohajerani, A., Bakaric, J., & Jeffrey-Bailey, T. (2017). The urban heat island effect, its causes, and mitigation, with reference to the thermal properties of asphalt concrete. Journal of Environmental Management, 197, 522–538. https://doi.org/10.1016/j.jenvman.2017.03.095

Mora, C., Dousset, B., Caldwell, I. R., Powell, F. E., Geronimo, R. C., Bielecki, C. R., Counsell, C. W. W., Dietrich, B. S., Johnston, E. T., Louis, L. V., Lucas, M. P., Mckenzie, M. M., Shea, A. G., Tseng, H., Giambelluca, T. W., Leon, L. R., Hawkins, E., & Trauernicht, C. (2017). Global risk of deadly heat. Nature Climate Change 2017 7:7, 7(7), 501–506. https://doi.org/10.1038/nclimate3322

Morabito, M., Crisci, A., Gioli, B., Gualtieri, G., Toscano, P., Di Stefano, V., Orlandini, S., & Gensini, G. F. (2015). Urban-Hazard Risk Analysis: Mapping of Heat-Related Risks in the Elderly in Major Italian Cities. PLOS ONE, 10(5), e0127277. https://doi.org/10.1371/JOURNAL.PONE.0127277

Nationale Klimaatadaptatiestrategie (NAS). (2019). Handreiking Lokaal Hitteplan - Klimaatadaptatie. https://klimaatadaptatienederland.nl/hulpmiddelen/overzicht/lokaal-hitteplan/

Oke, T. R. (1982). The energetic basis of the urban heat island. Quart. J. R. Met. Soc, 108(455), 551.

Oudin Åström, D., Bertil, F., & Joacim, R. (2011). Heat wave impact on morbidity and mortality in the elderly population: A review of recent studies. Maturitas, 69(2), 99–105. https://doi.org/10.1016/J.MATURITAS.2011.03.008

Peng, S., Piao, S., Ciais, P., Friedlingstein, P., Ottle, C., Bréon, F.-M., Nan, H., Zhou, L., & Myneni, R. B. (2012). Surface Urban Heat Island Across 419 Global Big Cities. Environmental Science & Technology, 46(2), 696–703. https://doi.org/10.1021/es2030438

Perkins, S. E., & Alexander, L. V. (2013). On the measurement of heat waves. Journal of Climate, 26(13), 4500–4517. https://doi.org/10.1175/JCLI-D-12-00383.1

Peterson, T., Folland, C., Gruza, G., Hogg, W., & Mokssit, A. (2001). Report on the activities of the working group on climate change detection and related rapporteurs. Geneva: World Meteorological Organization. https://core.ac.uk/download/pdf/9700748.pdf

Raines, G. L., Sawatzky, D. L., & Bonham-Carter, G. F. (2010). Incorporating expert knowledge – New fuzzy logic tools in ArcGIS. https://www.esri.com/news/arcuser/0410/fuzzylogic.html

Reiners, P., Sobrino, J., & Kuenzer, C. (2023). Satellite-Derived Land Surface Temperature Dynamics in the Context of Global Change—A Review. Remote Sensing 2023, Vol. 15, Page 1857, 15(7), 1857. https://doi.org/10.3390/RS15071857

RIVM. (2023). Social vulnerability to heat. KEA. https://www.klimaateffectatlas.nl/en/social-vulnerability-to-heat

RIVM. (2024). GGD-richtlijn medische milieukunde: hitte en gezondheid. https://www.rivm.nl/ggd-richtlijn-mmk-hitte-gezondheid

Russo, S., Sillmann, J., & Fischer, E. M. (2015). Top ten European heatwaves since 1950 and their occurrence in the coming decades. Environmental Research Letters, 10(12), 124003. https://doi.org/10.1088/1748-9326/10/12/124003

Sheridan, S. C., & Kalkstein, L. S. (2004). Progress in Heat Watch–Warning System Technology. Bulletin of the American Meteorological Society, 85(12), 1931–1942. https://doi.org/10.1175/BAMS-85-12-1931

Smoyer-Tomic, K. E., Kuhn, R., & Hudson, A. (2003). Heat Wave Hazards: An Overview of Heat Wave Impacts in Canada. Natural Hazards 2003 28:2, 28(2), 465–486. https://doi.org/10.1023/A:1022946528157

Staiger, H. , Bucher, K., & Jendritzky G. (1997). Die physiologisch gerechte Bewertung von Wärmebelastung und Kältestress beim Aufenthalt im Freien in der Maßzahl Grad Celsius. Annalen der Meteorologie. Annalen Der Meteorologie, 33, 100–107.

Steadman, R. G., Steadman, & G., R. (1984). A Universal Scale of Apparent Temperature. JApMe, 23(12), 1674–1687. https://doi.org/10.1175/1520-0450(1984)023

Steeneveld, G. J., Koopmans, S., Heusinkveld, B. G., Van Hove, L. W. A., & Holtslag, A. A. M. (2011). Quantifying urban heat island effects and human comfort for cities of variable size and urban morphology in the Netherlands. Journal of Geophysical Research Atmospheres, 116(20). https://doi.org/10.1029/2011JD015988

Stewart, I. D., & Oke, T. R. (2012). Local Climate Zones for Urban Temperature Studies. Bulletin of the American Meteorological Society, 93(12), 1879–1900. https://doi.org/10.1175/BAMS-D-11-00019.1

Stone, B., Vargo, J., Liu, P., Hu, Y., & Russell, A. (2013). Climate change adaptation through urban heat management in Atlanta, Georgia. Environmental Science & Technology, 47(14), 7780–7786. https://doi.org/10.1021/ES304352E

Sun, Y., Li, Y., Ma, R., Gao, C., & Wu, Y. (2022). Mapping urban socio-economic vulnerability related to heat risk: A grid-based assessment framework by combing the geospatial big data. Urban Climate, 43. https://doi.org/10.1016/J.UCLIM.2022.101169

Taherdoost, H., & Madanchian, M. (2023). Multi-Criteria Decision Making (MCDM) Methods and Concepts. Encyclopedia, 3(1), 77–87. https://doi.org/10.3390/encyclopedia3010006

TAUW, & Amsterdam University of Applied Science. (2021). Distances to Cooling. KEA. https://www.klimaateffectatlas.nl/en/distance-to-cooling

The Guardian. (2023). Severe heatwave engulfs Asia causing deaths and forcing schools to close. https://www.theguardian.com/weather/2023/apr/19/severe-heatwave-asia-deaths-schools-close-india-china

The Guardian. (2024). The story of a heat death: David went to work in his new job on a French building site. By the end of the day he was dead. https://www.theguardian.com/environment/article/2024/jul/13/the-story-of-a-heat-death-david-went-to-work-in-his-new-job-on-a-french-building-site-by-the-end-of-the-day-he-was-dead

The Lancet. (2018). Heatwaves and health. The Lancet, 392(10145), 359. https://doi.org/10.1016/S0140-6736(18)30434-3

The New York Times. (2023). Heat Waves Around the World Push People and Nations 'to the Edge' - The New York Times. https://www.nytimes.com/2022/06/24/climate/early-heat-waves.html

Tomlinson, C. J., Chapman, L., Thornes, J. E., & Baker, C. J. (2011). Including the urban heat island in spatial heat health risk assessment strategies: A case study for Birmingham, UK. International Journal of Health Geographics, 10. https://doi.org/10.1186/1476-072X-10-42

Tong, S., Prior, J., McGregor, G., Shi, X., & Kinney, P. (2021). Urban heat: an increasing threat to global health. BMJ, 375. https://doi.org/10.1136/BMJ.N2467

Twents Waternet. (2023). https://twn.klimaatmonitor.net

US EPA. (n.d.). Learn About Heat Islands | US EPA. Retrieved July 10, 2024, from https://www.epa.gov/heatislands/learn-about-heat-islands

U.S. Geological Survey (USGS). (2024). Landsat 8 Level 2, Collection 2, Tier 1 Surface Reflectance and Land Surface Temperature. https://earthengine.google.com

van Daalen, K. R., Romanello, M., Rocklöv, J., Semenza, J. C., Tonne, C., Markandya, A., Dasandi, N., Jankin, S., Achebak, H., Ballester, J., Bechara, H., Callaghan, M. W., Chambers, J., Dasgupta, S., Drummond, P., Farooq, Z., Gasparyan, O., Gonzalez-Reviriego, N., Hamilton, I., … Lowe, R. (2022). The 2022 Europe report of the Lancet Countdown on health and climate change: towards a climate resilient future. The Lancet Public Health, 7(11), e942–e965. https://doi.org/10.1016/S2468-2667(22)00197-9

Van Der Hoeven, F., & Wandl, A. (2015). Amsterwarm: Mapping the landuse, health and energy-efficiency implications of the Amsterdam urban heat island. Building Services Engineering Research and Technology, 36(1), 67–88. https://doi.org/10.1177/0143624414541451

Van Der Hoeven, F., & Wandl, A. (2018). Hotterdam: Mapping the social, morphological, and land-use dimensions of the Rotterdam urban heat island. Urbani Izziv, 29(1), 58–72. https://doi.org/10.5379/URBANI-IZZIV-EN-2018-29-01-001

Van Loenhout, J. A. F., Rodriguez-Llanes, J. M., & Guha-Sapir, D. (2016). Stakeholders' Perception on National Heatwave Plans and Their Local Implementation in Belgium and The Netherlands. International Journal of Environmental Research and Public Health 2016, Vol. 13, Page 1120, 13(11), 1120. https://doi.org/10.3390/IJERPH13111120

van Merwijk, K., Zuurbier, M., & Klaassen, P. (2023). Wie houdt het hoofd koel? https://www.awgl.nl/projecten/verkoeling-bij-hitte

Vanderplanken, K., van den Hazel, P., Marx, M., Shams, A. Z., Guha-Sapir, D., & van Loenhout, J. A. F. (2021). Governing heatwaves in Europe: comparing health policy and practices to better understand roles, responsibilities and collaboration. Health Research Policy and Systems, 19(1), 1–14. https://doi.org/10.1186/S12961-020-00645-2

Vicedo-Cabrera, A. M., Scovronick, N., Sera, F., Royé, D., Schneider, R., Tobias, A., Astrom, C., Guo, Y., Honda, Y., Hondula, D. M., Abrutzky, R., Tong, S., Coelho, M. de S. Z. S., Saldiva, P. H. N., Lavigne, E., Correa, P. M., Ortega, N. V., Kan, H., Osorio, S., … Gasparrini, A. (2021). The burden of heat-related mortality attributable to recent human-induced climate change. Nature Climate Change 2021 11:6, 11(6), 492–500. https://doi.org/10.1038/s41558-021-01058-x

Voelkel, J., Hellman, D., Sakuma, R., & Shandas, V. (2018). Assessing Vulnerability to Urban Heat: A Study of Disproportionate Heat Exposure and Access to Refuge by Socio-Demographic Status in Portland, Oregon. International Journal of Environmental Research and Public Health 2018, Vol. 15, Page 640, 15(4), 640. https://doi.org/10.3390/IJERPH15040640

Wageningen Environmental Research. (2016). Warm Nights. KEA. https://www.klimaateffectatlas.nl/en/warm-nights

WHO. (2023). Heatwaves. https://www.who.int/health-topics/heatwaves/#tab=tab_1

Wolf, T., & McGregor, G. (2013). The development of a heat wave vulnerability index for London, United Kingdom. Weather and Climate Extremes, 1, 59–68. https://doi.org/10.1016/J.WACE.2013.07.004

World Weather Attribution. (2022). Climate Change made devastating early heat in India and Pakistan 30 times more likely. https://www.worldweatherattribution.org/climate-change-made-devastating-early-heat-in-india-and-pakistan-30-times-more-likely/

World Weather Attribution. (2023). Extreme heat in North America, Europe and China in July 2023 made much more likely by climate change. https://www.worldweatherattribution.org/extreme-heat-in-north-america-europe-and-china-in-july-2023-made-much-more-likely-by-climate-change/

World Weather Attribution. (2024a). Dangerous humid heat in southern West Africa about 4°C hotter due to climate change. https://www.worldweatherattribution.org/dangerous-humid-heat-in-southern-west-africa-about-4c-hotter-due-to-climate-change/

World Weather Attribution. (2024b). Extreme heat killing more than 100 people in Mexico hotter and much more likely due to climate change. https://www.worldweatherattribution.org/extreme-heat-killing-more-than-100-people-in-mexico-hotter-and-much-more-likely-due-to-climate-change/

Yang, J., Wu, Z., Menenti, M., Wong, M. S., Xie, Y., Zhu, R., Abbas, S., & Xu, Y. (2023). Impacts of urban morphology on sensible heat flux and net radiation exchange. Urban Climate, 50, 101588. https://doi.org/10.1016/j.uclim.2023.101588

Yang, J., Yin, P., Sun, J., Wang, B., Zhou, M., Li, M., Tong, S., Meng, B., Guo, Y., & Liu, Q. (2019). Heatwave and mortality in 31 major Chinese cities: Definition, vulnerability and implications. Science of The Total Environment, 649, 695–702. https://doi.org/10.1016/J.SCITOTENV.2018.08.332

Zaidi, R. Z., & Pelling, M. (2015). Institutionally configured risk: Assessing urban resilience and disaster risk reduction to heat wave risk in London. Urban Studies, 52(7), 1218–1233. https://doi.org/10.1177/0042098013510957

Zinzi, M., & Santamouris, M. (2019). Introducing Urban Overheating—Progress on Mitigation Science and Engineering Applications. Climate 2019, Vol. 7, Page 15, 7(1), 15. https://doi.org/10.3390/CLI7010015

9 APPENDIX

9.1 KNMI daily weather station summary

The KNMI weather station data availability and type summary is as follows (Table 9–1), TX at stations (in **Bold**) with type of (automatic weather station) AWS, AWS/ Aerodrome, AWS/Mistpost were chosen for this study.

Table 9–1 Weather station summary

	ID	Location	Start Date	End Date	Type
0	209	IJmond	2001/1/30	up to date	Windmast
1	210	Valkenburg Zh	1951/1/1	2016/5/4	
2	215	**Voorschoten**	**2014/7/15**	**up to date**	AWS/Mistpost
3	225	IJmuiden	1971/1/1	up to date	Windmast
4	229	Texelhors	2017/12/13	up to date	Windmast
5	235	**De Kooy**	1906/1/1	up to date	AWS/Aerodrome
6	240	**Schiphol**	1951/1/1	up to date	AWS/Aerodrome
7	242	**Vlieland**	1996/1/1	up to date	AWS/Aerodrome
8	248	Wijdenes	1994/7/15	up to date	Windmast
9	249	**Berkhout**	1999/3/12	up to date	AWS
10	251	**Hoorn Terschelling**	1994/5/26	up to date	AWS
11	257	**Wijk aan Zee**	**2001/4/30**	**up to date**	AWS
12	258	Houtribdijk	2006/2/1	up to date	Windmast
13	260	**De Bilt**	1901/1/1	up to date	AWS
14	265	Soesterberg	1951/9/1	2008/11/16	
15	267	**Stavoren**	1990/6/18	up to date	AWS
16	269	**Lelystad**	1990/1/17	up to date	AWS/Aerodrome
17	270	**Leeuwarden**	1951/1/1	up to date	AWS/Aerodrome
18	273	**Marknesse**	1989/1/1	up to date	AWS
19	275	**Deelen**	1951/1/1	up to date	AWS/Aerodrome
20	277	**Lauwersoog**	1991/3/18	up to date	AWS
21	278	**Heino**	1991/1/1	up to date	AWS
22	279	**Hoogeveen**	1989/9/26	up to date	AWS
23	280	**Eelde**	1906/1/1	up to date	AWS/Aerodrome
24	283	**Hupsel**	1989/10/16	up to date	AWS
25	285	Huibertgat	1981/1/1	up to date	Windmast
26	286	**Nieuw Beerta**	1990/1/17	up to date	AWS
27	290	**Twenthe**	1951/1/1	up to date	AWS
28	308	Cadzand	1972/1/1	up to date	Windmast
29	310	**Vlissingen**	1906/1/1	up to date	AWS

30	311	Hoofdplaat	1997/1/31	2016/2/1	Windmast
31	312	Oosterschelde	1982/1/1	up to date	Windmast
32	313	Vlakte van De Raan	1997/1/31	up to date	Windmast
33	315	Hansweert	1997/1/31	up to date	Windmast
34	316	Schaar	1983/1/1	up to date	Windmast
35	319	**Westdorpe**	1991/6/25	up to date	AWS
36	323	**Wilhelminadorp**	**2017/12/15**	**up to date**	AWS
37	324	Stavenisse	1997/9/30	up to date	Windmast
38	330	**Hoek van Holland**	1971/1/1	up to date	AWS
39	331	Tholen	1981/1/1	up to date	Windmast
40	340	**Woensdrecht**	1993/4/1	up to date	AWS/Aerodrome
41	343	Rotterdam Geulhaven	1991/1/1	up to date	Windmast
42	344	**Rotterdam**	1956/10/1	up to date	AWS/Aerodrome
43	348	**Cabauw Mast**	1986/3/1	up to date	AWS
44	350	**Gilze-Rijen**	1951/1/1	up to date	AWS/Aerodrome
45	356	**Herwijnen**	1989/9/26	up to date	AWS
46	370	**Eindhoven**	1951/1/1	up to date	AWS/Aerodrome
47	375	**Volkel**	1951/2/1	up to date	AWS/Aerodrome
48	377	**Ell**	1999/5/1	up to date	AWS
49	380	**Maastricht**	1906/1/1	up to date	AWS/Aerodrome
50	391	**Arcen**	1990/6/18	up to date	AWS

9.2 Data availiability of Landsat 8 during heatwave days from 2013 until 2022

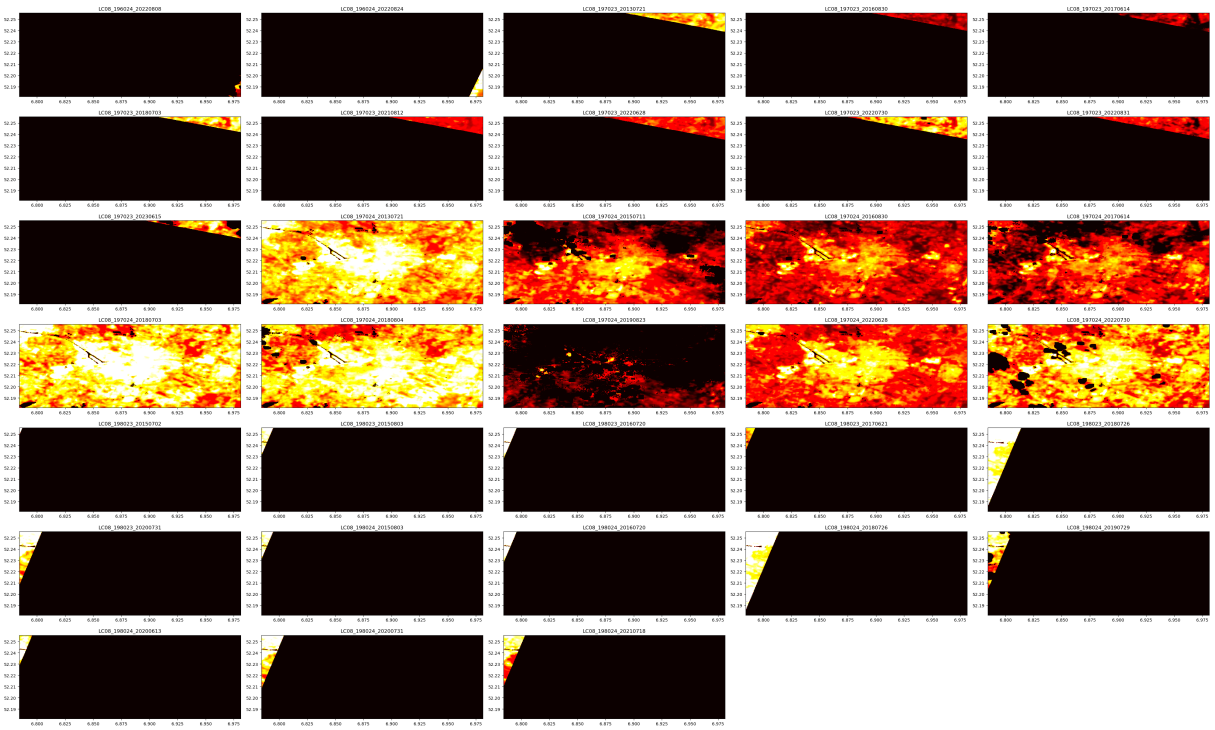

9.3 Range used for normalisation of each indicators

Table 9–2 Range used for normalisation of exposure indicators

Risk Level	Normalised values	SUHI	PET	Warm Nights	Population Density
1	< 0.2	(-3.82, -3.82)	(41.13, 41.23)	(0.0, 0.0)	(7.33, 18.19)
2	0.2-0.4	(-0.95, 1.08)	(41.24, 41.33)	(nan, nan)	(31.29, 37.11)
3	0.4-0.6	(1.25, 3.72)	(41.34, 41.44)	(nan, nan)	(43.0, 60.44)
4	0.6-0.8	(3.84, 6.03)	(41.46, 41.54)	(0.42, 0.56)	(62.33, 77.04)
5	0.8-1.0	(6.33, 8.83)	(41.57, 41.65)	(0.57, 0.7)	(78.84, 96.46)

Table 9–3 Range used for normalisation of vulnerability-sensitivity indicators

Risk Level	Normalised values	65 and older Frailty Health (%) y	Percentage 65 years and older (%) y	Births per 1000 inhabitants y	Severe Lonely aged 75+ per km2 y	18 and older Severe Overweight (%) y	18 and older Limited mobility (%) y	Percentage of social minimum households (%) y	Percentage rental properties (%) y
1	< 0.2	(0.0, 0.0)	(0, 6)	(0, 6)	(0, 39)	(0.0, 0.0)	(0.0, 5.5)	(0.0, 4.2)	(0, 17)
2	0.2-0.4	(nan, nan)	(7, 13)	(7, 12)	(40, 78)	(6.6, 9.0)	(7.0, 12.9)	(4.8, 9.4)	(19, 36)
3	0.4-0.6	(18.5, 27.6)	(14, 20)	(14, 14)	(89, 89)	(11.1, 15.9)	(13.2, 18.7)	(9.6, 14.1)	(37, 55)
4	0.6-0.8	(28.4, 36.6)	(21, 27)	(22, 22)	(152, 152)	(16.8, 21.1)	(20.2, 25.9)	(14.2, 18.8)	(56, 73)
5	0.8-1.0	(36.9, 46.1)	(28, 34)	(33, 33)	(180, 196)	(21.9, 26.5)	(30.2, 32.5)	(19.8, 23.6)	(74, 92)

Table 9–4 Range used for normalisation of vulnerability-adaptive capacity indicators

Risk Level	Normalised values	Percentage of Green Space in Public	Percentage of Green Space non-Public	Percentage of Water	Distance to cooling space
1	< 0.2	(67, 81)	(64, 76)	(19.69, 19.69)	(0.59, 0.93)
2	0.2-0.4	(53, 65)	(51, 62)	(15.28, 15.28)	(0.95, 1.27)
3	0.4-0.6	(39, 52)	(36, 46)	(8.54, 9.95)	(1.31, 1.62)
4	0.6-0.8	(25, 37)	(22, 35)	(4.49, 7.17)	(1.66, 1.87)
5	0.8-1.0	(10, 24)	(8, 21)	(0.0, 3.48)	(2.0, 2.35)